

**ROAD TRAFFIC ACCIDENT ANALYSIS
USING A NON METRIC CAMERA.//**

by

JOHN BOSCO KYALO KIEMA

THIS THESIS HAS BEEN ACCEPTED FOR
THE DEGREE OF..... *MSc 1993*
AND A COPY MAY BE PLACED IN THE
UNIVERSITY LIBRARY.

A thesis submitted in partial fulfilment for the Degree of Master
of Science (Surveying & Photogrammetry) in the University of
Nairobi.

THIS THESIS HAS BEEN ACCEPTED FOR
THE DEGREE OF..... *MSc 1993*
AND A COPY MAY BE PLACED IN THE
UNIVERSITY LIBRARY.

August, 1993

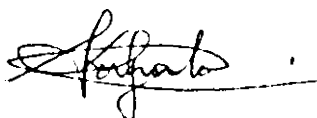
UNIVERSITY OF NAIROBI LIBRARY



0145093 1

DECLARATIONS.

This thesis is my original work and has not been presented for a degree to any other University.



JOHN BOSCO KYALO KIEMA

This thesis has been submitted for examination with my approval as University Supervisor.



Prof. H.N. NAGARAJA
Department of Surveying
University of Nairobi

ABSTRACT.

The road traffic accident (RTA) situation in Kenya is, to say the least, simply appalling. Accordingly, the RTA analysis methodology used is not only inefficient and inaccurate, but is also susceptible to criminal distortion. This thesis set out to investigate into the RTA analysis locally practiced while seeking to establish a low investment and operational cost, albeit speedy, photogrammetric method that could be used for the same purpose. This would also preferably provide a permanent record that may be admissible in the courts of law.

The Departmental non-metric (Mamiya C3) camera was identified and adopted as a low cost data acquisition tool. As is the requirement in non-metric photogrammetry, an elaborate data reduction scheme was required. The Direct Linear Transformation (DLT) approach was used in this respect. To this the two DLT restrictions were added.

Data was collected from various diverse sources. Several trips were made in the company of traffic police officers to different RTA scenes. The type, nature and rigour of observations and measurements made by these officers was carefully noted. An inventory was also later made into the police RTA files. Photographs of various "live" and "simulated" RTA scenes were also taken. The required photocoordinates were then made from a Zeiss Stereocord and on the Wild A8 stereo-plotter for comparison purposes. Relevant data was analyzed on the Vax 6310 mainframe computer located at University of Nairobi.

It was established that an RTA plan of scale 1/100 or even larger, was easily accomplished under the proposed

methodology using either of the above comparators. Also, different perspective views of any RTA scene were possible. This methodology on the average, reduced the time required at the RTA scene by at least ten minutes.

The results from this thesis tend to strongly suggest that an RTA analysis methodology akin to the one proposed should be used henceforth. This would not only change the old technology to a new one in local RTA analysis strategies, but also improve the collection, accuracy, preservation and presentation of metric RTA data. Further, this would also add a new dimension into understanding how RTAs occur and how to handle them properly; something that is long overdue in Kenya.

ACKNOWLEDGMENT.

This thesis would not have been duly completed without the contribution, guidance, challenge, inspiration, and indeed frustration by many individuals and organizations; a few of whom are mentioned here-under.

Firstly, I would like to thank the Deans committee of the University of Nairobi for kindly awarding me through my supervisor, a grant that made it possible to undertake this research.

Special thanks rightly go to Prof. H.N. Nagaraja my supervisor, for his ready advice, comments and guidance.

I also wish to express my gratitude to Dr-Ing F.W.O. Aduol, Chairman Department of Surveying & Photogrammetry, for his insight in the choice of this thesis and his inspiration and assistance all through in the course of its preparation.

Sincere appreciation is also accorded to the Traffic Department Nairobi Area Police and especially to the Divisional Traffic Officers at Kasarani and Buru-Buru Police Divisions.

I am also indebted to salute the Institute of Computer Science (ICS) University of Nairobi, in particular, messrs Mungai and Odeny for their cooperation.

Finally, I wish to record my profound thanks to my dear colleague Mr. Mulei Musyoka for challenge and inspiration throughout our study period.

DEDICATION.

To my future family, though undefined precisely presently, but vividly clear in the kaleidoscope of my mind, to my parents and brothers, and to all those Kenyans who have lost their lives as a direct result of road traffic accidents, is this thesis dedicated.

LIST OF FIGURES.

<u>Figure</u>	<u>Page</u>
1.1 Conceptualization of an RTA.	1
2.1 The Kenya Police-Traffic Department Accident Report form.	155
2.2 Graphical representation of RTA classification in Kenya over the last decade.	17
2.3 The RTA Sketch Plan.	157
5.1 The Control frame (Plan view).	67
5.2 The Control frame (Front view).	68
5.3 Shape of the control frame targets.	69
5.4 Subtense bar measurements.	73
5.5 Data acquisition set-up...the normal case of close range photogrammetry.	75
5.6 Generalized curves showing the relationship of standard deviation in the Object Space with the angle of convergence for a two-station reduction.	79
6.1 Horizontal coordination of a control point.	85
6.2 Vertical coordination of a control point.	87
6.3 Modified approach to the vertical coordination of a control point.	88

LIST OF TABLES.

<u>Table</u>	<u>Page</u>
2.1 Classification of RTAs in Kenya over the last decade.	16
6.1 Variation of the mean positional errors with the type of height coordination.	92
6.2 Effect of the variation in the interior orientation parameters with the number of control points for 11 unknowns.	96
6.3 Variation in the average mean square errors with the number of control points before incorporating the two DLT restrictions.	96
6.4 Variation in the average mean square errors with the number of control points after incorporating the two DLT restrictions.	97
6.5 Variation in the average mean square errors with the number of control points for photocoordinate measurements on the Zeiss Stereocord.	97
6.6 Variation in the average mean square errors with the number of control points for photocoordinate measurements on the Wild A8 Stereoplotter.	98
6.7 The variation of the average mean square errors with the number of unknown parameters.	98
6.8 Variation in the number of unknown parameters with the bare (theoretically) minimum number of control points required for a solution.	101

LIST OF PLATES.

<u>Plate</u>		<u>Page</u>
5a-5d	Sample illustrations of live road traffic accident (RTA) stereo-pairs.	81
5e-5h	Sample illustrations of simulated road traffic accident (RTA) stereo-pairs.	82

TABLE OF CONTENTS.

	Page
DECLARATION	(ii)
ABSTRACT	(iii)
ACKNOWLEDGMENT	(v)
DEDICATION	(vi)
LIST OF FIGURES	(vii)
LIST OF TABLES	(viii)
LIST OF PLATES	(ix)

CHAPTER 1. INTRODUCTION.

1.1	General	1
1.2	Statement of the problem	2
1.3	Organization of the report	7
1.4	Review of related literature	8
1.4.1	Close-range photogrammetry	8
1.4.2	RTA analysis in Kenya	10
1.4.3	Non-metric cameras and their use in RTA analysis.	11

CHAPTER 2. ROAD TRAFFIC ACCIDENT ANALYSIS IN KENYA.

2.1	Objectives of RTA analysis	14
2.2	RTA reporting and classification	14
2.3	Action at the RTA scene	18
2.3.1	Personnel and equipment required	18
2.3.2	Handling of the vehicles involved in the RTA	19
2.3.3	Sketch Plan Drawing	21
2.3.4	Measurements made at the RTA scene	22
2.3.5	Skid marks and Braking Impressions	22
2.4	Processing of RTA documents	24
2.5	Analysis and Interpretation of RTA documents	25
2.6	Expected accuracy of this methodology	27
2.7	Advantages and Disadvantages of RTA analysis	28

Methodology used in Kenya.

2.7.1	Disadvantages	28
2.7.2	Advantages	30
2.7.3	Discussion.	31

CHAPTER 3. THE DIRECT LINEAR TRANSFORMATION (DLT).

3.1	Transformation from comparator coordinates system into image coordinates system	32
3.2	Transformation from image coordinates system to object-space coordinates system	34
3.3	The Direct Linear Transformation (DLT) from comparator coordinates system to the object coordinates system	37
3.4	The Mathematical model of DLT considering random and systematic errors in the image coordinates	38
3.5	Calculation of the object-space coordinates from DLT coefficients for two photos	39
3.6	Estimation of inner orientation parameters of non-metric cameras from DLT coefficients	40
3.7	Extension of the mathematical model	44
3.8	Advantages and Disadvantages of DLT.	45

CHAPTER 4. SYSTEMATIC ERRORS IN NON-METRIC CAMERAS.

4.1	Lens distortions in non-metric cameras	47
4.2	The theoretical mathematical model used to represent symmetrical lens distortion	48
4.2.1	Factors affecting symmetrical lens distortion	49
4.2.2	The adopted mathematical model for symmetrical lens distortion	49
4.3	Asymmetrical lens distortion	51
4.3.1	The asymmetrical lens distortion due to the	51

	reference point not being the point of symmetry	
4.3.2	The asymmetrical lens distortion due to decentring of the lens elements	53
4.3.3	The adopted mathematical model for asymmetrical lens distortion	53
4.4	Film deformation in non-metric cameras	54
4.4.1	Film deformation outside the camera	55
4.4.2	Film deformation inside the camera	56
4.4.3	Total film deformation	57
4.5	Complete mathematical model for film deformation in non-metric cameras.	58

CHAPTER 5. DATA ACQUISITION.

5.1	Possible approaches to the determination of camera parameters while using a non-metric camera	60
5.1.1	Camera self calibration	61
5.1.2	Camera calibration using ground survey control	62
5.1.3	Control frame	62
5.2	Design of the control frame	63
5.2.1	Design criteria	64
5.2.2	Design specifications	65
5.2.3	Target design	69
5.3	Coordination of the control points	70
5.3.1	Reconnaissance	71
5.3.2	Types of observations	72
5.3.3	Instrumentation	72
5.3.4.1	Base measurement	72
5.3.4.2	Observation of horizontal directions	73
5.3.4.3	Determination of the heights of observation points	76
5.4	Photography	76
5.4.1	Specifications of the camera used	77
5.4.2	Photographic configurations used for the	78

RTA photography	
5.4.3 Measurement of the photocordinates.	80
<u>CHAPTER 6. ROAD TRAFFIC ACCIDENT DATA REDUCTION</u>	
<u>AND ANALYSIS.</u>	
6.1 Three-Dimensional coordination of the control frame	83
6.1.1 General	83
6.1.2 Base length computation	84
6.1.3 Horizontal coordination	85
6.1.4 Vertical coordination	86
6.2 Coordination of imaged RTA points	89
6.3 Results	91
6.3.1 Three dimensional coordination of the control frame	92
6.3.2 Three dimensional coordination of the imaged RTA points	92
6.4 Discussion.	99
<u>CHAPTER 7. CONCLUSIONS AND RECOMMENDATIONS.</u>	
7.1 Conclusions	103
7.2 Recommendations.	105
REFERENCES AND BIBLIOGRAPHY.	107
<u>APPENDIX A. STRUCTURE OF THE DLT.</u>	
A.1 The DLT formulation	114
A.2 Determining the unknown parameters	116
A.3 The form of the weight matrix	120
A.4 The variance-covariance matrix of the unknowns	121
A.5 The number of unknowns carried in the solution	121

A.6 Computation of the interior orientation
elements 122

A.7 Computation of the object space coordinates. 122

APPENDIX B. PROGRAM FLOW CHARTS.

B.1 Main program COORD 127

B.2 Main program DLT 132

B.3 Subroutine SORT 138

B.4 Subroutine XPYPC 140

B.5 Subroutine OBJECT 141

B.6 Subroutine OBTWO. 144

APPENDIX C.

C.1 Simplified version of the DLT restrictions 147

C.2 The elements of the restriction design
matrix 148

C.3 Coordinate list of the control frame 150

C.4 The Kenya Police-Traffic Department Accident
Report form. 155

C.5 The RTA Sketch Plan 157

C.6 Program listings. 159

1.1 General.

Right from the outset one may ask what Road Traffic Accidents (RTAs) are, and further, what causes them. In brief, an RTA results when there is lack of harmony in either one, two or even all of the following; road user, vehicle and environment. Alternatively, an RTA may be conceptualized as an event resulting once the system demand exceeds the driver performance (see Fig 1.1)

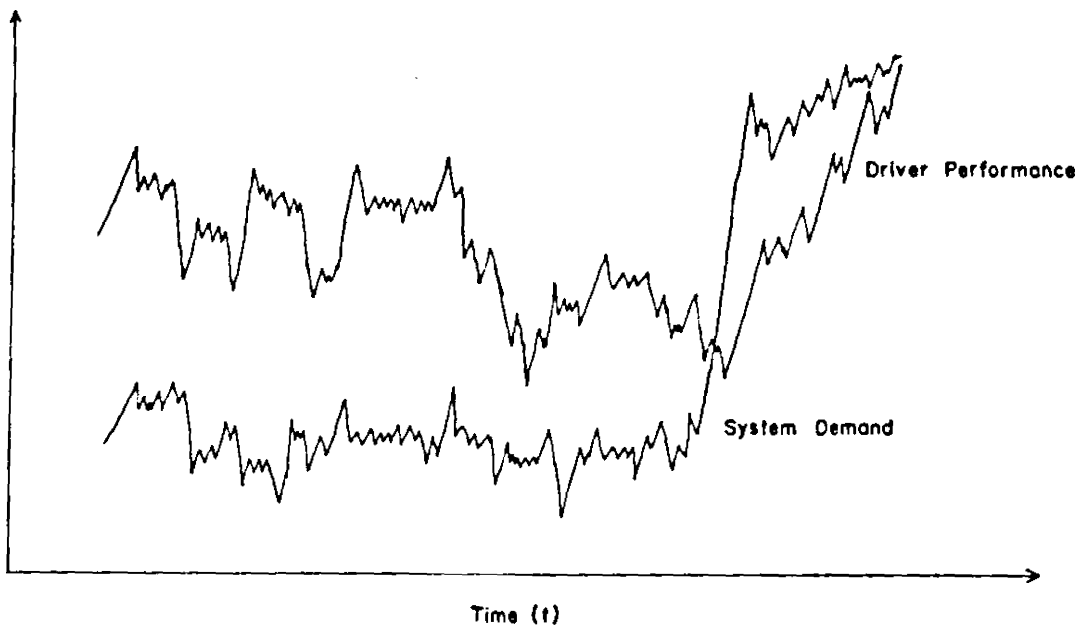


Fig 1.1 Conceptualization of an RTA

The exhaustive reasons as to why RTAs occur and why they occur where they do so, have not yet been fully determined. But some of the common known causes of RTAs include;

- poor road design,
- vehicular congestion on roads,
- distortion on the part of some of the road users from a normal psychological and/or physiological condition, and
- mechanical failure of the vehicle(s).

RTAs have rightly been referred to as "the biggest epidemic

of our time. Kenya has had more than its fair share of agony from this menace. Hardly any day goes by without at least five lives, on the average, being "sacrificed" on the increasingly dangerous Kenyan roads. Salient, though equally frightening, is the lofty, unchecked number of human beings who as a result end up permanently crippled. Regretfully, this is mostly the "bread winning" bracket in our society.

This scenario leads, and has indeed led, to untold economic strains and difficulties for the affected families. Not surprising is a statement advanced by one tour agent through the local dailies sometimes last year. This was to the effect that, apart from the threat of the dreaded Acquired Immune Deficiency Syndrome (AIDS), tourists were very worried about their safety on Kenyan roads. Apparently, the situation appears to have run out of hand. Not even the spirited campaign by the Daily Nation newspaper in 1991 could "prevent 2000" lives being lost through RTAs.

Among the most glaring weaknesses in the present efforts to reduce RTAs is that too often those concerned follow a "single-focus" approach. Engineers may think only of improvements in vehicle or road, educators of training for drivers and pedestrians, and law-enforcement and licensing officials of control and punishment. This is unfortunate and ought to be discouraged. It is in the spirit of diversified though homogeneous contribution that the possible contribution of photogrammetry, and by extension that of this thesis, ought to be recognized.

1.2 Statement of the problem.

The importance of comprehensive RTA recording strategies cannot be overemphasized. It is on the strength of resultant

RTA analysis, that remedial steps in the form of traffic-management and/or -engineering can be adopted accordingly.

Throughout history, RTAs have occurred. And they will definitely continue to take place. Or are they caused? It has become routine practice over the ages to attempt to determine their cause(s). This is in line with efforts to establish the liability of such RTAs. The legal implications of this are well known (eg. insurance claims). Society has continued to rely upon the police in establishing the validity of such and other related claims. Unfortunately, however, in practically most developing countries, including Kenya, police officers even to this day still pace distances and measure with tapes in recording evidence at RTA scenes, much as was done elsewhere seventy years ago [eg. Salley, 1964].

The major drawback of the above practice is fourfold. Firstly, these measurements are often critical in determining the liability of RTAs. But it is difficult to adequately measure the site with a tape. This may further be aggravated if measurements were to be done under poor lighting conditions. Implicitly, the reliability and precision of such measurements is quite low, besides the approach being relatively subjective. Moreover, the susceptibility of blunders resulting is much more enhanced, especially given the apparently low training in measurement that these officers undergo. Ironically, measurements obtained from such procedures continue to be unsuspectingly recognized by law as foolproof!

Secondly, the time element is critical. This is because RTA victims must be cared for and damaged vehicles cleared off the roads for smooth traffic flow. Conventional RTA

reconstruction methods have tended to risk the occurrence of further RTAs. This is due to the impatience that they create on other road users. Indeed, the event of jams being created by traffic personnel in the course of execution of their work after RTAs, though avoidable, is quite common in this country.

Thirdly, due to the slow data acquisition methodology conventionally adopted, RTA related court cases by extension are bound to pend more, even for periods extending over many years. Unfortunately, as pointed out earlier on, most of the bereaved families do suffer untold economic difficulties upon demise of their loved ones. Hence, since "justice delayed is justice denied", existing poor RTA documentation methods do negatively add further to the detriment of the affected siblings.

Finally, the RTA analysis report is a very important piece of document. It is not only admissible to the courts of law but indeed takes precedence over any other form of evidence that may be adduced therein. Any slight distortion in this document may drastically influence the balance of unbiased judgement thereof [Quinn, 1979;1984]. However, the very nature of this document, especially that resulting from conventional RTA analysis, exposes it to criminal distortion. Some other form of evidence that is not easily susceptible to this alteration is thus better suited for RTA analysis.

From the foregoing, it is imperative that RTA reconstruction techniques that effectively address to the above shortcomings be adopted. Close range photogrammetry does offer desirable attributes which may conveniently be adopted in this respect [Robertson, 1990(a)]. Use has been made of stereo-metric cameras, especially in the developed world, in

order to achieve this [Ghosh, 1981]. This approach has however, received only lukewarm acceptance in most Third World countries. The main reasons for this, one would reasonably infer are; unawareness of the significant potentials of close range photogrammetry, prohibitive cost of the necessary equipments and scarcity of trained personnel.

It is an open secret that most police departments or even other personnel who deal with RTAs in developing countries are faced with severe lack of funds. Thus, much as they would like to keep abreast with these modern RTA analysis techniques, it is practically impossible for them to realise this.

Whereas on the one hand, it is obvious that RTA analysis techniques currently used in most developing countries fall short of expectation, it is hard reality that most of these countries cannot afford these modern expensive techniques. Indeed, most of the countries in this bracket would justify that there are other many pressing issues worth more urgent attention. There is therefore the need to develop an RTA analysis technique which, while on the one hand compares with those commonly used in developed countries, is also within reasonable financial reach of everybody; particularly to third world countries.

Over the last decade or so, a lot of research effort has been directed towards this end [eg. Abdel-Aziz, 1974; Faig, 1976; Adams, 1980 etc.]. Out of this has emerged the promising potential use of non-metric (or amateur) cameras. These are simple, hand-held (or otherwise), "off-the-shelf" cameras. Though not designed for photogrammetric purposes per se (in general they all lack fiducial marks), it has been established that highly

accurate results can be achieved through use of these cameras, provided that an appropriate analytical data reduction scheme is adopted. Moreover, apart from their general availability, non-metric cameras are also significantly cheaper than their metric counterparts. Nothing could be more encouraging.

To tackle some of the issues raised here-above, it is proposed in this thesis to empirically evaluate the extent to which non-metric cameras can be applied to RTA analysis in Kenya. It is further proposed to evaluate and adapt this technique to the solution of the local RTA problem. Specifically, this study sets out to demonstrate the effectiveness of the photogrammetric application of non-metric cameras for RTA reconstruction in Kenya. The main objectives inherent include the following:

1. To investigate into the RTA analysis methodology currently practiced in Kenya with a view to evaluating its merits and demerits.
2. To establish an efficient photogrammetric technique that could be adopted for RTA analysis in Kenya.
3. To devise a methodology that could speed up the RTA measuring process in the field with a view to ensuring a quick return to the normal flow of traffic and the speedy release of the RTA vehicles to their respective owners.
4. To design a permanent, and preferably admissible in court, high quality record of the RTA scene in the form of a photograph and/or stereo image. This should assist among others, the police as well as the legal and insurance professions.

Generally, it is necessary to fully understand and appreciate a problem before one embarks upon solving it. A

proper feeling of such a problem is required. The hypothesis of this thesis is that, techniques locally used for RTA reconstruction seem to have missed this point. Apparently, on a local framework, we seem not to have fully understood RTAs; why they occur, how they do so and further, why they occur where and when they do so. No wonder the undeterred escalating trend of RTAs prevalent in Kenya. It is hoped that by the end of this study an insight, however small, will have been obtained into the quest to curb RTAs in Kenya.

1.3 Organization of the report.

Contained in this section is a synopsis of the report content. Chapter 2 is an attempt to investigate into the RTA analysis methodology currently practiced in Kenya. Discussed herein are the objectives of RTA analysis, the RTA reporting and classification, the action which follows at the RTA scene, the processing, analysis and interpretation of resultant RTA documents and the expected accuracy of this methodology. As the main highlight of this chapter follows a listing of the advantages and disadvantages identified in this methodology.

Chapters 3 and 4 give an exposition on the theoretical analysis of the proposed RTA analyses methodology. In particular, chapter 3 discusses in depth the details of the Direct Linear Transformation (DLT) approach. This was used as the data reduction technique in the adoption of non-metric cameras for RTA analysis. In chapter 4 is discussed the two main sources of systematic errors in non-metric cameras; namely, lens distortion and film deformation. The different mathematical models that were used in modelling these error sources are also discussed.

The diverse aspects considered in the data acquisition are discussed in chapter 5. Contained therein is the design, fabrication and subsequent calibration of the control frame. Also, the different photographic configurations used and the measurement of the photocoordinates is given. Chapter 6 dwells mostly on the various resultant computations made and on the obtained results. A discussion of the obtained results is also outlined. The pertinent conclusions and recommendations are then pointed out in the final chapter 7.

1.4 Review of related literature.

1.4.1 Close-Range Photogrammetry.

Upon its discovery, close-range photogrammetry was exclusively used as a fast, economic and efficient system for topographic mapping. The non-topographic applications of this technique have since unprecedentedly, grown over the last two decades or so. Interestingly, the scope of application in this field continues to expand [Ayeni, 1985]. Some common non-topographic applications of close-range photogrammetry include; biostereometrics, accident investigations, archaeological studies, industrial applications, environmental studies, machine vision, and many other branches of science. It has been acknowledged that non-topographic applications of close-range photogrammetry in general, display a greater variety of problems and solutions due to availability of analogical, analytical and digital based photogrammetric instrumentation and also due to the size of the object, accessibility, accuracy, control points and so on [Simonsson, 1980].

Close-range photogrammetry was used in investigating Road Traffic Accidents (RTAs) as early as 1933 and 1935 in Switzerland and Germany respectively [Salley, 1964; Ghosh,

1981]. Since then this technique has successfully been applied in other parts of Europe, the United States and Japan. The amazing advantages in this method overwhelmingly justify its use. It is worth noting that in Japan for example, no RTA related court case, as a direct result of the use of this method, pends beyond one week after the RTA [Ghosh, 1981].

Photogrammetry in general and close-range photogrammetry in particular, has extensively been used in various studies wherein the ultimate goal has been to curb RTAs. The mapping of street intersections using close-range photogrammetry has been done in this spirit [Kobelin, 1976]. Close-range photogrammetry has also been identified as enabling several different traffic parameters to be covered in one study for example, traffic-speeds, -acceleration, -volumes, -flows and patterns, parking inventories etc [Garner and Uren, 1973]. Traffic flow studies have also been carried out in order to prevent RTAs and ease traffic congestion especially in this motorization era [Hashimoto and Murai, 1990].

In industry, photogrammetric techniques have been adopted in determining the optimum design of vehicles in view of existing road designs [Bruhn and Schneider, 1990]. The use of these methods in establishing the optimum driver eye height [Turpin and Lee, 1961] has been particularly apt. Faig et.al [1992] suggest a low investment and operational cost system for car collision investigation. The design of this photogrammetric system is based on the non-metric stereo-camera concept, and utilizes the enlarger-digitizer procedure. This is expected to provide essential information for the automobile design study and its monitoring.

From the foregoing, it is implicit that, close-range photogrammetry has found immense use in RTA analyses. The

main reason(s) for accepting this technique as the 'in-house' operational tool for RTA analysis stems from its inherent advantages. This method does possess some gorgeous prospects which may be exploited in this direction. Several authors have dwelt on this satisfactorily [eg. Abdel-Aziz, 1974; Karara and Faig, 1980; Robertson, 1990(a)]. The saying that "a picture is worth a thousand words" is reflective of this [Shortis, 1983]. The advantages of photogrammetry have also enabled this method coupled with image processing to be further adopted in evaluating aircraft accidents and occurrences [Robertson, 1990(a)].

After an RTA has occurred, the police officer is usually under great pressure to record accurately and rapidly the scene of the RTA so as to facilitate the speedy restoration of normal traffic flow. Close-range photogrammetry has been used in the developed world by the police to accomplish this important money and life saving task. In order to specifically address to this work, there has thus arisen the need to develop the required equipment. To this end, universal stereo metric systems have been designed [Schernhorst; Karara, 1967]. Additional new instrumentation for RTA analysis has also been suggested [Robertson, 1990(b)]. The need for stereometric investigations in RTAs was empirically ascertained by Lillesand and Clapp [1971]. In general, when compared with conventional RTA analysis techniques, this method was found to significantly improve the collection, accuracy, preservation, and the presentation of metric accident data.

1.4.2 RTA analysis in Kenya.

The rampant, undeterred trend of RTAs in Kenya has caught the grim concern of many a citizen. As a result, local RTAs

have and still do demand a lot of research if a successful attempt is to be made in understanding them. Agoki [1988] discusses the fundamental characteristics and causal factors related to local RTA occurrence. He also develops predictive models for Kenya at both the macro and micro levels. This is hopefully expected to be used in the monitoring of RTAs and the performance of road safety improvement programmes and also to facilitate a proper understanding of the behavior of RTAs in relation to road design elements. Various other researchers have also studied local RTA trends and implications [eg. Kwamina et.al; Miyanji, 1976; Maina, 1978; Mang'oli, 1979 etc].

Putting forward the premise that; in order to solve any particular problem one needs to have an in-depth understanding of it, then one is tempted to relate the high RTA trend prevalent in Kenya to the lack of respect for this observation. Seemingly, on a local framework we have not yet fully understood RTAs. Methods used for RTA analysis seem to attest to this. Local police officers still pace distances and measure with tapes in recording evidence at RTA scenes much as was done elsewhere seventy years ago [Salley, 1964].

1.4.3 Non-metric cameras and their use in RTA analysis.

In recent years, a lot of research effort has been directed towards enhancing the accuracy and reliability of close-range photogrammetric techniques [eg. Kenefick, 1971; Hottier, 1976; Bopp and Krauss, 1978; Fraser, 1980; Torlegard, 1981; Kubik and Merchant, 1987; Faig et.al., 1990 etc]. Resultant from these is that quantitative evidence obtained from photographs is now regarded as evidence of great weight. Indeed, the admissibility in court of photogrammetric products is no longer doubtful for

"pictures don't lie" [Quinn, 1979; 1984].

It is interesting to note that poor RTA analysis techniques initially adopted in developing countries have not been altered. This is in spite of the conspicuously desirable attributes that have become associated with the use of modern approaches. There has arisen therefore, the practical need to develop alternative RTA analysis procedures which, while their accuracy compares with that of already developed modern methods, are also financially within reach. The realization of the potential in non-metric cameras has been achieved in this perspective.

Non-metric or simple cameras unlike their metric counterparts are endowed with desirable attributes such as, flexibility in focussing, high resolution, general availability and low prices. Invigorated studies on the potentials and use of non-metric cameras have been widely done [eg. Abdel-Aziz, 1974; Kolbl, Faig, 1976; Adams, Murai et.al; Karara and Faig, 1980; Hartzopoulos, 1985]. Out of these studies has emerged the same consensus that, "non-metric cameras can now be conveniently used in cases initially thought only possible via the use of metric cameras". This has led to their ever-increasing use in virtually all fields of non-topographic photogrammetry. The stand that it's "metric or none" which had been upheld and adhered to rather conservatively, does not "hold water" any more [Karara and Faig, 1980].

However, there is a small price to be paid. Successful use of non-metric cameras does necessitate use of efficient analytical data reduction schemes. Among the algorithms developed for data reduction of non-metric photogrammetry are the Direct Linear Transformation (DLT) developed at the University of Illinois [Abdel-Aziz and Karara, 1971], the

11-parameter solution [Bopp and Krauss, 1978], and a simplified version of the 11-parameter solution [Adams, 1980]. Calibration of a non-metric camera is also more demanding than that for a metric camera. Two calibration approaches have successfully being identified and used for non-metric cameras namely; On-the-job-calibration [Zolfaghari, Salmenpera, 1980; Murai et.al, 1984] and Self-calibration [Kenefick et.al, 1972; Mutfurglu and Aytac, 1980; Ghosh et.al, 1990].

The revelation of the immense potentials in non-metric cameras is bound to appeal to, and interest many photogrammetrists and non-photogrammetric users. Karara [1985], rightly predicts an insurgence into the adoption and use of photogrammetry as an invaluable tool for measurement purposes. It is also observed that pertinent studies in RTA analysis are bound to increase as a result of the use of affordable non-metric cameras [Waldhausl and Kager, 1984]. Attempts have successfully been made to draw close-range photogrammetry closer to the "people".

2.1 Objectives of RTA analysis.

In Kenya, the mandate to investigate into road traffic accidents (RTAs) falls wholly on the auspices of the Kenya Police. They are the personnel charged with the responsibility of establishing the cause of any RTA and prosecuting appropriate persons, if need be. The objectives of RTA analysis from the perspective of the police, includes;

1. to ascertain the cause,
2. to prevent re-occurrence, and
3. to prosecute persons who are primarily responsible.

In order to address to these objectives adequately, it is necessary that the investigating officers make certain measurements at the scenes of RTAs. Often, it is on the strength of these measurements that relevant persons are charged in the law courts. Therefore, in order for proper and correct court verdicts to be arrived at, it is imperative that the concerned police officers make an impartial recording and analysis at any one RTA scene.

2.2 RTA reporting and classification.

RTA national statistics though alarming do not reveal the full extent of the problem; last year (1991), 2216 RTA fatal cases were reported. These are based on details of personal injury RTAs reported to the police and recorded on the Traffic Department Accident Report form known as FP41 (see Fig 2.1). The information required for the completion of this form is relatively comprehensive. This form seeks to establish details pertinent to the circumstances, the vehicles involved and the casualties. There is, however, no

general requirement in Kenya for RTAs to be reported to the police.

A comparison in the UK of hospital and police records [Atkinson, 1990], estimated that one-third of slight, and one-sixth of serious injuries had arisen in unreported RTAs. The extent of under-reporting was found to depend on the category of road user involved. Injuries to car occupants were under-reported by 14%, pedestrians by about 27% and pedal cyclists by about 60%. From these figures it seems probable that there is greater under-reporting of RTAs involving slight injury. The position in Kenya could not be any different.

Furthermore, the information available for those RTAs that are reported is, for various reasons, frequently incomplete. Often the police have to rely on the goodwill of eye-witnesses. But unfortunately, most of the eye-witnesses often do not want to volunteer complete evidence for fear of resultant legal complications. Moreover, the investigating officer may not have attended the scene and may not have details of vehicles or others involved, and may be vague about the RTA location. The apparent accuracy that may be needed to specify location of RTAs often is spurious in many cases. Inaccuracies are more likely to occur in rural areas where the number of identifying features available to assist the description of the accident unambiguously will generally be far fewer than in built-up regions.

Classification of the severity of the RTA is also recorded by the police on the FP41 form. This is logically determined by the severity of the most seriously injured casualty involved, either slight, serious or fatal, using the following criteria:

- a) Slight injury - an injury of a minor character such as a sprain, bruise, cut or laceration not judged to be severe, or slight shock requiring roadside attention.
- b) Serious injury - an injury for which a person is detained in hospital as an 'in-patient', or any of the following injuries whether or not detention results: fractures, concussion, internal injuries, crushings, severe cuts and lacerations, severe general shock requiring medical treatment, injuries causing death 30 or more days after the RTA.
- c) Fatal - death from injuries sustained, resulting less than 30 days after the RTA.

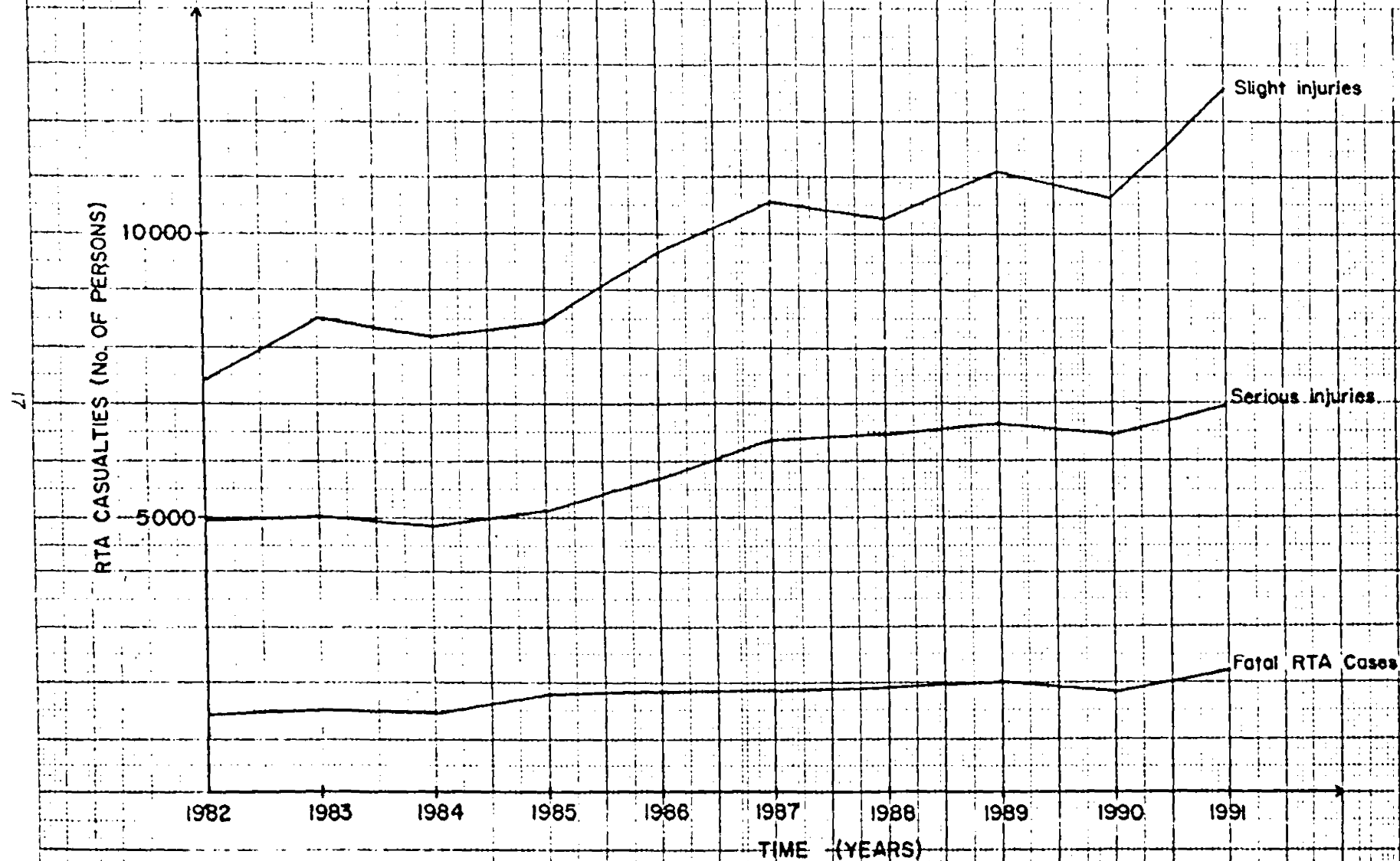
Table 2.1 portrays the classification of RTAs in Kenya over the last decade while Fig 2.2 is a graphical representation of the same [The Kenya Police RTA Statistics, 1992].

Table 2.1 Classification of RTAs in Kenya over the last decade.

Year	Fatal RTA	Serious injuries	Slight injuries	Total
1982	1462	4978	7400	13840
1983	1515	5017	8509	15041
1984	1490	4856	8220	14566
1985	1800	5113	8476	15389
1986	1832	5701	9676	17209
1987	1889	6385	10540	18814
1988	1919	6460	10280	18659
1989	2014	6650	11094	19758
1990	1856	6455	10619	18930
1991	2216	6958	12546	21720

An injured casualty is coded by the police as "seriously" or "slightly" injured on the basis of information

FIG. 2.2 GRAPHICAL REPRESENTATION OF RTA CLASSIFICATION IN KENYA OVER THE LAST DECADE



available within a short time after the RTA. This generally will not include the results of a medical examination, but may include the fact of being detained in hospital. Death within 30 days should subsequently be notified to the police and the FP41 record amended as necessary. However, awareness of changes between "slight" and "serious" classification is much less likely, in which case, if a case is suspected as being "serious" though it appears "slight", then it should be recorded as "serious".

There is little that one can do to rectify, retrospectively, these shortcomings in existing data. It is therefore only prudent that the shortcomings and limitations in RTA data be clearly borne in mind and allowance made for them wherever possible.

2.3 Action at the scene of a road traffic accident.

2.3.1 Personnel and equipment required.

On receiving the report of a RTA the police officer records the name and address of the person reporting the accident. All RTAs reported to the police are supposed, under the law, to be entered into the accident register of the police station concerned. Ideally the RTA scene should be visited promptly.

Before leaving the police station or before visiting the scene, the police officer should remember to carry with him sufficient equipment to enable him to deal with the RTA without undue difficulties. Mentioned here-under are some of the things which are often included;

1. A light hard board on which to write.
2. Statement forms or writing papers which can be used for recording statements at the scene and drawing

sketch plans.

3. Pieces of water proof chalk which can be used to mark on the tarmac surface during wet weather.
4. A pen and a pencil (a pencil can be used when it is raining).
5. A tape measure, often 30 metres long.
6. Traffic signs eg. "ACCIDENT AHEAD", Blinking or flashing lights.

It is important that the investigating officer be accompanied by other police officers who could help him in diverting traffic at the scene. Maximum care is usually taken to prevent the re-occurrence of more accidents at the scene.

On arrival at the scene the investigating officer is supposed to first of all attend to the injured persons and arrange for them to be removed to hospital. Where possible the officer could cautiously apply first aid on the casualties.

On busy roads or streets when there is an RTA it is likely for vehicles to form a jam. If it is possible, traffic should be diverted when the sketch plan is being drawn or measurements are being taken. After marking the positions of vehicles and any other relevant objects, these can be removed and the road be cleared.

Where there is possibility of prosecuting any of the involved drivers, or when there is injury, or a Government vehicle is involved, a sketch plan must be taken. In addition, when the RTA is serious or likely to amount to a fatal case, photographs must also be taken.

The investigating officer should look for witnesses and if

possible record their statements.

2.3.2 Handling of the vehicles involved in the RTA.

If an expert is available he should check on the condition of the vehicles at the scene. If not, they should not be interfered with before they are inspected. A police officer has power to detain vehicles involved in a RTA for the purpose of inspecting or cause them to be inspected. This is laid down under section 105(1) of the Traffic Act, which states that; "It shall be lawful for any police officer in uniform to stop any vehicle, and for any police officer, licensing officer or inspector

- a) to enter any vehicle;
- b) to drive any vehicle or cause any vehicle to be driven;
- c) upon reasonable suspicion of any offence under this Act, to order and require the owner of any vehicle to bring the vehicle to him,

for the purpose of carrying out any examination and test of any vehicle with a view to ascertaining whether the provisions of this Act are being complied with or with a view to ascertaining whether any vehicle is being used in contravention of this act".

When there is no evidence of prosecuting any of the involved drivers and that there are no injuries and the damage to the vehicles is negligible, the vehicle owners or drivers can be referred to civil remedy (this cannot apply to Government vehicles as these are not insured). The investigating officer(s) could be called upon by the concerned parties to arbitrate between them.

Scientific assistance is of great value when the accident is

"HIT AND RUN". Scenes of crime personnel should be called in such a case. It is important that the nearest relatives of the persons killed or taken to hospital are informed.

2.3.3 Sketch Plan Drawing.

The necessity for this arises whenever in an RTA a person is injured whether slightly or seriously, or a Government vehicle is involved, or there is possibility of prosecuting one or more drivers involved in the RTA whether there is injury or not.

On arrival at the RTA scene a police officer should take measurements and draw a rough sketch plan whether the scene has been disturbed or not. The purpose of drawing the sketch plan is to present the picture of the RTA scene in an abstract manner. The RTA sketch plan is a most valuable tool, since it indicates graphically the nature of the RTA record at any particular location (see Fig. 2.3). This plan usually shows by arrow indications the movements which led to each RTA.

At the RTA scene the investigating officer chooses two or more fixed points and then constructs a baseline on which all the measurements are to be based eg. the shortest distance from the object to the baseline from the rear / front corners of the vehicle(s). The fixed points should be permanent in such a way as to enable the investigating officer(s) to pin-point where the vehicles and any other objects were, should it be necessary for such an officer to go back to the RTA scene and explain to the court how he/she drew the sketch plan.

In many instances it becomes desirable to supplement the sketch plans / collision diagrams with a scaled drawing or

photographs illustrating the location of road signs and markings, pedestrian crossings, traffic signals, bus stops, parking locations, slight obstructions, fronting land use etc. This is most useful for it could clarify whether or not physical features did influence the RTA experience.

2.3.4 Measurements made at the RTA scene.

Several particular measurements are usually made at the RTA scene. Some of these include;

1. width of the road surface,
2. width of the pavement, footpaths etc.,
3. track marks, skid marks, braking impressions,
4. positions of the vehicles and the directions they were facing after the RTA,
5. dimensions of the vehicles,
6. broken glasses, dry mud from the collision and any other debris,
7. road directions, and the
8. markings of the road traffic signs.

All these measurements should be checked in order to reduce the possibility of errors. The weather conditions and the state of the road should also be included.

Care should be taken regarding the track marks. These should be dealt with as soon as possible after the RTA and before the vehicles are removed from the scene. The reason for this is in order to avoid uncertainty as to the vehicle which made them. Where opportunity presents itself the treads of the tyres should be compared with the road tracks.

2.3.5 Skid marks and Braking impressions.

It is important that the terms "skid marks" and "braking

impressions be distinguished and used in their proper senses. A skid mark is caused by various circumstances, but often, it can be attributed to lack of observation on the part of the driver for example, in failing to notice a dangerous road surface or bad driving. The tyre condition does of course play an important role in connection with braking. A tyre that has worn smooth will not exert the same grip on the road surface as one which has reasonable amount of tread.

Some common causes of skid marks include;

1. rapid acceleration on a greasy surface,
2. hitting an object and subsequently diverting from the proper course, and
3. mechanical failure.

There are two types of skid marks, which could result from;

1. locking of wheels by braking which usually leaves behind continuous heavy marks along the road surface, or
2. wheels sliding sideways due to high speeds or rapid acceleration especially around corners. In such cases the markings are always wide. In addition, where the vehicle has been driven at a high speed round the corner, the wheels which are on the outside are bound to make heavier indications because of the weight transferred to them.

The difference between the skid marks and braking impressions is that the latter form a distorted impression on the tyre tread which has been transmitted to the road surface. In a normal two-wheel drive vehicle, when brakes are applied heavily, more weight goes to the front wheels to make heavier marks than the rear ones. Infact, sometimes the

rear wheels lock completely and make skid marks over brake impressions made by the front wheels which are revolving. It is imperative therefore, that the investigating officer(s) examine the marks carefully before coming to any conclusion. Although everything at the scene should be included in the sketch plan, it should not be defined that where there is broken glass is a point of impact. The decisions must be left to the court, [eg. Nzioka vs. Republic CR.App.No. 429/1972 High Court of Kenya].

2.4 Processing of RTA documents.

Care should be taken to ensure that all the required information is documented before leaving the RTA scene. Also, it is critical that the well specified procedures and methodology for data collection at the RTA scene be adhered to. This is necessary because it might not always be possible, though it is desirable, for the same investigating officer at the RTA scene to compile the police report.

A traffic police file should be opened for the RTA depending on it's injury nature as discussed in section 2.3.3. The FP41 police form should be properly filled and cross-checked. Any doubtful or contradictory evidence should be verified apriori. A fair copy of the sketch plan is then drawn and together with the draft copy is included in the police file. Any photographs, in case of fatal RTAs, are also supposed to be included in the respective police files. Statements from driver(s), casualties and any witnesses should be recorded. In this respect an objective strategy should be adopted. Any other relevant documents eg. P3 forms, should also be recorded and all the above included in the traffic file. Then finally, the investigating officer should on the strength of one's experience and training, state ones's view as to who was primarily responsible for

the RTA. Although the investigating officer's opinion is to be professionally respected, the court is under no legal obligation whatsoever, to accept the former's view. Rather, the court is supposed to draw its own ruling based solely on its interpretation of the RTA documents contained in any such police file.

These and many other reasons make the RTA police file highly confidential. The author established that locally, the RTA police files generally required between 2 weeks up to 1 year or even more for complete compilation depending on the state of the RTA casualties. Upon compilation of the RTA file and summoning of all witnesses, in liaison with the police, the court then fixes dates for hearing. It is interesting to note that insurance firms often liaise with the police systematically if they have an interest in any RTA case.

2.5 Analysis and Interpretation of RTA documents.

A fair and impartial analysis of RTAs is a very onerous task. It ideally requires the presence of the investigating officer at the RTA scene at the time of the accident. More often-than-not however, the investigating officer is not present at the scene at the time of the RTA occurrence. Rather, he/she is expected by law to report at the RTA scene promptly upon report of any RTA which falls under his/her jurisdiction.

After reporting to the RTA scene, the investigating officer is expected to collect all physical evidence through the necessary measurements. He/she should then proceed on to collect evidence from any eye-witnesses. Care should be taken to ensure impartiality from the eye-witnesses. Perhaps a random sampling of these could be taken. Important site features eg. road signs, sharp bends etc. should also be

taken note of. Naturally, it is expected that before leaving the RTA scene the investigating officer has developed some tentative opinion as to the RTA cause.

Back at the office, after thorough assessment of the recorded site features, physical evidence recorded at the scene eg. sketch plans, and a study of witness statements, the investigating officer should be in a suitable position to point out at the RTA cause. Proper reasons should be forwarded, if necessary, justifying the officers "reasoning" to account for any conclusions made. In this respect, usually the officer's training and experience comes in handy.

It is worth noting that the investigating officer's findings should be authenticated up the steps of hierarchy in the traffic police ranks up to the Division Traffic Officer (DTO). What is forwarded to the courts of law becomes indeed, the official position of the state in as far as any RTA case is concerned.

Serious RTAs may perhaps need to be studied more elaborately. Specialized police RTA investigation units comprising senior police officers are usually involved in this. It is entirely upon the police findings that charges may be preferred against any person(s) suspected of causing any RTA. The type of charge preferred may vary from civil libel to criminal prosecution.

In the court the prosecutor (state counsel) is expected to portray the State's official position while highlighting the police findings. The judge is supposed to give the court's verdict in any such RTA case and ideally does not need to subscribe to the State's view. In some cases it does become necessary for the courts to actually visit the RTA scene to

verify any ambiguity in the RTA documents.

It is important to note that, not only are RTA records useful for fair dissemination of justice, but they are also indispensable tools for traffic management. It is only after patiently collecting and objectively analyzing RTA records that the traffic engineer can determine whether or not remedial / corrective measures are within his/her scope. This therefore, goes on to stress at the immense care that should be taken when analyzing and interpreting RTA documents. It also goes on to point out at the highly important job that the police are entrusted with.

2.6 Expected accuracy of current methodology.

Assessing the accuracy that could be derived from the RTA police documents is a very challenging task. This is basically because this involves evidence which greatly varies in dimension, nature and also in depth; varying from sketch plans to witness statements. Moreover, in some cases it might result that the statements from different eye-witnesses, for example, conflict if not contradict.

In the local scenario studied, it was realized that measurements were made to the nearest inch. This would have suggested a suitable plotting scale of about 1/100 [Highway Capacity Manual, 1965]. However, to complicate the matter "sketch plans" are not drawn to scale under the present local practice. Basing his arguments on the random checks that the author made, the resulting sketch could not be drawn to a scale any better than about 1/500. This suggests that no measurements better than 5 inches in accuracy could be deciphered from the sketch plan, were it to be drawn to scale.

It is the author's opinion that the present practice did initially cater for some accuracy element for example, measurements been taken to the nearest one inch. However, with time most probably due to the high RTA phenomenon resulting in extra work burden, this initial accuracy aspect was shelved, from whence sketch plans were drawn totally ignorant of scale. Indeed, it is also the author's strong conviction that erroneous court verdicts must have been, at one or more times, made as a result of this inept practice.

2.7 Advantages and Disadvantages of RTA analysis

Methodology Used in Kenya.

Though the current RTA analysis methodology used in Kenya is understandably good, the author did recognize several flaws in this practice. It is interesting to note that all these and other conclusions were arrived at upon the author accompanying different traffic officers at Buru Buru- and Kasarani- Divisional Police Headquarters to about 50 RTA scenes at random times. This randomness does of course support the argument that these observations made here-under, portray the current practice reasonably well.

2.7.1 Disadvantages.

1. The current RTA analysis methodology practiced in Kenya is quite time consuming. A lot of time is lost in taking various measurements and in drawing the required sketch plan. As expected, emanating from these are delays and jams which further present a suitable environment for the re-occurrence of more RTAs. It appears that this initial delay sparks off further ones inevitably ending up in court delays. The author observed that RTA related court cases pend from six months up to two or more years in Kenya. It was also

established that on average the time required for RTA data collection was between 30 minutes and 3 hours.

2. From a survey point of view, in a 2-D network, a minimum of two fixed points are required to overcome the 4 datum defects present viz., 2 translation, 1 scale and 1 rotation. This is incidentally, what the investigating officers are required to do as per the Traffic Act. However, this is not adhered to in practice. As the author observed in virtually all the field trips he went to, only one fixed point was taken. The meaning of this from a survey perspective is that there either resulted a singular situation or a non-unique one thereof. In defense, upon query, the traffic officers upheld that they did this due to lack of time and that it was also "acceptable".
3. "Sketch plans" are not drawn to scale. Therefore, no reliable evidence can confidently be derived therefrom although these are religiously treated as foolproof in our courts of law. In the author's view, this is done by the traffic officers in order to exonerate themselves from liabilities in case of erroneous measurements. In addition it was observed that no caution whatsoever was given on the fairly copied sketch plans eg. "sketch not to scale".
4. The susceptibility of committing blunders is high. This is further compounded by the fact that most RTAs are recorded under poor lighting conditions. Ironically, no field techniques are used to re-check any measurements made. Furthermore, due to the pressure of making the RTA measurements as quickly as possible, the probability of the police inadvertently omitting some of the required measurements (as discussed in section 2.3.4) is significant.
5. There is lack of indication of the general direction

(eg. North) on the sketch even if not drawn to scale. This insertion could perhaps provide a more descriptive scenario at any RTA scene.

6. It was noted by the author during the many trips he made that no rigorous steps were taken in order to ensure that off-sets were correctly taken from a survey view point.

2.7.2 Advantages.

However, the current RTA analysis methodology locally practiced was observed to have some desirable attributes. Some of these include;

1. It is cheap.
2. It is relatively easy to train new personnel to the practice.
3. By recording evidence from eye-witnesses this approach enables the provision of some sort of independent check.
4. Although done from an ignorant point of view, measurements were recorded to the nearest 1 inch (no technical reason was given for this). This incidentally, is quite ideal if the sketch plans were to be drawn at a desirable scale of 1/100. According to the author such a scale would be generally ideal.
5. The current practice is also labour intensive as ideally only three traffic officers are required. However, the author observed that in all the times he accompanied the officers to the different RTA scenes only a maximum of two officers were present and on two occasions only one!

2.7.3 Discussion.

In light of the above advantages and disadvantages

identified in the current RTA analysis methodology, two points are to be noted. Firstly, it is fitting to congratulate the local traffic police force for the tremendous job that they have done and continue to do, despite many unfavorable conditions.

The major problems that the author identified was the lack of efficient mobility and insufficient personnel. In the divisional headquarters that the author was stationed only one vehicle was on "stand-by" for traffic duties. Therefore, the same officers were required to attend to multi-RTAs as these tended to occur more-or-less at the same times - peak hours. Lack of enough personnel results in overworking the skeleton staff present which has the long term effect of demoralizing them.

Secondly, from a technical point of view the current practice is questionable. The kind and accuracy of measurements made, the time required for this, and the sketch plans drawn therefrom, raise a lot of doubts. This does therefore, necessitate the need for alternative efficient, economic approaches to the same problem. However, it should be encouraged that any such alternative solution ought to be tailored to the local requirements.

CHAPTER 3. THE DIRECT LINEAR TRANSFORMATION (DLT).

The absence of fiducial marks in non-metric cameras did over many years inhibit their use in photogrammetry. However, with the development of the Direct Linear Transformation approach in 1971 a major breakthrough was realised. This facilitated a direct transformation from the comparator coordinate system into the object space coordinate system. The presence, or absence, of fiducial marks was there-after rendered insignificant as the coordinates in the image system were no longer mandatory.

In this chapter is presented the mathematical formulation and basis of the Direct Linear Transformation approach.

Normally in analytical photogrammetry the required measurements of the image points are carried out on a comparator. Subsequently, the transformation from the comparator coordinates system to the desired object coordinates system is conveniently done in two steps:

- a) Transformation from comparator coordinates system to image / plate coordinates system with the origin at the principal point.
- b) Transformation from image coordinates system into object-space coordinates system.

3.1 Transformation from Comparator Coordinates System into Image Coordinates System.

Coordinates from a photograph are usually measured using a comparator. Often, for correction of the various systematic errors inherent, it is mathematically convenient to have these coordinates referred to the principal point in an image coordinate system. It is therefore necessary to transform the observed comparator coordinates to equivalent

image coordinates. The transformation of the comparator coordinates into image coordinates has conventionally been done in the following manner:

$$\bar{x} - \bar{x}_0 = a_1 + a_2 x + a_3 y \quad (3.1.1)$$

$$\bar{y} - \bar{y}_0 = a_4 + a_5 x + a_6 y \quad (3.1.2)$$

where:

\bar{x}, \bar{y} are the image coordinates referred to image coordinates system.

\bar{x}_0, \bar{y}_0 are the coordinates of the principal point referred to image coordinates system.

x, y are the image coordinates referred to comparator coordinates system.

a_1, a_2, \dots, a_6 are affine transformation constants.

Using matrix notation Equations (3.1.1) and (3.1.2) can be rewritten as:

$$\begin{bmatrix} x \\ y \end{bmatrix} = \begin{bmatrix} a_1 \\ a_4 \end{bmatrix} + \begin{bmatrix} a_2 & a_3 \\ a_5 & a_6 \end{bmatrix} \begin{bmatrix} x \\ y \end{bmatrix} \quad (3.1.3)$$

after taking

$$x = \bar{x} - \bar{x}_0$$

$$y = \bar{y} - \bar{y}_0$$

The above equations represent the two-dimensional affine coordinate transformation model. This model accommodates for two different scale factors along x and y axes and takes into account possible errors of non-perpendicularity in the comparator axes.

From equations (3.1.1) and (3.1.2) there results 8 unknowns in two equations. Thus the coordinates of a minimum of four

points need to be known in both the comparator and the image coordinate systems for subsequent transformation(s). In metric cameras the above corrections are usually applied by using the known (calibrated) coordinates of four or more fiducial marks.

However, in non-metric cameras there are no fiducial marks. The absence of these marks in non-metric cameras makes it difficult to apply such corrections. Incidentally, however, since this model accounts for film shrinkage (see section 4.4) which one expects to be quite significant in non-metric cameras, it has to be incorporated in somehow.

3.2 Transformation from Image Coordinates System to Object-Space Coordinates System.

A basic problem in photogrammetry is the transformation of the observed image coordinates to their equivalent object-space coordinates. The observed image coordinates could be in any one plate system. Similarly, the desired object-space coordinates could be in some object coordinate system. Solution of this basic problem is realised if and when a suitable mathematical relationship is formulated relating both the image coordinates and their corresponding object-space coordinates.

The collinearity condition equation expresses the relationship between image coordinates system and object-space coordinates system. This equation expresses the central projection of a point from three or two-dimensional object-space onto a two-dimensional image space and vice-versa. It expresses the fact that in a perspective projection the image point, the center of projection, and the corresponding object point all lie on one straight line.

Thus, given the image point- and projection center-coordinates the corresponding object point coordinates may be determined after invoking the collinearity principle. Often, collinearity equations are used in analytical photogrammetry as a universal approach for expressing the relationship between the correct image coordinates and the object-space coordinates. This relationship is mathematically expressed in the form:

$$\begin{bmatrix} \bar{x}_l - \bar{x}_o \\ \bar{y}_l - \bar{y}_o \\ -c \end{bmatrix} = \lambda_l \begin{bmatrix} m_{11} & m_{12} & m_{13} \\ m_{21} & m_{22} & m_{23} \\ m_{31} & m_{32} & m_{33} \end{bmatrix} \begin{bmatrix} X_l - X_o \\ Y_l - Y_o \\ Z_l - Z_o \end{bmatrix} \quad (3.2.1)$$

where:

\bar{x}_l, \bar{y}_l are the image coordinates of any point i

\bar{x}_o, \bar{y}_o are the coordinates of the principal point relative to image (fiducial axes) coordinate system

X_l, Y_l, Z_l are the object-space coordinates of point i

c is the camera constant

λ_l is a scale factor which has different values for different points

X_o, Y_o, Z_o are the object-space coordinates of the exposure station

$m_{l,j}$'s are the coefficients of transformation.

Implicit in these are the angular elements of exterior orientation; say ω, ϕ, κ .

Equation (3.2.1) can alternatively be put in the following form:

$$\bar{x}_l - \bar{x}_0 = -c \frac{m_{11}(X_l - X_0) + m_{12}(Y_l - Y_0) + m_{13}(Z_l - Z_0)}{m_{31}(X_l - X_0) + m_{32}(Y_l - Y_0) + m_{33}(Z_l - Z_0)} \quad (3.2.2)$$

$$\bar{y}_l - \bar{y}_0 = -c \frac{m_{21}(X_l - X_0) + m_{22}(Y_l - Y_0) + m_{23}(Z_l - Z_0)}{m_{31}(X_l - X_0) + m_{32}(Y_l - Y_0) + m_{33}(Z_l - Z_0)} \quad (3.2.3)$$

The relationship between (\bar{x}_l, \bar{y}_l) and (X_l, Y_l, Z_l) can be determined if the coefficients in the above two equations (3.2.2) and (3.2.3) are known. These coefficients are the inner orientation parameters $(\bar{x}_0, \bar{y}_0, c)$, the object space coordinates of the exposure station (X_0, Y_0, Z_0) , and the implicit three orientation angles (ω, ϕ, κ) which define the elements of the rotation matrix with coefficients m_{ij} 's.

Equations (3.2.2) and (3.2.3) are non-linear for the above coefficients. In order to obtain the values of these coefficients one has to have initial approximate values for these. Linearization of these two equations can then be performed about their approximate values using Taylor's series expansion. The solution is obtained by iterating accordingly until the corrections to the coefficients become very small and can be neglected.

The possibility of having a solution and the number of iterations necessary depends on the closeness of the initial approximate values of the coefficients to the corresponding true values and the geometric validity of the model.

The number of unknowns in the above two equations (3.2.2) and (3.2.3) is nine, if the inner orientation parameters $(\bar{x}_0, \bar{y}_0, \text{and } c)$ are unknown, or six if they are known. The number of unknowns dictates the minimum number of control

points needed to be observed in both the image- and object-coordinate systems to barely solve for the unknowns.

3.3 The Direct Linear Transformation (DLT) from Comparator Coordinates System to the Object Coordinates System.

The above two transformations (comparator-to-image and image-to-object-space) can be combined into one linear transformation. This transformation expresses a linear transformation directly from comparator coordinates system into object-space coordinates system without passing through the intermediate image coordinate system.

Normally, fiducial marks define the image coordinate system axes. The absence of these and/or other marks renders the definition of the image coordinate system technically impossible. It would thus be a token opportunity for restitution systems without fiducial marks if this direct transformation were possible.

Substituting the values of $(\bar{x}_l - \bar{x}_o)$ and $(\bar{y}_l - \bar{y}_o)$ from equations (3.1.1) and (3.1.2) into equations (3.2.2) and (3.2.3) respectively one gets:

$$\begin{aligned}
 a_1 + a_2 x_l + a_3 y_l &= \\
 -c \frac{m_{11}(X_l - X_o) + m_{12}(Y_l - Y_o) + m_{13}(Z_l - Z_o)}{m_{31}(X_l - X_o) + m_{32}(Y_l - Y_o) + m_{33}(Z_l - Z_o)} & \quad (3.3.1)
 \end{aligned}$$

$$\begin{aligned}
 a_4 + a_5 x_l + a_6 y_l &= \\
 -c \frac{m_{21}(X_l - X_o) + m_{22}(Y_l - Y_o) + m_{23}(Z_l - Z_o)}{m_{31}(X_l - X_o) + m_{32}(Y_l - Y_o) + m_{33}(Z_l - Z_o)} & \quad (3.3.2)
 \end{aligned}$$

After simplification and grouping (as discussed in Appendix

A) the above two equations can be put in the form:

$$x_l + \frac{L_{1l}X + L_{2l}Y + L_{3l}Z + L_{4l}}{L_{9l}X + L_{10l}Y + L_{11l}Z + 1} = 0 \quad (3.3.3)$$

$$y_l + \frac{L_{5l}X + L_{6l}Y + L_{7l}Z + L_{8l}}{L_{9l}X + L_{10l}Y + L_{11l}Z + 1} = 0 \quad (3.3.4)$$

The above two equations take the following linearized form:

$$x_l + L_{1l}X + L_{2l}Y + L_{3l}Z + L_{4l} + L_{9l}xX + L_{10l}xY + L_{11l}xZ = 0 \quad (3.3.5)$$

$$y_l + L_{5l}X + L_{6l}Y + L_{7l}Z + L_{8l} + L_{9l}yX + L_{10l}yY + L_{11l}yZ = 0 \quad (3.3.6)$$

These two equations are used as the basis for the DLT and are similar to equations used in optics for the transformation between three-dimensional space to two-dimensional space.

3.4 The Mathematical Model of DLT Considering Random and Systematic Errors in the Image Coordinates.

In the previous sections (\bar{x}, \bar{y}) were considered as image coordinates free from any systematic and/or random error. However, the measured image coordinates are subject to two kinds of errors: random errors of the point i (V_{x_i} and V_{y_i}) and systematic errors inherent in the j th photograph (Δx_j and Δy_j). The relationship between $(\bar{x}$ and $\bar{y})$ and (x, y) can empirically be written in the form:

$$\bar{x}_l = x_l + \Delta x_j + Vx_l \quad (3.4.1)$$

$$\bar{y}_l = y_l + \Delta y_j + Vy_l \quad (3.4.2)$$

Substituting the above formulae (3.4.1) and (3.4.2) into equations (3.3.5) and (3.3.6) one gets:

$$(x_l + Vx_l + \Delta x_j)(L_{9l} X + L_{10l} Y + L_{11l} Z + 1) + L_{1l} X + L_{2l} Y + L_{3l} Z + L_{4l} = 0 \quad (3.4.3)$$

$$(y_l + Vy_l + \Delta y_j)(L_{5l} X + L_{6l} Y + L_{7l} Z + 1) + L_{5l} X + L_{6l} Y + L_{7l} Z + L_{8l} = 0 \quad (3.4.4)$$

The linearized form of the above equations takes this form:

$$AV_{xl} + A\Delta x_j + x_l + L_{1l} X + L_{2l} Y + L_{3l} Z + L_{4l} + L_{9l} x X + L_{10l} x Y + L_{11l} x Z = 0 \quad (3.4.5)$$

$$AV_{yl} + A\Delta y_j + y_l + L_{5l} X + L_{6l} Y + L_{7l} Z + L_{8l} + L_{9l} y X + L_{10l} y Y + L_{11l} y Z = 0 \quad (3.4.6)$$

where

$$A = L_{9l} X + L_{10l} Y + L_{11l} Z + 1 \quad (3.4.7)$$

L_1, L_2, \dots, L_{11} are the DLT parameters.

Several mathematical models have been used for Δx and Δy to represent the systematic components of the errors caused by film deformation and lens distortion. These are discussed in the following chapter(4).

3.5 Calculation of the Object-Space Coordinates from DLT Coefficients for two Photos.

After solving Equations (3.4.5) and (3.4.6) for the right and left photographs one has the following results:

- a) The coefficients of DLT $(L_1 \dots L_{11})$ and $(L_1 \dots L_{11})$ for the right and left photos

respectively.

- b) The coefficients of systematic errors (film deformation and lens distortion) for the right and left photos.

Knowing the coefficients which describe systematic errors, one can obtain the correct image coordinates for point (i), (\bar{x}_i, \bar{y}_i) and $(\bar{\bar{x}}_i, \bar{\bar{y}}_i)$ for right and left photos respectively.

$$\text{eg } \bar{x}_i = x_i + \Delta x_j \quad \bar{y}_i = y_i + \Delta y_j$$

where Δx_j and Δy_j are the x and y contributions of the systematic errors in the jth photograph.

The object space coordinates $X_i, Y_i,$ and Z_i for a point i can be obtained by solving the following four equations:

$$(\bar{x}_i L_9 - L_1) X_i + (\bar{x}_i L_{10} - L_2) Y_i + (\bar{x}_i L_{11} - L_3) Z_i + (\bar{x}_i - L_4) = 0 \quad (3.5.1)$$

$$(\bar{y}_i L_9 - L_5) X_i + (\bar{y}_i L_{10} - L_6) Y_i + (\bar{y}_i L_{11} - L_7) Z_i + (\bar{y}_i - L_8) = 0 \quad (3.5.2)$$

$$(\bar{\bar{x}}_i L_9 - L_1) X_i + (\bar{\bar{x}}_i L_{10} - L_2) Y_i + (\bar{\bar{x}}_i L_{11} - L_3) Z_i + (\bar{\bar{x}}_i - L_4) = 0 \quad (3.5.3)$$

$$(\bar{\bar{y}}_i L_9 - L_5) X_i + (\bar{\bar{y}}_i L_{10} - L_6) Y_i + (\bar{\bar{y}}_i L_{11} - L_7) Z_i + (\bar{\bar{y}}_i - L_8) = 0 \quad (3.5.4)$$

3.6 Estimation of Inner Orientation Parameters of Non-metric cameras from DLT Coefficients.

In DLT the constant terms of inner orientation, outer orientation parameters, and the linear components of film deformations are grouped into eleven parameters (L_1, \dots, L_{11}) . However, it is necessary to determine the

coordinates of the principal point (x_0, y_0) to be used as a reference point for symmetrical and asymmetrical lens distortion. The estimation of x_0, y_0 , and c can be undertaken as a by-product of the DLT solution, based on the values of the eleven parameters $(L_1 \dots L_{11})$.

The image coordinates system is an arbitrary system. One can, without a loss of generality, take the image coordinates axes to be parallel to the comparator axes. In this case, Equations (3.1.1) and (3.1.2) will take this form:

$$\bar{x} - \bar{x}_0 = \lambda_1 (x - x_0) \quad (3.6.1)$$

$$\bar{y} - \bar{y}_0 = \lambda_2 (y - y_0) \quad (3.6.2)$$

where:

x_0, y_0 are the principal point coordinates relative to comparator coordinate axes.

λ_1, λ_2 are scalars

The other parameters are as defined in Section 3.1

Substituting Equations (3.6.1) and (3.6.2) into Equations (3.2.2) and (3.2.3) respectively and dropping the subscripts one gets:

$$\lambda_1 (x - x_0) = -c \frac{m_{11}(X - X_0) + m_{12}(Y - Y_0) + m_{13}(Z - Z_0)}{m_{31}(X - X_0) + m_{32}(Y - Y_0) + m_{33}(Z - Z_0)} \quad (3.6.3)$$

$$\lambda_2 (y - y_0) = -c \frac{m_{21}(X - X_0) + m_{22}(Y - Y_0) + m_{23}(Z - Z_0)}{m_{31}(X - X_0) + m_{32}(Y - Y_0) + m_{33}(Z - Z_0)} \quad (3.6.4)$$

The above two equations can be put in this form:

$$x - x_0 = -C_x \frac{m_{11}(X - X_0) + m_{12}(Y - Y_0) + m_{13}(Z - Z_0)}{m_{31}(X - X_0) + m_{32}(Y - Y_0) + m_{33}(Z - Z_0)} \quad (3.6.5)$$

$$y - y_0 = -C_y \frac{m_{21}(X - X_0) + m_{22}(Y - Y_0) + m_{23}(Z - Z_0)}{m_{31}(X - X_0) + m_{32}(Y - Y_0) + m_{33}(Z - Z_0)} \quad (3.6.6)$$

As in section 3.3, the above two equations, in turn, can be put in this form:

$$x + L_1 X + L_2 Y + L_3 Z + L_4 + L_9 x X + L_{10} x Y + L_{11} x Z = 0 \quad (3.6.7)$$

$$y + L_5 X + L_6 Y + L_7 Z + L_8 + L_9 y X + L_{10} y Y + L_{11} y Z = 0 \quad (3.6.8)$$

where

$$L_1 = (x_0 m_{31} - C_x m_{11})/L \quad (3.6.9)$$

$$L_2 = (x_0 m_{32} - C_x m_{12})/L \quad (3.6.10)$$

$$L_3 = (x_0 m_{33} - C_x m_{13})/L \quad (3.6.11)$$

$$L_4 = (-x_0 (m_{31} X_0 + m_{32} Y_0 + m_{33} Z_0) + C_x (m_{11} X_0 + m_{12} Y_0 + m_{13} Z_0))/L \quad (3.6.12)$$

$$L_5 = (y_0 m_{31} - C_y m_{21})/L \quad (3.6.13)$$

$$L_6 = (y_0 m_{32} - C_y m_{22})/L \quad (3.6.14)$$

$$L_7 = (y_0 m_{33} - C_y m_{23})/L \quad (3.6.15)$$

$$L_B = (-y_0 (m_{31} X_0 + m_{32} Y_0 + m_{33} Z_0) + C_y (m_{11} X_0 + m_{12} Y_0 + m_{13} Z_0)) / L \quad (3.6.16)$$

$$L_9 = m_{31} / L \quad (3.6.17)$$

$$L_{10} = m_{32} / L \quad (3.6.18)$$

$$L_{11} = m_{33} / L \quad (3.6.19)$$

$$L = -m_{31} X_0 - m_{32} Y_0 - m_{33} Z_0 \quad (3.6.20)$$

The rotational matrix M is orthogonal. From the special properties of M , one can have the following relationships, as given in Abdel-Aziz (1974):

$$L_9^2 + L_{10}^2 + L_{11}^2 = 1/L^2 (m_{31}^2 + m_{32}^2 + m_{33}^2) = 1/L^2 \quad (3.6.21)$$

$$\begin{aligned} L_1^2 + L_2^2 + L_3^2 &= 1/L^2 (X_0^2 (m_{31}^2 + m_{32}^2 + m_{33}^2) \\ &+ C_x^2 (m_{11}^2 + m_{12}^2 + m_{13}^2) - \\ &2X_0 C_x (m_{11} m_{31} + m_{12} m_{32} + m_{13} m_{33})) \\ &= 1/L^2 (X_0^2 + C_x^2) \end{aligned} \quad (3.6.22)$$

$$\begin{aligned} L_1 L_9 + L_2 L_{10} + L_3 L_{11} &= 1/L^2 (X_0 (m_{31}^2 + m_{32}^2 + m_{33}^2) \\ &- C_x (m_{31} m_{11} + m_{32} m_{12} + m_{33} m_{13})) = 1/L^2 X_0 \end{aligned} \quad (3.6.23)$$

similarly one can have

$$L_5^2 + L_6^2 + L_7^2 = 1/L^2 (y_0^2 + C_y^2) \quad (3.6.24)$$

$$L_5 L_9 + L_6 L_{10} + L_7 L_{11} = 1/L^2 y_0 \quad (3.6.25)$$

From Equations (3.6.21), (3.6.22), (3.6.23), (3.6.24) and (3.6.25) one has:

$$x_0 = (L_1 L_9 + L_2 L_{10} + L_3 L_{11}) L^2 \quad (3.6.26)$$

$$y_0 = (L_5 L_9 + L_6 L_{10} + L_7 L_{11}) L^2 \quad (3.6.27)$$

$$C_x^2 = -x_0^2 + L^2 (L_1^2 + L_2^2 + L_3^2) \quad (3.6.28)$$

$$C_y^2 = -y_0^2 + L^2 (L_5^2 + L_6^2 + L_7^2) \quad (3.6.29)$$

$$C = (C_x + C_y) / 2 \quad (3.6.30)$$

Equations (3.6.26), (3.6.27), (3.6.28), (3.6.29) and (3.6.30) give the values of x_0 , y_0 , C_x , C_y and C as a by-product of DLT.

3.7 Extension of the Mathematical model.

Equations (3.3.3) and (3.3.4) can be re-written as follows;

$$x_l + \Delta x_j = \frac{L_1 X + L_2 Y + L_3 Z + L_4}{L_9 X + L_{10} Y + L_{11} Z + 1} \quad (3.7.1)$$

$$y_l + \Delta y_j = \frac{L_5 X + L_6 Y + L_7 Z + L_8}{L_9 X + L_{10} Y + L_{11} Z + 1} \quad (3.7.2)$$

where Δx_j and Δy_j are the contributions of systematic errors in the x and y observed image coordinates respectively implicit in the j th photograph. These are discussed in the following chapter (4).

Bopp and Krauss [1978] while extending the basic 11-parameter (DLT) solution for on-the-job calibration of

non-metric cameras identified two geometrical conditions that should be fulfilled. The two constraints are;

$$(L_1^2 + L_2^2 + L_3^2) - (L_5^2 + L_6^2 + L_7^2) + \frac{C^2 - B^2}{D} = 0 \quad (3.7.3)$$

$$A - \frac{B.C}{D} = 0 \quad (3.7.4)$$

where

$$A = L_1 L_5 + L_2 L_6 + L_3 L_7$$

$$B = L_1 L_9 + L_2 L_{10} + L_3 L_{11}$$

$$C = L_5 L_9 + L_6 L_{10} + L_7 L_{11}$$

$$D = L_9^2 + L_{10}^2 + L_{11}^2$$

For an optimum solution therefore, the above two restrictions should be incorporated into the extended mathematical model as defined through Equations (3.7.1) and (3.7.2) here-above.

3.8 Advantages and Disadvantages of DLT.

Abdel-Aziz and Karara [1971] investigated the main advantages and disadvantages of DLT. According to them, DLT has the following advantages:

- a) It yields at least the same accuracy as the conventional solution.
- b) It is a direct solution and needs no initial approximations for the unknowns. Thus a solution is obtained by DLT even in cases where the conventional collinearity approach fails due to the lack of reasonable approximations for the unknown parameters (inner and outer orientations).
- c) The proposed solution is relatively easy to program since it does not involve partial derivatives of the

coefficients of the observation equation.

- d) The computer executing time and the computer memory needed are less than those in the conventional approach.

In case the inner orientation parameters are known, which is not the case of non-metric cameras, one has to solve for eleven unknowns in the DLT approach, while the solution using the conventional collinearity equations involves only six unknowns (i.e the elements of exterior orientation).

CHAPTER 4. SYSTEMATIC ERRORS IN NON-METRIC CAMERAS.

The correction for systematic errors is a very important matter when dealing with non-metric cameras. Indeed, it is largely the extent to which one successfully corrects for this type of error that influences the precision and accuracy of any parameters determined thereof. In metric restitution instruments, systematic errors are routinely corrected for during the process of camera calibration. On the other hand, in non-metric cameras, systematic errors are corrected for through the use of mathematical models, often in the process of data reduction.

In this chapter is treated the two main sources of systematic errors encountered in the use of non-metric cameras. These include systematic errors due to lens distortion and those resulting from film deformation.

4.1 Lens distortions in non-metric cameras.

In a non-metric camera, usually two kinds of lens distortions are present, namely; symmetrical and asymmetrical lens distortions. For a perfectly centred lens, the lens distortion is ideally symmetrical about the optical axis and is thus called symmetrical lens distortion. Asymmetrical lens distortion otherwise known as decentring lens distortion, is the error due to decentering of the lens elements.

Different mathematical models have been proposed over the years to correct for the above systematic error in non-metric cameras. Generally, most of these models have the following characteristics:

- a) The symmetrical lens distortion is represented by an odd polynomial.

b) The asymmetrical lens distortion is represented by one of the following models:

- 1) Neglecting the asymmetrical lens distortion and using the point of symmetry as the reference point for symmetrical lens distortion.
- 2) Neglecting the asymmetrical lens distortion and using the principal point as the reference point for symmetrical lens distortion.
- 3) The asymmetrical lens distortion is included while the principal point is taken as the reference point for symmetrical lens distortion.
- 4) The asymmetrical lens distortion is included while the optical axis of symmetry is taken as the reference point for symmetrical lens distortion.

It is essential that, especially for non-metric cameras, all the above systematic errors are modelled out and thus adequately accounted for. Most of the models that have been suggested run into several terms, degrees, and orders. In order to determine the required optimum parameters a statistical significance test is usually done.

4.2 The theoretical Mathematical model used to represent symmetrical lens distortion.

The mathematical model for symmetrical lens distortion has been studied rigorously by several different researchers and a common consensus reached.

It is widely acknowledged that the symmetrical lens distortion may be represented by an odd polynomial as

$$\Delta r = K_1 r + K_2 r^3 + \dots + K_n r^{2n-1} \quad (4.2.1)$$

where

$$r^2 = (x - x_s^2) + (y - y_s^2)$$

(x, y) the coordinates of any point

(x_s, y_s) the coordinates of the point of symmetry

$(2n-1)$ is the degree of the polynomial

K_1, K_2, \dots, K_n are constants

4.2.1 Factors affecting symmetrical lens distortion.

Contrary to the long considered belief in photogrammetry that the symmetrical lens distortion was a function of the lens used only, several other factors have been found to influence this. It has been established that the most important changes in symmetrical lens distortion are:

- a) the changes caused by different principal distances,
- b) the changes for out-of-focus points, and
- c) the changes caused by different aperture openings.

The magnitude and nature of these changes vary from one arrangement to the other. Abdel-Aziz [1974] has intensively studied the above phenomena.

4.2.2 The adopted mathematical model for symmetrical lens distortion.

The symmetrical lens distortion polynomial can be represented theoretically by an odd order polynomial. In practical applications however, sometimes it is necessary to represent lens distortion with a complete polynomial. Accordingly, one has the choice between an odd- or a complete-polynomial to represent symmetrical lens distortion. Each has its advantages and disadvantages. In using an odd polynomial, one will run into one of the

following:

- a) the model used is the correct model (the symmetrical lens distortion is an odd one), or
- b) the model used is the wrong model (the symmetrical lens distortion is not an odd one).

Evidently, there is no problem in case a) if the model used is the correct model. However, in case b) one is using a different model from the correct one. A good example of this is using an odd polynomial to represent the symmetrical lens distortion of the Super-Aviogon lens. The symmetrical lens distortion of this lens is best represented by full polynomial in the form:

$$\Delta r = K_1 r + K_2 r^2 + K_3 r^3 + \dots \quad (4.2.2.1)$$

The number of terms that would be needed if one used an odd/even polynomial to represent Equation (4.2.2.1) is undefined, and would depend mainly on the even/odd terms of the complete polynomial. From a mathematical point of view one would hence not have a solution to Equation (4.2.2.1) by using an odd/even polynomial whatever the number of terms used.

Alternatively, using a complete polynomial, one will run into one of the following;

- a) the model used is the correct model (the symmetrical lens distortion is a complete polynomial), or
- b) the model used is the wrong model (the symmetrical lens distortion is an odd/even polynomial).

There is no problem in case (a), the model used is the correct model, while in case (b), one will have a solution, but the number of coefficients carried in the solution will

be increased by $\left(\frac{n-1}{2}\right)$ coefficients where n is the power of the odd/even polynomial [Abdel-Aziz, 1974].

For the work undertaken in this study, an even order polynomial was initially used to represent the symmetrical lens distortion. No additional parameters could be obtained therefrom. On the other hand, when an odd polynomial was used only the K_1 term could be determined. As a result, the full polynomial was then adopted and successfully used.

4.3. Asymmetrical lens distortion.

By stating that the symmetrical lens distortion is strictly symmetrical about the optical axis, one implicitly acknowledges the following assumptions:

- a) the symmetrical lens distortion is referred to the point of symmetry, and
- b) the lens components are perfectly centered.

Violation of any or both of the above assumptions results in the introduction of asymmetrical lens distortion.

4.3.1 The asymmetrical lens distortion due to the reference point not being the point of symmetry.

According to Seidel's aberration theory, the symmetrical lens distortion Δx and Δy can be expressed as:

$$\Delta x = (\bar{x} - x_s)Kr^2 \quad (4.3.1.1)$$

$$\Delta y = (\bar{y} - y_s)Kr^2 \quad (4.3.1.2)$$

where

$$r^2 = (\bar{x} - x_s)^2 + (\bar{y} - y_s)^2$$

(\bar{x}, \bar{y}) are the image coordinates referred to any image coordinate system (usually the principal point is taken as an origin), and

(x_s, y_s) are the coordinates of the point of symmetry referred to the above coordinate system.

K is a constant.

The error $d\Delta x$ and $d\Delta y$ due to the assumption that $x_s = y_s = 0$ (i.e., the reference point coincides with the point of symmetry) can be calculated by applying the law of error propagation to Equations (4.3.1.1) and (4.3.1.2). Accordingly, one finds out that

$$d\Delta x = A_1 (r^2 + 2x^2) + 2A_2 \bar{x}y \quad (4.3.1.3)$$

$$d\Delta y = A_2 (r^2 + 2y^2) + 2A_1 \bar{x}y \quad (4.3.1.4)$$

where

A_1 and A_2 are constants.

The above errors described by Equations (4.3.1.3) and (4.3.1.4) are insignificant in the following cases;

- a) the symmetrical lens distortion has small values, and
- b) the difference between the point of symmetry and the reference point is small.

In case of higher degree polynomials being used to model symmetrical lens distortion, the symmetrical lens distortion Δx and Δy could be expressed as:

$$\Delta x = (\bar{x} - x_s)(K_1 r^2 + K_2 r^4 + \dots + K_n r^{2n}) \quad (4.3.1.5)$$

$$\Delta y = (\bar{y} - y_s)(K_1 r^2 + K_2 r^4 + \dots + K_n r^{2n}) \quad (4.3.1.6)$$

The error $d\Delta x$ and $d\Delta y$ could similarly be obtained by applying the law of propagation of errors to equations (4.3.1.5) and (4.3.1.6).

4.3.2 The asymmetrical lens distortion due to decentring of the lens elements.

Conrady's model is the mostly accepted model which represents the error due to the decentring of the lens elements in photogrammetry. According to this model, the error due to the decentring of the lens elements is:

$$d\Delta x = \left[P_1 (r^2 + 2x^2) + 2P_2 xy \right] \left(1 + P_3 r^2 + P_4 r^4 + \dots \right) \quad (4.3.2.1)$$

$$d\Delta y = \left[P_2 (r^2 + 2y^2) + 2P_1 xy \right] \left(1 + P_3 r^2 + P_4 r^4 + \dots \right) \quad (4.3.2.2)$$

where

$$x = \bar{x} - x_s$$

$$y = \bar{y} - y_s$$

P_1, P_2, P_3 and P_4 are constants

$x_s, y_s, \bar{x}, \bar{y}$, and r are as already defined in section 4.3.1.

In most practical applications of this model in close-range photogrammetry, as in Faig [1972] and Brown [1971] only P_1 and P_2 are the significant terms.

Accordingly, the model for asymmetrical lens distortion is:

$$d\Delta x = P_1 (r^2 + 2x^2) + 2P_2 xy \quad (4.3.2.3)$$

$$d\Delta y = P_2 (r^2 + 2y^2) + 2P_1 xy \quad (4.3.2.4)$$

4.3.3 The adopted mathematical model for asymmetrical lens distortion.

From discussions in sections 4.3.1 and 4.3.2 the total asymmetrical lens distortion would take the form:

$$\Delta x = b_1 (r^2 + 2x^2) + 2b_2 xy \quad (4.3.3.1)$$

$$\Delta y = b_2(r^2 + 2y^2) + 2b_1xy \quad (4.3.3.2)$$

where

b_1 and b_2 are constants.

The above model would take care of decentring lens distortion and of the error due to the reference point not being the point of symmetry.

4.4 Film deformation in non-metric cameras.

Film deformation presents itself as a very notorious source of systematic error in non-metric cameras. Indeed, it has been recognised as the main limiting factor for non-metric photogrammetry. This problem is not improved much given the uncontrolled, increasingly wide variety of 35mm films in the market today. A thorough study of film characteristics and film deformation is thus necessitated. The study of film deformation in metric cameras concerns two main issues:

a) the film deformation, and b) the correction to film deformation.

Previously, the film deformation problem had not been taken into account by most non-metric camera users. However, Abdel-Aziz and Karara [1971], Faig [1972], Adams, Muftuoglu, Murai et.al [1980], Torlegard [1981], Ghosh et.al [1990], among others have reported correction of the film deformation in the non-metric camera. These authors in general introduce an affine model for correcting film deformation.

The main source of film deformation is film unflatness at the time of exposure. In the use of metric cameras, special film flattening devices are used to correct for this. However, non-metric cameras do not have this facility. Mechanical disorder in the film manufacture could also be

another source of film deformation.

The film deformations may be categorized in many different ways. In the following sections they are dealt with in two categories, viz;

- 1) deformation occurring outside the camera, which is a function of the film material and the laboratory conditions, and
- 2) deformation occurring inside the camera while the film is loaded, which is a function of the mechanism of the camera.

Of the above two categories of film deformation logically, one intuitively expects the magnitude of film deformation outside the camera to be greater than that inside the camera. This is arrived at after considering the great pains to which virtually all camera manufacturers go to when designing and fabricating these data acquisition instruments. However, an objective analysis of this is possible only after critically assessing each of these.

4.4.1 Film deformation outside the camera.

The deformation of the film outside the camera encompasses the deformation of the film during processing and storage. The quantitative studies of such deformation have been done by using either the Glass grid plate or the Moire pattern methods as discussed by Abdel-Aziz [1974].

The magnitude of film deformation outside the camera is a function of:

- a) the physical and chemical properties of the film used,
- b) the method of processing, and
- c) the temperature and the relative humidity of the

laboratory materials and the storage room.

Naturally, one would expect the same deformation in metric and non-metric cameras if the same film were used in both, and both films were developed under the same conditions. However, experimental results obtained by metric camera films are meaningless when applied to non-metric cameras. This is mainly due to the fact that

- a) different types and sizes of films are used in non-metric cameras as opposed to those used in metric cameras, and that
- b) there is generally a lack of control over temperature and humidity during processing and storage of non-metric films.

In studying deformation of films used in non-metric cameras, an important point should be upheld. It is worth acknowledging that the number and types of films that could be used for non-metric cameras continues to ever increase. However, different film types have different characteristics and therefore an exhaustive up-to date comparative analysis of these is very difficult in practice.

4.4.2 Film deformation inside the camera.

Errors in this category are mainly due to the lack of film flatness during exposure and the tension of the film during, before, and after exposure. In estimating such errors one has to appreciate that the film has to be processed before any measurements can be made on it. Therefore a direct estimation of the film deformation inside the camera is not possible.

But estimation of film deformation after processing gives a combination of deformation both inside and outside the

camera. Thus an estimate of film deformation inside the camera could be obtained by subtracting that outside the camera from the total deformation inside and outside the camera.

4.4.3 Total film deformation.

The total film deformation (inside and outside the camera) is the function of:

- a) the camera used,
- b) the film used, and
- c) the environmental conditions during processing and storage.

Change in any one of the above factors produces an alteration in the total film deformation. Due to the lack of flatness of the film and the lack of control over the laboratory conditions used for processing the films employed in non-metric cameras, it would be expected that the combined error due to such deformation in non-metric cameras would be higher than that in metric cameras.

The estimation and the correction of film deformation in metric cameras has been done by using one of these two methods:

- a) using fiducial marks,
- b) using a reseau.

Unfortunately, most non-metric cameras do not have fiducial marks or reseau. This means that these approaches cannot be used for non-metric cameras. Instead, one could use a control array with precisely determined object-space coordinates.

In this case, it is impossible to separate film deformation

from lens distortion. The estimated values of RMS would then be the residual errors due to unrepresented film deformation, unrepresented lens distortion, and the random errors in the measurements.

4.5 Complete mathematical model for film deformation in non-metric cameras.

As discussed in section 4.4 there are two main sources of film deformation, viz:

- a) film deformation outside the camera and
- b) film deformation inside the camera.

Several researchers (eg Abdel-Aziz and Karara [1971], Faig [1972], Ghosh et.al [1990] etc) have experimentally proved that an affine model is sufficient to represent film deformation outside the camera. Also, Fryer et.al [1990], confirmed that film unflatness resulted in a radial-like distortion of the image. They further examined the hypothesis that the effect of film unflatness was absorbed into the parameters describing the radial lens distortion. This was found not to be the case, rather it was the affine scaling of image coordinates in the interior orientation phase which partially offset the effect of film unflatness.

Thus, film deformation can be partially arrested through the use of an affine transformation represented by two polynomials of first degree with 6 unknowns as follows:

$$x = a_1 + a_2 \bar{x} + a_3 \bar{y} \quad (4.5.1)$$

$$y = a_4 + a_5 \bar{x} + a_6 \bar{y} \quad (4.5.2)$$

This model takes into account two different scale factors, along x and y, and the error due to non-perpendicularity between x and y axes of the comparator. Also, as discussed

in section 4.4.3 the above model is good enough to represent the total film deformation inside and outside the camera. However, in view of section 4.4.2, one has to be cautious when using such a model to represent film deformations in non-metric cameras.

CHAPTER 5. DATA ACQUISITION.

The acquisition of relevant data forms a very important stage in any study. Indeed, this constitutes an integral part of the research. The previous chapter (four) appraises the various systematic errors that one is likely to encounter in the use of non-metric cameras. It further goes on to discuss several mathematical models that have successfully been used to correct for these systematic errors. This and other afore-discussed chapters however, do not reveal much about gross and/ or random error types.

The very nature of both gross and random errors hinders the use of mathematical models to correct for them. However, significant reduction or even elimination of both these error types could be achieved through an articulate data acquisition scheme. Therefore, any data acquisition approach, if it is to be deemed adequate and comprehensive, should be tailored to this end.

This chapter discusses the various aspects that are considered important in the acquisition of data for the above study. It basically incorporates the design of the control frame, its fabrication and subsequent calibration. Also, the different photographic configurations used in the reconstruction of the various RTA cases studied, together with the respective photocoordinate measurements are presented.

5.1 Possible approaches to the determination of camera parameters while using a non-metric camera.

Photogrammetric restitution from metric cameras does not necessarily warrant the provision of control. This is because these cameras are designed for measurement purposes per se, and although they may incorporate external control

they are not inexplicably tied down to this. Camera calibration directly enables the determination of the desired interior orientation elements.

However, use of non-metric cameras demands the determination of camera parameters in one or more forms. Three different approaches to the provision of this could be adopted namely;

- a) camera self calibration,
- b) camera calibration by use of ground survey control,
- c) control frame.

5.1.1 Camera Self calibration.

Camera calibration basically involves the determination of precise values for the elements of interior orientation and also the resolution of a camera. This is usually done after manufacture and prior to use of any such camera. Recently however, self-calibration has been favored as a means to camera calibration. This technique involves the determination of the above unknowns after photography and in real time together with other desired parameters. Several authors have successfully dealt with this practice [eg Mutfurglu and Aytac, 1980; Ghosh et.al, 1990].

The resolution of a camera may be calibrated using any of two methods commonly encountered. The lens resolving power may be expressed through a direct count of the maximum number of lines per millimeter that can be reproduced by the lens. This may also be determined from density scans taken across test patterns resulting in the modulation transfer function (MTF) [eg. Wolf, 1983].

5.1.2 Camera calibration using ground survey control.

Though rarely used in close-range photogrammetry as a means to provision of control, the above techniques are almost exclusively adopted for the same purpose in aerial photogrammetry. Field survey methods may involve either pre- or post-marking of certain surveyed signals before photography. There is need to incorporate both horizontal and vertical control in the above methodology. Surveying techniques such as triangulation, trilateration, traversing etc., may be used for the horizontal control. Vertical control on the other hand may be provided through heighting techniques such as spirit levelling, trigonometric heighting etc.

Provision of control through these techniques is not only expensive but also notoriously time consuming. This more-or-less explains why these techniques are rarely used as the in-house control tools in close range photogrammetry.

5.1.3 Control frame.

In an effort to design efficient means of providing control especially in the use of non-metric cameras, the use of a control frame has been suggested by among others; Dohler, Gracie, [1971], Ghosh, [1972], Abdel-Aziz, [1974] etc. In this approach a control frame is fabricated on the understanding that control is best utilized in an interpolative mode. Most of the above authors have recommended the construction of a 3 Dimensional frame with more control in the direction of the camera axis. This is due to the fact that it is in this direction that errors propagate uncontrollably due to a poor ray intersection.

It has further been suggested that for the 2 Dimensional coordination of the targets on the frame, either a metric

camera or a theodolite could be adopted depending on the depth of field considerations and also on the required accuracy of the test area. The height coordination may be facilitated through either the measurement of vertical angles using a theodolite and/or through precise levelling.

5.2 Design of the control frame.

Of the above three possible approaches to the determination of camera parameters discussed, the control frame technique was the most enterprising one for the study undertaken. This was basically because, in the use of a non-metric camera for RTA analysis, control should be provided for in a portable mode. Especially from the point of view of time, camera self-calibration and field survey techniques were unacceptable for this study.

The reasons for adopting the use of a theodolite for the 3D coordination of the control frame, were as follows:

- 1) The expected accuracy of any control point determined by using a theodolite is about 0.5mm in the X and Y coordinates and about 2.7mm in the Z coordinates.
- 2) The focusing distance of the theodolite ranges between 1m to 40Km.

Also, from an accuracy point of view, precise levelling strategies were used in establishing the plane of collimation followed by measurement of vertical angles. This had been identified as a more accurate means for vertical coordination than the direct measurement of vertical angles.

5.2.1 Design criteria.

Considered here is the general strategy that was used in the design of the control frame. Various ideal considerations had been postulated. To what extent these were adhered to in the actual fabrication is considered in the following section. Some of the criteria that were emphasized in the design of the control frame included:

a) Size of the control frame.

The basic contention was that control should have been used in an interpolative mode. Approximating the maximum size of an RTA to be 12 metres, say in the X-direction (assuming about 3 vehicles involved), the control frame should ideally have been of size 12 x 3 metres. Moreover, the control frame designed should have been flexible enough such that it could be used for a considerable variation in photographic scales.

b) Design material.

For portability reasons the control frame should have been fabricated in parts which could be easily joined up at the RTA scene. In this respect it was desirable to use aluminium instead of iron, for example.

c) Design characteristics.

The control frame should be rigid and stable. This could be ensured by using larger cross section sizes in the fabrication of the frame.

d) Control configuration.

There was need for more object space control in the direction of the camera axis. This was because, it was in this direction that errors propagated very fast due to poor ray intersection. Hence, the necessity for control in at least three separate object planes.

e) Target design.

For clear identification and subsequent measurement the targets used ought to have contrast with the background. The size of these targets should be at least twice the size of the measuring mark at model scale.

5.2.2 Design Specifications.

Several of the design criteria discussed in the preceding section appeared too ideal to be practical. In most of these instances therefore, the ideal considerations were trimmed down to their realistic practical levels.

With respect to the size of the control frame the following argument was forwarded. Approximating the general size of an RTA involving two vehicles to be about 7 metres (in the X-direction), then this presents the general size of frame required i.e 7 x 3 metres. However, upon considering that single vehicle RTAs do occur and bearing in mind the portability of the frame, two similar frames of sizes 3.5 x 1.8 metres that could be hinged up together were fabricated. In order to facilitate versatility for various RTA scenes of different sizes, the distance between the frame and the actual RTA scene could be adjusted accordingly.

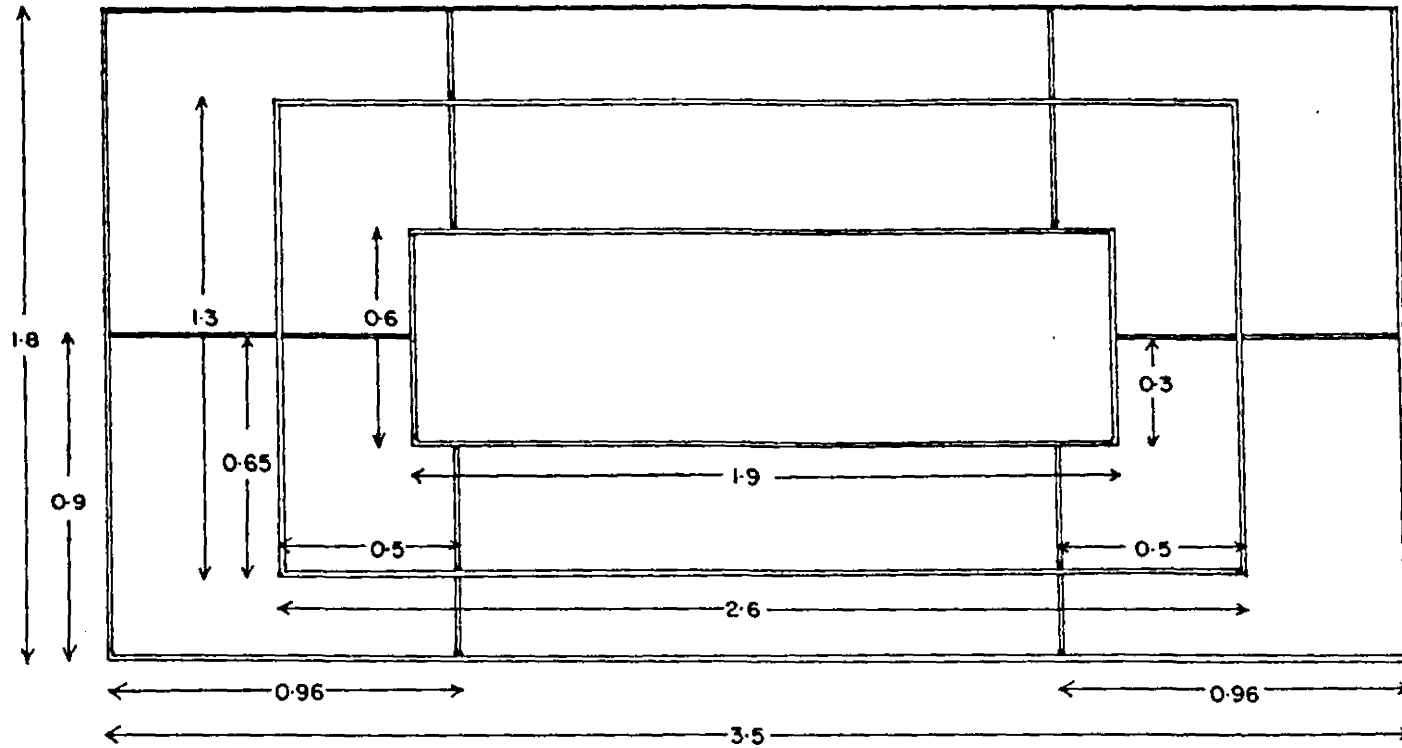
Upon lengthy discussions with relevant personnel, the design material used was substituted to mild steel in pieces of square tubes. These were welded together resulting in frames as in Fig. 5.1. Aluminium was discarded, in spite of its superior characteristics, because of its poor welding characteristics. For each frame 40, 30 and 20 targets were set in the front, middle and rear planes respectively, thus resulting in a total of 180 targets altogether.

Again, it was felt that since an efficient, time conscious

RTA analysis methodology was desired, the idea of the frame being set up from its component parts at the RTA scene would defeat this purpose. It was generally felt that this setting up of the frame was to take between 30mins to 1 hr. This would have been utterly unacceptable. Therefore, the frame was designed and fabricated as two similar/equal parts. Square tubes were used instead of metallic bars in order to reduce the weight of the resulting frame however marginally.

Most of the other design criteria were adhered to. This included the design characteristics, control configurations and aspects of target design. Both the plan and front elevations of the frame fabricated are as shown in Figures - 5.1 and - 5.2 respectively.

CONTROL FRAME (Front Elevation)



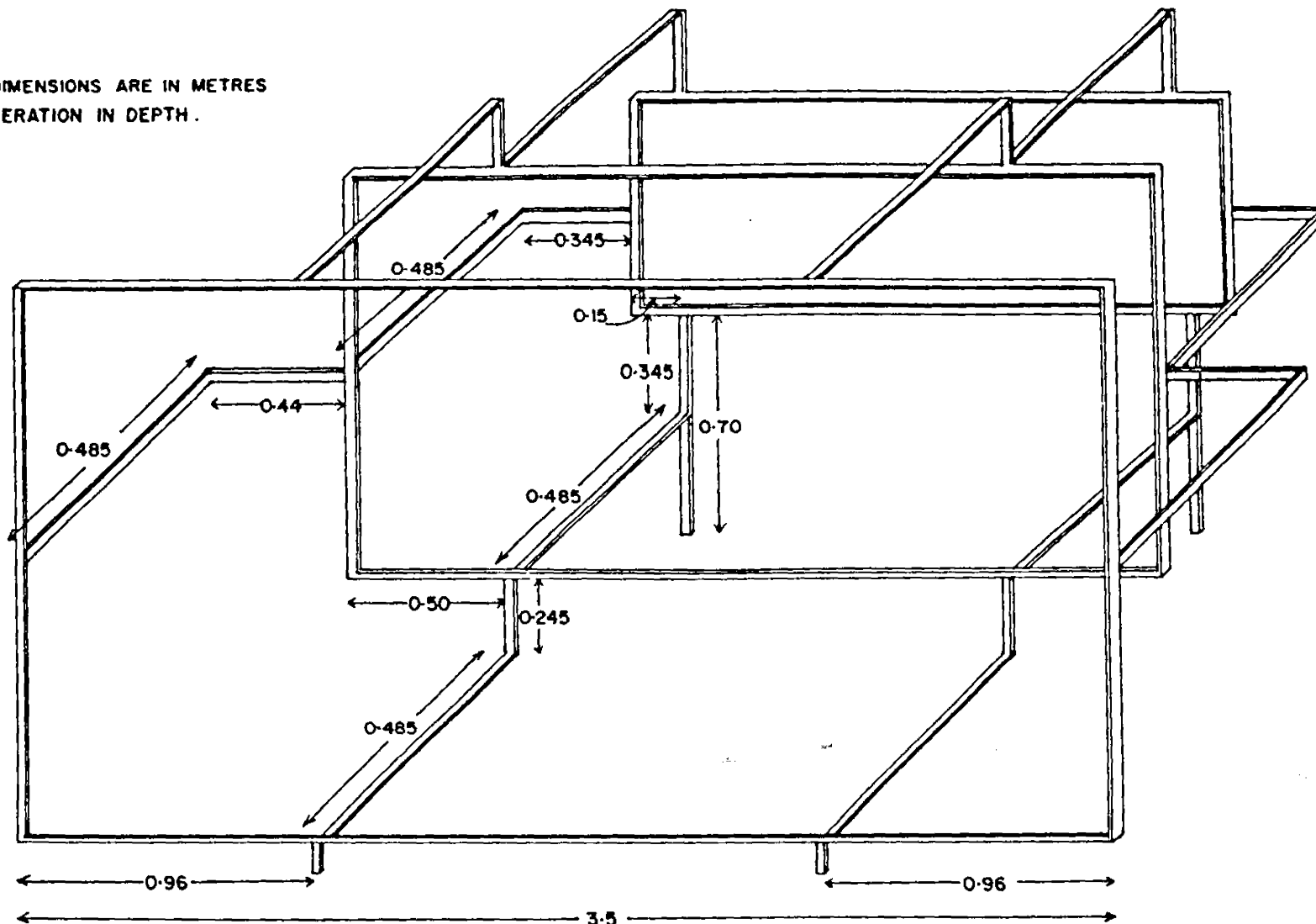
NB. ALL DIMENSIONS ARE IN METRES

SCALE 1 : 20

FIG. 5-1

FIG. 5.2 CONTROL FRAME (Front Isometric View)

NB. ALL DIMENSIONS ARE IN METRES
EXAGGERATION IN DEPTH.



SCALE 1 : 20

5.2.3 Target Design.

Elaborate target design forms an extremely important part in any photogrammetric mission. Poor design of targets may lead to incorrect coordinate measurements or even into absence of imaged targets in the resultant image all together. In the extreme case this could even render the whole undertaking useless. One therefore, cannot afford to haphazardly design the targets as this could lead to monumental losses in one's project.

This section attempts to discuss some desirable considerations which would result in targets that were best suited for RTA photography. Three aspects of the target design were investigated into, namely; shape, size and colour.

From various studies undertaken by different authors (eg. Torlegård, 1981), the best shape for targets is as shown in figure 5.3. This type of target is easy to design and it enhances the well known fact that the best intersection for any two lines is at 90 degrees. Various complicated shapes for targets have been suggested and evaluated. However, given that this study aspires to establish a comprehensive albeit, simple RTA analysis methodology, it was strongly felt that this simple shape would suffice.

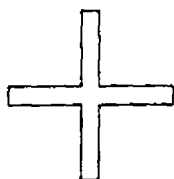


Fig 5.3 Shape of the control frame targets

The size of the targets adopted was constrained by the desire to obtain reliable measurements upon placing the

measuring mark on the target image accurately. The minimum diameter of the targets was not expected to be any smaller than that of the measuring mark at model scale, since the aim was to center the measuring mark accurately on the target image. On the other hand, this was not expected to be too large as to render its centering inaccurate.

Ideally, the size of these targets was constrained to vary from one to two times the size of the measuring mark at model scale. Accordingly, if T_s (mm) is the target size at model scale then

$$(0.06 / S)\text{mm} < T_s(\text{mm}) \leq 2(0.06 / S)\text{mm}$$

where 0.06mm is the size of the measuring mark (eg. for the Wild A8) and S is the model scale. To cater for the diverse range of scales likely to be encountered in RTA photography an average target size of 4mm was adopted.

The colour of the targets was chosen so as to contrast with the background. The chosen colour would have been more critical if a colour film was used for photography than when a Black/White one was adopted. This is because of the greater grey level separation range in the latter than in the former one. In any case, since the control frame was painted black, then the most ideal contrast colour for the targets was white.

5.3 Coordination of the control points.

The basic purpose of using the control frame was in order to provide the required control. Aspects of design for the control frame including the targets are discussed in the preceding section. This section considers points respected in the coordination of the control points on the frame. Also considered is the resulting accuracy of these control points

together with the various sources of errors encountered in the coordination.

In order to determine the 3-dimensional coordinates the following methods were adopted. Surveying by intersection, involving triangulation principles, was used for the horizontal coordination. In this method a baseline was measured and targets intersected through horizontal directions from two observation stations. Trigonometric principles were adopted for the vertical coordination. Obviously, it was envisaged necessary to carry out a thorough reconnaissance before the actual observations were made.

5.3.1 Reconnaissance (Recce).

The objective of the recce was to establish the most suitable positions for the survey stations defining the base. Several criteria were considered in this, namely;

- all the target points were required to be visible from both the observation points,
- generally, it was considered desirable to ensure that strong intersection angles were maintained (approx. 90 degrees),
- the survey stations were chosen so as to provide suitable positions for setting up the theodolite, and
- the survey stations were suitably separated by at least two metres in order to ensure a high measurement precision for the base.

The control frame was placed in the test field and left undisturbed for the whole of these observations. Two survey points which satisfied the above criteria were then chosen and marked down on the ground.

5.3.2 Types of observations.

The observation scheme adopted was dictated by the types of observations required. Three categories of observations were identified, namely;

- 1) observations for the determination of the base,
- 2) observations of horizontal directions to the targets on the control frame, and
- 3) trigonometric observations of vertical angles for determination of relative heights of the control points.

5.3.3 Instrumentation.

Basic instruments used in acquiring data for the above three observation categories included;

- 1) one second theodolite and its tripod,
- 2) precise level plus the accompanying precise staff, and
- 3) subtense bar with its tripod (Wild).

The theodolite was used for the horizontal direction and vertical angle measurements. The subtense bar for the base measurement and the precise level and staff for establishing the horizontal plane of collimation.

5.3.4.1 Base measurement.

The base between the observation stations was measured with a subtense bar. A theodolite was set up at station A and the subtense bar at station B. The angle γ subtended by the marks on the subtense bar was measured twenty times using different circles and on both face-left and -right. The same procedure was repeated for base measurements from station B.

For observation the bar was set horizontal on a tripod, with the horizontality being ensured through one end of the invar

rod. Further, the bar was oriented such that it was perpendicular to the line of sight; this was achieved through a diopter located on one arm of the bar.

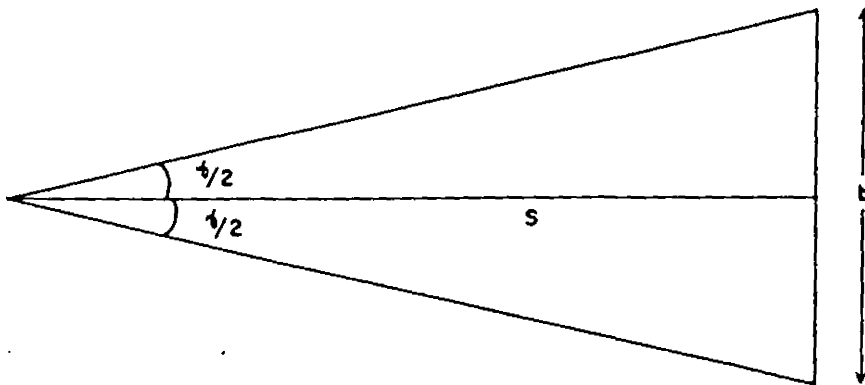


Fig 5.4 Subtense bar measurements

With the above precautions taken in order to eliminate blunders and account for systematic errors, from Fig 5.4 the following relationship was easily derived;

$$s = \frac{b}{2} \cot \frac{\gamma}{2} \quad (5.3.4.1.1)$$

but normally $b = 2$ metres, giving

$$s = \cot \frac{\gamma}{2} \quad (5.3.4.1.2)$$

The base (s) was then obtained from equation (5.3.4.1.2).

5.3.4.2 Observation of horizontal directions.

The theodolite was set up at one observation station and oriented to the other, whereupon an arbitrary reading was set on the circle. Directions to all the target points on the control frame were then made. This procedure was repeated for both face-left and -right theodolite settings. After this, the theodolite was transferred to the other station, oriented back to the former one and the whole procedure repeated. It was explicity necessary that the whole control frame set-up in the test field be undisturbed

throughout the entire observation period.

As discussed in section 2.7.2, the author observed that a plan scale of 1/100 was most suitable for general RTA mapping. The coordination of the control points was made with this point borne in mind. At this scale a cartographic resolution of 0.2mm on the map corresponded to 2cm on the object.

The accuracy of the object-space coordinates X, Y, and Z derived using the normal case of photogrammetry (see Fig 5.5) is given by Equations 5.3.4.2.1 through 5.3.4.2.3, [Abdel-Aziz, 1974] reproduced here-below;

$$\sigma X = \frac{D}{c} \sigma x \quad 5.3.4.2.1$$

$$\sigma Y = \frac{D}{c} \sigma y \quad 5.3.4.2.2$$

$$\sigma Z = \frac{D/c}{B/D} \sqrt{2} \sigma x \quad 5.3.4.2.3$$

where σX , σY , and σZ , are the accuracy on the object-space coordinates X, Y, and Z respectively.

σx , σy are the mean accuracy on the x and y photo-coordinates respectively.

B is the distance between the two exposures.

D is the average distance between the object points to the base B.

c is the average principal distance of photos 1 and 2.

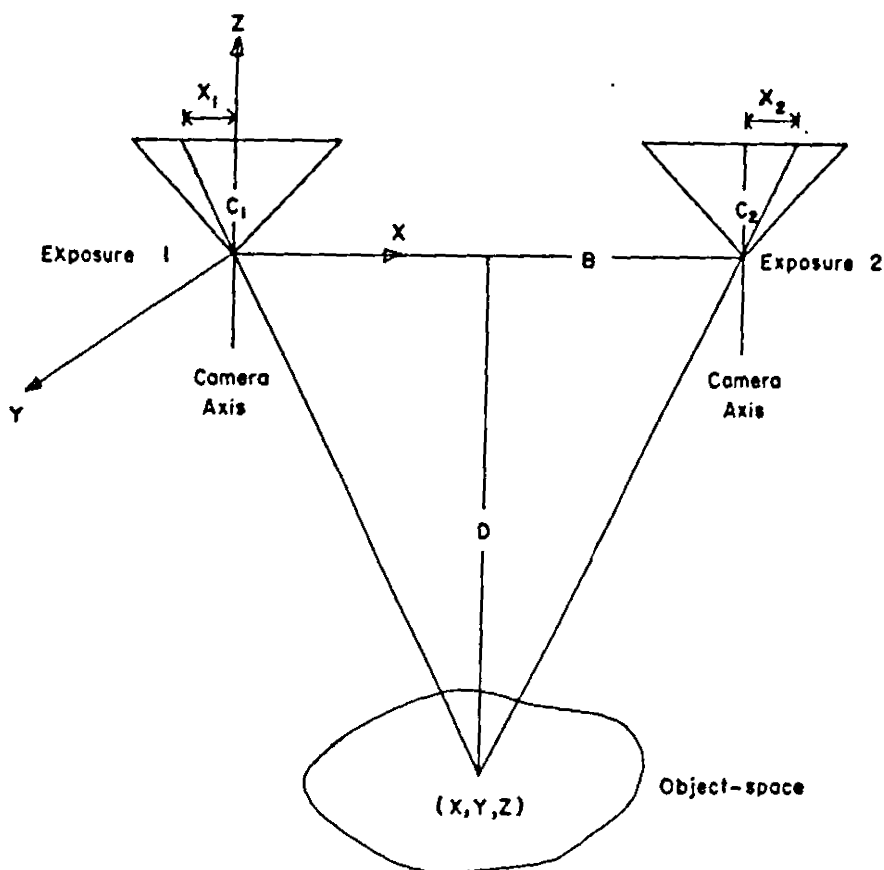


Fig 5.5 Data acquisition set up...Normal case of close range photogrammetry.

For the study undertaken the maximum values of the above parameters were about $D = 15\text{m}$, $c = 200\text{mm}$, $\sigma_x = \sigma_y = 8\mu\text{m}$, $B = 13\text{m}$ giving the accuracy of the plan coordinates as about 0.85mm . The general magnitude of the parameter values has been obtained by a generalisation of values given in table 6.3. From the above preanalysis therefore, the safe tolerable error in the plan control was judiciously taken as $\pm 0.5\text{mm}$.

Experimentally, it was found that the accuracy of a complete round of observations for coordination of a control point was about 1.5mm . Hence the required number of rounds of observations to achieve a standard error of $\pm 0.5\text{mm}$ was 9.

However, as a safety strategy and for the balancing out of instrumental errors in the field observations, a total of 10 rounds of horizontal observations were made to each control point. More specifically, at each station 5 rounds of each face-left and -right observations were made to all control targets thus resulting in a total of 3600 horizontal angle observations for estimation of all necessary planimetric control data.

5.3.4.3 Determination of the heights of observation points.

The plane of collimation at the observation stations was established using a precise level. Trigonometric principles were then used in determining the heights of the targets points. Vertical angles were observed from both observation stations to the targets and the mean heights of these established after using least squares adjustment procedures.

No correction was made for refraction since the observation distances involved were very small (all less than 10 metres). In any case the magnitude of the vertical displacement(s) resulting from this was not expected to exceed $\pm 1.0\text{mm}$ which was way within the tolerable error range [Rogers, 1981]. Along the same lines as discussed in the preceding section, at each station 5 rounds of vertical angles were made to each control point, thus resulting in a total of 1800 vertical angle observations.

5.4 Photography.

The data acquisition scheme discussed in the preceding sections of this chapter was generally geared towards coordinating the points on the control frame. This frame was to be used in the determination of the camera parameters

through the photography that was to follow suit.

When using a non-metric camera for RTA photography different photographic configurations are possible. Also, it is possible to vary different parameters during the photography. These may include the camera principal distance, the exterior orientation angles: ω, ϕ, κ , the base of stereophotography and the average object distance.

The accuracy of any photogrammetric system is determined by the accuracy of the object-space coordinates derived from any such system. This in turn depends on among others:

- the scale of photography,
- the accuracy of the inner and outer orientation parameters of the photographs as in the case of metric cameras, or the accuracy of the object-space controls as in the case of non-metric cameras,
- the configuration of the photography,
- accuracy in the measurement of the photocoordinates, and the
- approximations made underlying the data reduction scheme.

In the remainder of this chapter is treated the relationship between the above parameters as obtained in the different RTA cases studied. Incidentally, in the realisation of this, a combination of both "live" and "simulated" RTA scenes were used. The simulated RTA cases simply involved imitating RTA scenes. These were used because they presented an opportunity for a more rigorous study since the time delay incurred, was not critical as in the live data case.

5.4.1 Specifications of the camera used.

The specifications of the Mamiya C3 Flex camera used in this research were as follows:

- Focal length of the lens = 80mm / 135mm / 180mm
(interchangable)
- Camera format = 5.8cm x 5.8cm
- Serial number No. 230776
- Taking lens No. 862316 / 891669 / 976596
- Focussing lens No. 1005251 / 893415 / 846385
- Tripod (Slik) No. 4232

5.4.2 Photographic configurations used for the RTA photography.

Both the convergent and normal cases of close-range photogrammetry were used in the RTA photography. However, the angle of convergence was kept to a low value (not exceeding 20 degrees). This was done in an effort to avoid the effect of critical convergence angles on the accuracy, discussed in among others Kenefick [1971], Hottier [1976], Torlegard [1981], Faig et.al [1990], etc and reproduced in Fig 5.6.

In order to enhance the identification of the vehicles involved in the RTA, circular retroreflective targets of diameter 2cm were manually attached to the various edge intersections of these vehicles. Marks of diameter 4mm had been pasted onto these targets. As discussed in Baltsavias and Stallmann [1991], such targets improve the light reflectance by almost a thousand times. The control frame was then aligned to a suitable position (mostly adjacent) in the RTA object space.

The average object distance (D_{avg}) was determined depending mostly on the general terrain of the area where the RTA had occurred. A photographic base was then established perpendicular to D_{avg} . The appropriate focal length, aperture and shutter speed settings were then set on the

camera, the latter two being influenced by the weather

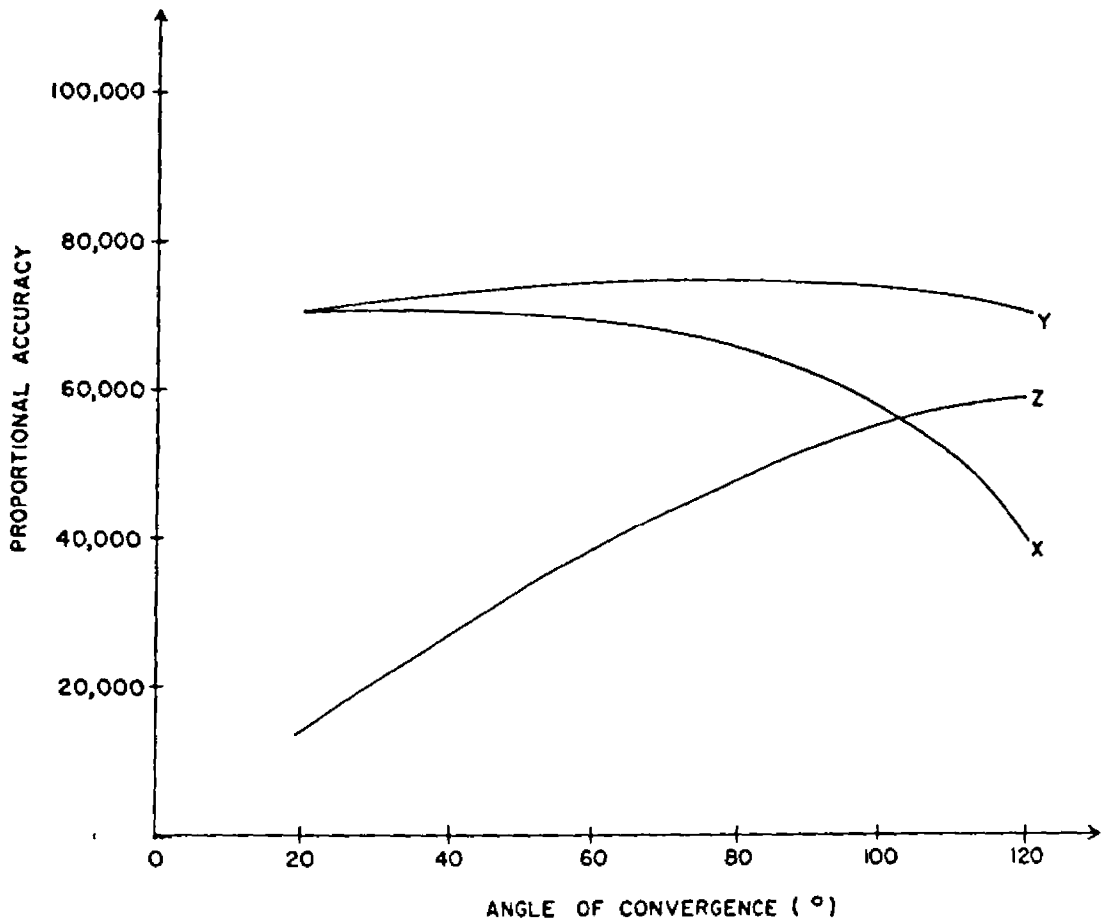


Fig 5.6 Generalized curves showing the relationship of standard deviation in the Object Space with the angle of convergence for a two-station reduction [Kenefick, 1971].

conditions. At selected camera stations located along this base, and at various convergent angles as discussed above, several photographs were taken after appropriately focussing the camera. The photographs were taken in such a way as to ensure that no large portion of the resulting image was featureless (eg. sky or road surface).

Plates 5a-5d are sample illustrations of "live" RTA stereo pairs while plates 5e-5h those of "simulated" RTA stereo pairs.

Throughout, it was ensured that at least two photographs

were taken from each camera station without changing the direction of the camera axis. The reason for this was merely one of a precaution. Also, if the photographs were taken from n camera stations, this was done in such a way as to ensure that at least $n/2$ stereo pairs resulted. The photographic scales used in this study varied between about $1/50 - 1/200$. The films used were;

- 1). Fujicolor Super HR 100, and
- 2). Kodak Verichrome Pan.

5.4.3 Measurement of the photocoordinates.

After photography, normal post card size prints were printed from commercial dealers. Depending on the clarity of the resulting photographs and on their successful stereo-matching, a few (preferably even number) of these were identified and chosen for measurement purposes. A minimum of 4 photographs were accepted. Measurements were done on both a $10\mu\text{m}$ Zeiss Stereocord and on the Wild A8 Stereo-plotter for comparison. The procedure and preparation of the photographs for measurement on these two comparators was different.

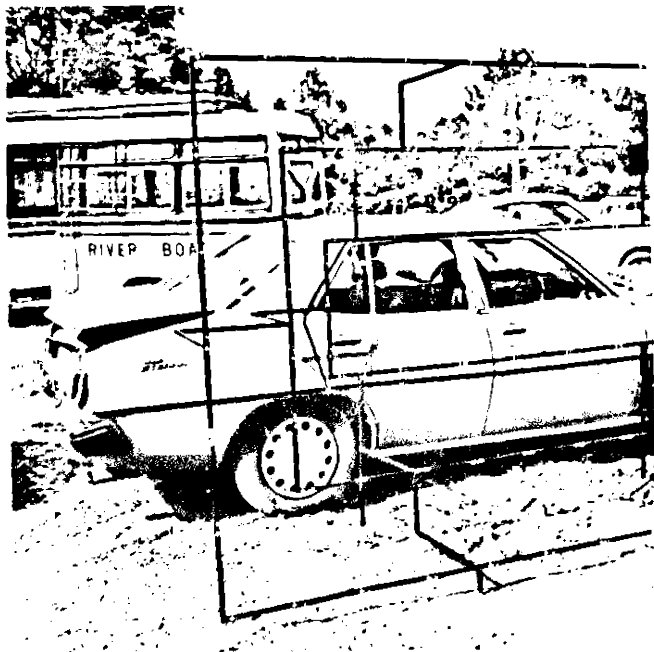
For the Zeiss Stereocord the photographs were enlarged to 5×7 and 8×10 paper print sizes. On the other hand, for the measurements on the A8, the developed original negatives were used directly. In this task the A8 was adapted and used as a mono-comparator as discussed in Ghosh [1979].



5a



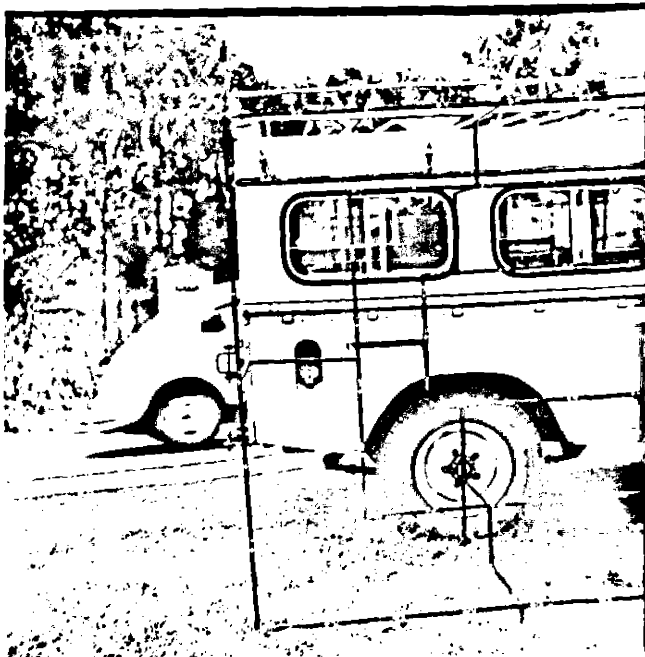
5b



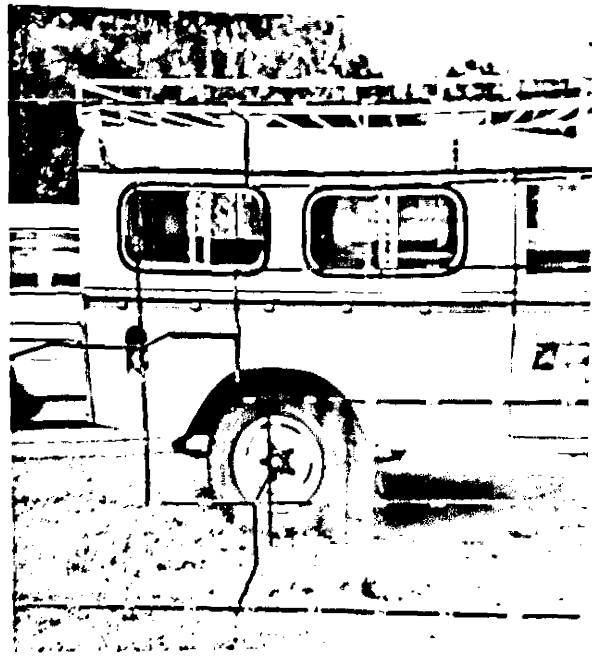
5c



5d



5e



5f



5g

5h

CHAPTER 6. ROAD TRAFFIC ACCIDENT DATA REDUCTION AND ANALYSIS.

In this chapter is considered all the various computations made. Basically, all these are geared towards photogrammetrically mapping any one RTA scene. In the first part of this, the least squares adjustment procedure used in establishing the control point coordinates on the control frame using the theodolite is given. The photogrammetric coordination of the imaged control and RTA points then follows. For this, the Direct Linear Transformation (DLT) strategy, discussed in chapter 3, was used. The various results obtained are also given together with the respective statistical analysis. A discussion of the obtained results is then finally outlined.

6.1 Three Dimensional coordination of the control frame.

6.1.1 General.

The simple Gauss-Markov model is fully described through the functional and stochastic models [Koch, 1988]:

$$Ax = E(y) \quad \text{with} \quad D(y) = \sigma_o^2 W_{yy}^{-1} \quad (6.1.1.1a)$$

where:

y is an $n \times 1$ vector of observations

x ,, $m \times 1$,, ,, unknowns parameters

A ,, $n \times m$ design matrix

W_{yy} ,, $n \times n$ positive definite weight matrix of y

and σ_o^2 is the variance of unit weight.

Since y is a stochastic parameter, it is associated with an observational error ε_y , so that one may rewrite Equation 6.1.1.1a in the form

$$y = Ax + \varepsilon_y \quad , \quad E(\varepsilon_y) = 0 \quad , \quad D(\varepsilon_y) = \sigma_o^2 W_{yy}^{-1} = D(y)$$

or alternatively

$$y = Ax + \varepsilon_y, \quad \varepsilon_y \sim (0, \sigma_o^2 W_{yy}^{-1}), \quad D(\varepsilon) = D(y) \quad (6.1.1.1c)$$

Under the least squares condition that $\hat{\varepsilon}' W \hat{\varepsilon}$ be minimum and provided that $n > m$ and A has full column rank, then

$$\hat{x} = (A'WA)^{-1}A'Wy \quad (6.1.1.2a)$$

$$D(\hat{x}) = \hat{\sigma}_o^2 (A'WA)^{-1} \quad (6.1.1.2b)$$

$$\hat{\sigma}_o^2 = \hat{\varepsilon}' W \hat{\varepsilon} / (n - m) \quad (6.1.1.2c)$$

where \hat{x} is the Best linear unbiased estimate (BLUE) of the unknown parameter x .

6.1.2 Base length computation.

Applying the least squares approach discussed in section 6.1.1 one would get the following relationships:

From Equation 5.3.4.1.2 $s = \text{Cot } \gamma / 2$

Thus $\frac{\partial s}{\partial \gamma} = \frac{1}{2} \text{Cosec}^2 \frac{\gamma}{2}$ giving $A := \frac{-2}{1 + s^2}$

after ignoring the insignificant errors in the length and the non-perpendicularity of the subtense bar.

$$\left. \begin{aligned} \gamma &= 2\text{Cot}^{-1} s & \gamma_c &= 2\text{Cot}^{-1} s_o \\ y &:= \gamma_{\text{obs}} - \gamma_c \\ x &:= \Delta s & s &= s_o + \Delta s \end{aligned} \right\} \quad (6.1.2.1)$$

where

s_o is the approximate base length

γ_{obs} is the observed subtense angle

γ_c computed

The rest of the above parameters are as defined before.

Equations 6.1.1.2 were then used to compute the base length and its standard error. The whole process was iteratively repeated until the correction to the base length was insignificant (say, less than $1\mu\text{m}$).

6.1.3 Horizontal coordination.

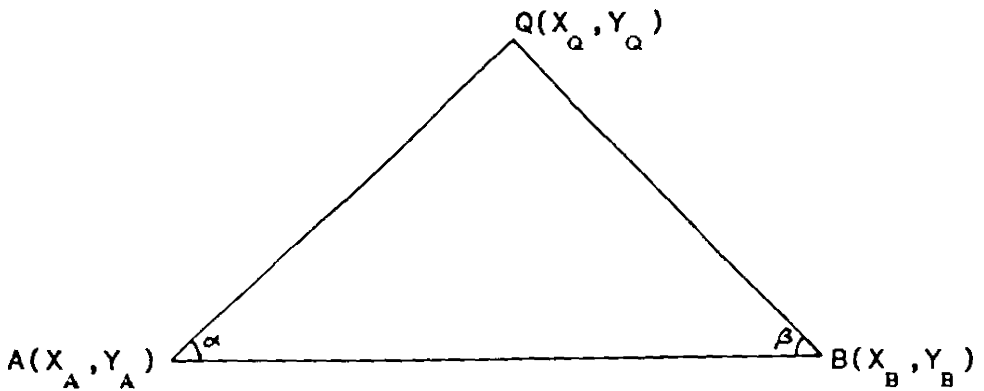


Fig 6.1 Horizontal coordination of a control point

Suppose a point Q is to be intersected from points A and B using intersection angles α and β respectively. The coordinates of point Q according to Bannister and Raymond [1986] would be given by

$$X_Q = \frac{X_A \cot\beta + X_B \cot\alpha + Y_B - Y_A}{\cot\alpha + \cot\beta} \quad (6.1.3.1)$$

$$Y_Q = \frac{Y_A \cot\beta + Y_B \cot\alpha + X_A - X_B}{\cot\alpha + \cot\beta}$$

After simplification and along similar lines as those discussed in section 6.1.1, if the angles α and β were observed n times in order to coordinate point Q, then the required coefficient matrices would be defined as;

$$A := \begin{bmatrix} \text{Cot}\alpha_1 + \text{Cot}\beta_1 & 0 \\ 0 & \text{Cot}\alpha_1 + \text{Cot}\beta_1 \\ \text{Cot}\alpha_2 + \text{Cot}\beta_2 & 0 \\ 0 & \text{Cot}\alpha_2 + \text{Cot}\beta_2 \\ \vdots & \vdots \\ \text{Cot}\alpha_L + \text{Cot}\beta_L & 0 \\ 0 & \text{Cot}\alpha_L + \text{Cot}\beta_L \\ \vdots & \vdots \\ \text{Cot}\alpha_n + \text{Cot}\beta_n & 0 \\ 0 & \text{Cot}\alpha_n + \text{Cot}\beta_n \end{bmatrix} \quad X := \begin{bmatrix} \Delta X_Q \\ \Delta Y_Q \end{bmatrix}$$

$$y := \begin{bmatrix} (X_A \text{Cot}\beta_1 + X_B \text{Cot}\alpha_1 + Y_B - Y_A) - (\text{Cot}\alpha_1 + \text{Cot}\beta_1) X_Q^0 \\ (Y_A \text{Cot}\beta_1 + Y_B \text{Cot}\alpha_1 + X_A - X_B) - (\text{Cot}\alpha_1 + \text{Cot}\beta_1) Y_Q^0 \\ (X_A \text{Cot}\beta_2 + X_B \text{Cot}\alpha_2 + Y_B - Y_A) - (\text{Cot}\alpha_2 + \text{Cot}\beta_2) X_Q^0 \\ (Y_A \text{Cot}\beta_2 + Y_B \text{Cot}\alpha_2 + X_A - X_B) - (\text{Cot}\alpha_2 + \text{Cot}\beta_2) Y_Q^0 \\ \vdots \\ (X_A \text{Cot}\beta_n + X_B \text{Cot}\alpha_n + Y_B - Y_A) - (\text{Cot}\alpha_n + \text{Cot}\beta_n) X_Q^0 \\ (Y_A \text{Cot}\beta_n + Y_B \text{Cot}\alpha_n + X_A - X_B) - (\text{Cot}\alpha_n + \text{Cot}\beta_n) Y_Q^0 \end{bmatrix}$$

(6.1.3.2)

where X_Q^0 and Y_Q^0 are the approximate coordinates of point Q.

The final coordinates of point Q are then given as:

$$X_Q = X_Q^0 + \Delta X_Q \quad (6.1.3.3)$$

$$Y_Q = Y_Q^0 + \Delta Y_Q$$

The above procedure was repeated iteratively in order to determine the planimetric coordinates of the point Q and the associated accuracy parameters.

6.1.4 Vertical Coordination.

Consider the following configuration

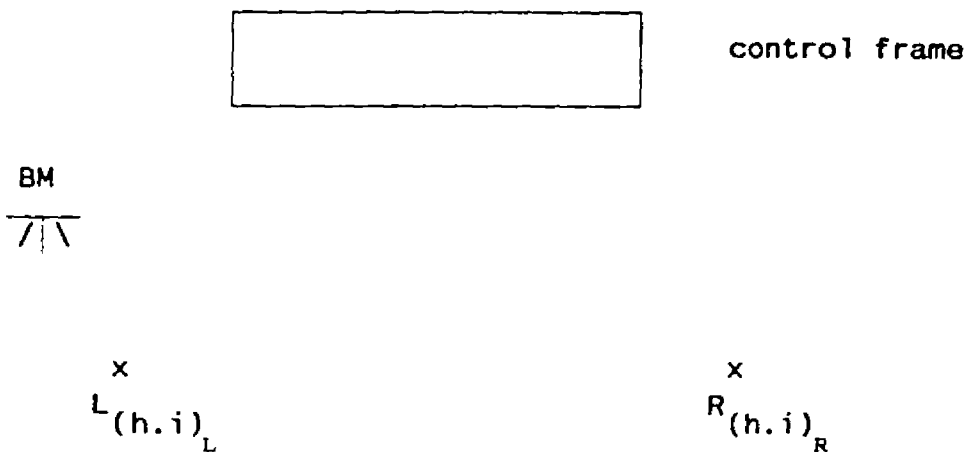


Fig 6.2 Vertical coordination of a control point

where L and R are the left and right theodolite stations,

$(h.i)_{L/R}$ is the height of the instrument at the left or right theodolite stations, and

BM is a suitably chosen bench mark.

From Fig 6.2 one obtains the following height relationships:

$$Z_{i(L)} = (RL)_L + (h.i)_L + \Delta Z_{i(L)} \quad (6.1.4.1a)$$

$$Z_{i(R)} = (RL)_R + (h.i)_R + \Delta Z_{i(R)} \quad (6.1.4.1b)$$

giving

$$Z_i = (Z_{i(L)} + Z_{i(R)})/2 \quad (6.1.4.2)$$

where $Z_{i(L/R)}$ is the height coordinate of point i computed from the left / right instrument station, $RL_{(L/R)}$ is the reduced level of the L / R station determined from BM, and

$\Delta Z_i = s_i \tan B_i$ with s_i and B_i as the horizontal distance and reduced vertical angle to point i respectively.

As discussed in section 5.3.4.3, the above formulation holds precisely if a single set-up of instrument is used at L and

R stations and all the necessary observations are made without changing/disturbing the entire instrument set-up. In this case the error incurred in measuring the instrument heights remains constant for all heights determined and cancels out while averaging results and hence can be ignored. However, due to the number of measurements required and the unreliable weather conditions present then, the instrument had to be disturbed after almost every two set-ups.

The result was that the standard error in the height coordinates was, on average, a poor 16 times worse off than for the corresponding plan coordinates. In order to improve this accuracy, more observations were definitely required. Five more rounds of vertical angle observations were then made but using a slightly different approach geared towards circumventing the height of instrument problem.

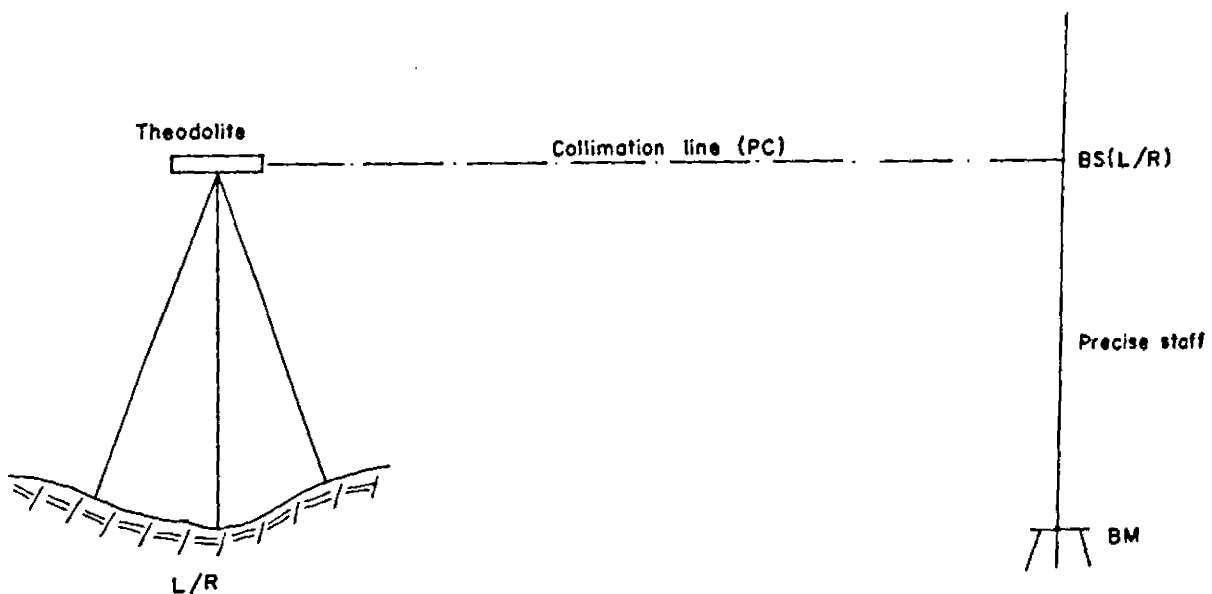


Fig 6.3 Modified approach to the vertical coordination of a control point.

The theodolite at station L/R was centred and oriented horizontally to define a line of collimation. A precise levelling staff was then used to determine the backsight

(BS) reading at the Bench mark (BM).

The height of this collimation line (PC) was given by:

$$PC_{(L/R)} = BM + BS_{(L/R)} \quad (6.1.4.3)$$

giving

$$Z_{i(L/R)} = PC_{(L/R)} + \Delta Z_{i(L/R)} \quad (6.1.4.4)$$

where all the above are as defined before.

6.2 Coordination of imaged RTA points.

Incorporation of the two constraints into the extended DLT mathematical model, as discussed in section 3.7, resulted in the over-constrained Gauss-Markov model with full rank. The adjusted DLT parameters were used to calibrate the camera as defined in section 3.6. The subroutine OBJECT in the same program DLT was used to recompute the 3D coordinates of the control points in the photogrammetric network. This computation was an aid to control quality of computer results. Finally, the subroutine OBTWO was then used to coordinate all the imaged RTA points along similar lines as those discussed in section 3.5

After simplification, the two DLT restrictions given in Equations (3.7.3) and (3.7.4) can be re-written

as:

$$\begin{aligned} r_1 = & L_1^2 L_{10}^2 + L_1^2 L_{11}^2 + L_2^2 L_9^2 + L_2^2 L_{11}^2 + L_3^2 L_9^2 + \\ & L_3^2 L_{10}^2 - L_5^2 L_{10}^2 - L_5^2 L_{11}^2 - L_6^2 L_9^2 - L_6^2 L_{11}^2 - \\ & L_7^2 L_9^2 - L_7^2 L_{10}^2 + 2(L_5 L_6 L_9 L_{10} + L_6 L_7 L_{10} L_{11} + \\ & L_5 L_7 L_9 L_{11} - L_1 L_2 L_9 L_{10} - L_1 L_3 L_9 L_{11} - L_2 L_3 L_{10} L_{11}) = 0 \end{aligned} \quad (6.2.1a)$$

$$\begin{aligned}
r_2 = & L_{15}L_{10}^2 + L_{15}L_{11}^2 + L_{26}L_9^2 + L_{26}L_{11}^2 + L_3L_7L_9^2 + \\
& L_3L_7L_{10}^2 - L_{16}L_9L_{10} - L_{17}L_9L_{11} - L_{25}L_9L_{10} - \\
& L_{27}L_{10}L_{11} - L_{35}L_9L_{11} - L_{36}L_{10}L_{11} = 0
\end{aligned}
\tag{6.2.1b}$$

In parameter estimation involving linear models, the overconstrained Gauss-Markov model with full rank is defined in general as follows;

$$y = Ax + \varepsilon_y \quad \varepsilon_y \sim (0, \sigma_0^2 W_{yy}^{-1}) \tag{6.2.2a}$$

$$r = Rx \tag{6.2.2b}$$

where the parameters in Equation (6.2.2a) are as defined in section 6.1.1, r in Equation (6.2.2b) is the $c \times 1$ vector of restrictions and R is the $c \times m$ design restriction matrix. By definition the matrix R is denoted by

$$R = \begin{bmatrix} \frac{\partial r_1}{\partial L_1} & \frac{\partial r_1}{\partial L_2} & \frac{\partial r_1}{\partial L_3} & \dots & \frac{\partial r_1}{\partial L_{11}} \\ \frac{\partial r_2}{\partial L_1} & \frac{\partial r_2}{\partial L_2} & \frac{\partial r_2}{\partial L_3} & \dots & \frac{\partial r_2}{\partial L_{11}} \end{bmatrix}
\tag{6.2.3}$$

The individual elements of this matrix are given in Appendix C.2.

According to Koch [1988], the pertinent Lagrangian function L is denoted by

$$L = \varepsilon' W \varepsilon + 2(Rx - r)' \lambda \tag{6.2.4}$$

where λ is the vector of Lagrangian multipliers.

The resultant normal equation matrix is then given by

$$\begin{bmatrix} A'WA & R' \\ R & 0 \end{bmatrix} \begin{bmatrix} x \\ \lambda \end{bmatrix} = \begin{bmatrix} A'Wy \\ r \end{bmatrix} \quad (6.2.5)$$

If $N := A'WA$ and $K := R N^{-1} R'$ then

$$\begin{aligned} \hat{x}_r &= \hat{x}_u + N^{-1} R' K^{-1} (r - R \hat{x}_u) \\ &= \hat{x}_u - N^{-1} R' K^{-1} R \hat{x}_u \quad \text{since } r \text{ is a null vector} \end{aligned}$$

$$\text{giving } \hat{x}_r = (I - N^{-1} R' K^{-1} R) \hat{x}_u \quad (6.2.6a)$$

$$\text{and } D(\hat{x}_r) = \hat{\sigma}_0^2 (N^{-1} - N^{-1} R' K^{-1} R N^{-1}) \quad (6.2.6b)$$

$$\text{where } \hat{\sigma}_0^2 = \frac{\hat{\epsilon}' W \hat{\epsilon}}{(n + c - m)} \quad (6.2.6c)$$

\hat{x}_r is the solution vector incorporating the restrictions

\hat{x}_u is the solution vector devoid the restrictions

$D(\hat{x}_r)$ is the dispersion matrix of the unknown parameters

obtained using the solution with restrictions.

I is the $(m \times m)$ identity matrix

Equations (6.2.6a), (6.2.6b) and (6.2.6c) were the ones used to compute the unknowns and additional parameters together with the accuracy parameters. These however had to be incorporated into the basic DLT formulation described in Appendix A.

6.3 Results.

In this section is presented an overview of the results obtained. These are conveniently divided into two broad parts. Those concerned with the coordination of the control frame and those concerned with the three dimensional coordination of the imaged RTA points. Logically, more

emphasis is placed on the second part.

6.3.1 Three dimensional coordination of the control frame.

The base length (s) between the observation stations together with its respective standard error was obtained as:

$$s = 11.090m \pm 0.13mm$$

After coordinating the control frame it was observed that the height coordinates were about 16 times worse off than their plan equivalents (case A). In order to improve upon this the approach as expressed through Equations (6.1.4.3) and (6.1.4.4) was used resulting in case B. It was established that this improvement was significant at 5% level of significance.

The results obtained are tabulated in table 6.1.

Table 6.1. Variation of the mean positional errors with the type of height coordination.

Case	Mean Positional errors (mm)			
	X	Y	Z	POS
A	0.453	0.453	7.081	7.110
B	0.439	0.439	2.676	2.747

The complete coordinate list plus accuracy parameters of case B is tabled in Appendix C.3.

6.3.2 Three dimensional coordination of the imaged RTA points.

The first investigation carried out here was to study the effect of the number of control points on the stochasticity of the interior orientation parameters. The results obtained are tabulated in table 6.2 and discussions follow in section

6.4.

To examine the significance of the 2 DLT constraints, for the same RTA scene the number of control points was varied and the resultant effect, with and without the constraints, on the average mean square errors observed. The obtained results are tabulated in tables 6.3 and 6.4 respectively.

Tables 6.5 and 6.6 reflect the results obtained for the same RTA scene upon varying the photocoordinate measurement from using the Zeiss Stereocord to the Wild A8 Stereoplotter respectively.

Finally, in order to appreciate the significance of the parameters involved in the mathematical modelling of systematic errors the following was done. The number of unknown parameters in the solution was varied and the effect of this on the average mean square errors observed. Table 6.7 gives a tabulated view of the obtained results.

In order to appreciate the magnitude of the unknown parameters together with their standard errors, those from one particular RTA scene obtained using 50 control points are given below. These figures do of course represent the general magnitude of the unknown parameters.

Computed values of unknowns and standard errors, Photo 1

DLT parameters	Standard errors
$L_1 = -0.47117540D+00$	0.43903150D-01
$L_2 = -0.44426165D+00$	0.68395172D-01
$L_3 = -0.93355599D-01$	0.48503526D-01
$L_4 = 0.10079009D+04$	0.30654441D+02
$L_5 = -0.47160336D+00$	0.51171148D-01
$L_6 = -0.44134440D+00$	0.65309054D-01
$L_7 = -0.99247118D-01$	0.59519877D-01

L_8	=	0.10113254D+04	0.18589174D+02
L_9	=	-0.46916779D-03	0.51145406D-04
L_{10}	=	-0.43948700D-03	0.63385095D-04
L_{11}	=	-0.92218487D-03	0.50223653D-04

Lens distortion coefficients Standard errors

K_1	=	0.42481965D-01	0.98917674D-02
K_2	=	-0.54101793D-03	0.20925728D-03
K_3	=	0.21502968D-05	0.10722571D-05
P_1	=	-0.21908037D-03	0.85749425D-04
P_2	=	0.75066828D-03	0.37128837D-04

Computed values of unknowns and standard errors, Photo 2

DLT parameters		Standard errors	
L_1	=	-0.70824739D+00	0.61779501D-01
L_2	=	-0.24662407D+00	0.62942714D-01
L_3	=	-0.12950082D+00	0.58054806D-01
L_4	=	0.10846312D+04	0.27643880D+02
L_5	=	-0.67991387D+00	0.69451519D-01
L_6	=	-0.24254340D+00	0.65121865D-01
L_7	=	-0.13404528D+00	0.71125545D-01
L_8	=	0.10567265D+04	0.25980851D+02
L_9	=	-0.64572686D-03	0.67169250D-04
L_{10}	=	-0.22685831D-03	0.64118089D-04
L_{11}	=	-0.12718479D-03	0.56354081D-04

Lens distortion coefficients Standard errors

K_1	=	0.14377639D-01	0.38706227D-02
K_2	=	-0.80848972D-04	0.40127150D-04
K_3	=	0.16209633D-06	0.10043032D-06
P_1	=	0.97542606D-03	0.46681999D-04
P_2	=	-0.25947192D-03	0.20265653D-04

As a general observation one can conclude that of the 11 DLT parameters only the L_4 and L_8 parameters have magnitudes and standard errors greater than 1. Equations (3.6.12) and (3.6.16) reproduced again here, give these two parameters as:

$$L_4 = \frac{(-x_0 (m_{31} X_0 + m_{32} Y_0 + m_{33} Z_0) + c (m_{11} X_0 + m_{12} Y_0 + m_{13} Z_0))}{L} \quad (6.3.2.1)$$

$$L_8 = \frac{(-y_0 (m_{31} X_0 + m_{32} Y_0 + m_{33} Z_0) + c (m_{21} X_0 + m_{22} Y_0 + m_{23} Z_0))}{L} \quad (6.3.2.2)$$

Of all the 11 DLT parameters it is only these two which have functions of the translation parameters X_0 , Y_0 , and Z_0 inherent in their numerator part. Therefore the magnitudes of L_4 and L_8 are greater than 1 most probably, because of the implicit translation parameters in them. Also, the K_1 parameter is the largest (by at least a hundred times) of all the lens distortion coefficients.

The final output from the proposed RTA analysis methodology are the coordinates of the imaged RTA and control points. RTA plans may be plotted from these using, probably a photogrammetric approach, and the methodology further adopted for an industrial production. On the other hand, the output from the traditional method of RTA analysis is an RTA sketch. The advantages and disadvantages of both final outputs and the methodologies in general, are discussed in section 2.7.

Table 6.2 Effect of the variation in the interior orientation parameters with the number of control points for 11 unknowns.

No of control points	Parameter	XP(mm)	YP(mm)	C(mm)
55	Left photo	1001.277	998.247	81.643
	Right photo	1002.426	999.182	204.215
50	Left photo	1001.032	998.523	81.242
	Right photo	1002.122	999.453	204.023
45	Left photo	1000.977	998.847	80.987
	Right photo	1001.876	1000.003	203.186
40	Left photo	1000.593	999.047	79.896
	Right photo	1001.607	1000.316	202.214
35	Left photo	1000.201	999.374	78.137
	Right photo	1001.346	1000.623	201.208

Table 6.3 Variation in the average mean square errors with the number of control points before incorporating the two DLT restrictions.

No. of control points	Average mean square errors (RMS)			
	X(mm)	Y(mm)	Z(mm)	POS(mm)
20	1.472	5.723	0.947	5.985
30	1.288	4.073	0.464	4.297
35	0.590	2.242	0.567	2.386
40	0.576	2.103	0.525	2.242
45	0.682	1.500	0.477	1.715
50	0.581	1.073	0.398	1.284
55	0.627	0.924	0.375	1.178

Table 6.4 Variation in the average mean square errors with the number of control points after incorporation the two DLT restrictions.

No. of control points	Average mean square errors (RMS)			
	X(mm)	Y(mm)	Z(mm)	POS(mm)
20	1.178	5.827	1.474	6.125
30	1.219	3.779	0.469	3.999
35	0.598	2.120	0.543	2.268
40	0.507	1.983	0.457	2.097
45	0.686	1.439	0.495	1.669
50	0.673	0.870	0.537	1.165
55	0.462	0.783	0.329	0.967

Table 6.5 Variation in the average mean square errors with the number of control points for photocoordinate measurements on the Zeiss Stereocord.

No. of control points	Average mean square errors (RMS)			
	X(mm)	Y(mm)	Z(mm)	POS(mm)
20	1.362	4.725	1.403	5.114
30	1.204	3.782	0.643	4.021
35	0.527	2.246	0.529	2.367
40	0.498	1.942	0.421	2.049
45	0.546	1.520	0.406	1.665
50	0.484	0.947	0.491	1.171
55	0.455	0.741	0.347	0.936

Table 6.6 Variation in the average mean square errors with the number of control points for photocoordinate measurements on the Wild A8 Stereoplotter.

No. of control points	Average mean square errors (RMS)			
	X(mm)	Y(mm)	Z(mm)	POS(mm)
20	0.619	1.890	0.539	2.061
30	0.668	1.351	0.326	1.542
35	0.251	0.864	0.311	0.952
40	0.184	0.669	0.214	0.726
45	0.303	0.563	0.145	0.656
50	0.210	0.379	0.205	0.479
55	0.175	0.365	0.145	0.430

Table 6.7 The variation of the average mean square errors with the number of unknown parameters.

Case	Number of unknowns (IP)	Average mean square error (RMS)			
		X(mm)	Y(mm)	Z(mm)	POS(mm)
A	11	0.976	3.147	1.381	3.573
	12	1.321	1.853	1.479	2.714
	14	6.159	20.914	5.512	22.488
	16	2.635	4.110	1.297	5.052
B	11	0.830	2.686	1.136	3.032
	12	1.726	4.172	1.932	4.910
	14	6.684	19.974	5.236	21.704
	16	1.142	1.766	1.004	2.330
C	11	0.747	2.798	0.323	2.914
	12	1.984	2.657	1.217	3.532
	14	6.263	15.362	5.139	17.367
	16	4.829	7.022	2.858	8.988

6.4 Discussion.

In the three dimensional coordination of the control frame the plan coordinates obtained were within the accuracy limits stipulated for at the design stage (see section 5.3.4.2). However, there was a problem in the height coordinates. As discussed in section 6.3.1 there was a significant accuracy improvement in Case B. Thus, from the results in table 6.1 one can only infer that, for trigonometric heighting involving short observation lines, the most critical source of error is that resulting from measurement of the instrument height.

As the number of control points in the photogrammetric network decreases so does the accuracy and the precision of the interior orientation parameters. This is reflected from the observations in table 6.2. The camera constant c , is particularly affected giving weight to the indication that camera related parameters are not independent. The problems resulting from the poor interior orientation, can be resolved to a certain extent by placing scale control in the object space, and limiting the measuring range in the direction of the depth of field [Faig et.al., 1992].

Errors propagate most rapidly in the direction of the camera axis which incidentally, coincides with the adopted Y axis in the study undertaken. This is portrayed in both tables 6.3 and 6.4 wherein on average, the RMS values in the Y coordinates are between 2 - 3 times larger than those in the X and Z directions. This agrees quite well with what has been discovered through previous studies (eg. Abdel-Aziz, 1974; Hottier, 1976; Ghosh et.al, 1990). The reason for this has been advanced as due to the poor ray intersection in the general direction of the camera axis. One possible solution to this problem is the provision of more object space

control in the Y direction to counteract this effect.

The magnitude of the average mean square errors in the X and Z directions are more-or-less the same and their overall influence on the mean positional errors is on average, less than 30%.

Tables 6.3 and 6.4 also reveal that indeed, the incorporation of the 2 DLT restrictions does improve the general solution but only marginally. For the same number of control points the mean positional errors in table 6.4 are generally slightly better, even though not significant at 5% level of significance, than those in table 6.3.

Also, for the RTA scene implicit in tables 6.3 and 6.4, not less than 45 control points should have been accepted for meaningful results. However, on a general framework there seems to be no deterministic number of control points which are mandatory for a stable solution. One can only infer that this is influenced perhaps by the distribution of these over the entire RTA scene. The more homogeneous is the distribution the better. Evidently, results seem to deteriorate as the number of control points decrease and a possibly poor distribution of control descends over the RTA scene. One can only further the opinion that the greater the number and the better the distribution of control over the entire RTA scene, the better the photogrammetric solution.

The bare minimum number of control points required for a solution is dependent upon the number of unknowns (IP) in the solution. Table 6.8 depicts this scenario.

Table 6.8. Variation in the number of unknown parameters with the bare (theoretically) minimum number of control points required for a solution.

No. of unknown parameters (IP)	No. of control points
11	6
12	6
14	7
16	8

The average standard errors of the mean comparator coordinates obtained after three (3) iterations from the Stereocord and A8 were 0.008mm and 0.003mm respectively. This resulted in more-or-less the same influence on the obtained object-space coordinates. That is, for any particular RTA the average mean square errors for the same number of control/image points resulting upon using the A8 for photocoordinate measurement was about 2-3 times less than that from the stereocord. Tables 6.5 and 6.6 depict this. Thus, the more precise the photocoordinates the higher the accuracy of the obtained object-space coordinates.

Usually a compromise must be struck between the obtained accuracy and the cost of the measuring equipment (or its hire). For example, the cost of an A8 Stereoplotter is at least five times that of the Zeiss Stereocord. However, the accuracy resulting from the use of a stereocord, or even possibly a digitizer, is sufficient for the accuracy stipulated for in local RTA mapping. These relatively low cost equipment(s) could hence be locally adopted for photocoordinate measurement in RTA mapping.

The accuracy and precision of photogrammetric networks in

general, improves with the inclusion of a small selection of additional parameters to the process of the bundle adjustment [Fryer and Mitchell, 1987]. However, Fraser [1982] indicates that although the continued inclusion of additional parameters may improve internal consistency (precision), the absolute accuracy of the computed coordinates may in fact deteriorate. The selection of the most suitable additional parameters is therefore very important.

Results obtained in table 6.7 seem to confirm Fraser's observation. For number of unknowns (IP) greater than 12 in general, the average mean square errors seem to deteriorate when compared with those for IP less or equal to 12.

Also, results in table 6.7 confirm that only the K_1 term is significant in the modelling of systematic errors for the non-metric camera used in this study. The significance test for this was performed using the F test at 5% level of significance. Further, it was established that for the lenses used both the even and odd mathematical models, though commonly used for modelling out symmetrical lens distortion, were unsuitable. Only use of the complete model (see section 4.2) resulted in the successful solution of additional parameters.

CHAPTER 7. CONCLUSIONS AND RECOMMENDATIONS.

Discussed in this chapter are the pertinent conclusions and relevant recommendations arrived at as a result of this study. The conclusions in particular, are drawn mainly from the advantages and disadvantages identified in both the current and proposed RTA analysis methodologies.

7.1 Conclusions.

From a technical view point the current RTA analysis practice falls short of expectation. The type, accuracy and reliability of the measurements made are often inadequate. As discussed in section 2.7.1 from a survey perspective the measurements made would result in either a singular situation or a non-unique one thereof. The susceptibility of committing blunders is high as measurements are often made under unfavorable conditions eg. under duress, or under poor lighting conditions.

The sketch plans drawn under the current RTA analysis practice are not to scale. Also, there is no indication of the general direction whatsoever. A serious time delay causing traffic jams usually results at virtually all RTA scenes during the process of measurement under the current practice. Moreover, the author views this as one of the spontaneous causes for the unacceptable pending of RTA related court cases.

All the above aspects do point out to one conclusion. That, the RTA analysis methodology locally practiced is seriously inadequate. Although it may have been adopted from basically a practical point of view, for example, it is cheap and relatively easy to train new personnel to the practice, the present time is really ripe for a change of methodology. This should not only be technically superior, but should

also be of comparative low cost and conscious of the time element.

The advantages in the proposed RTA analysis methodology do strongly point out to such an alternative. Under this new methodology an RTA plan of scale 1/100 or even better is easily accomplished. A photogrammetric approach could be used here. This methodology is also efficient in expenditure of time as at least a good 10 minutes is saved at the RTA scene. All the resultant photographs could be used to provide both needed illustrative and quantitative RTA information. Also, different perspective views of the RTA scene are possible. This may be used to provide more information otherwise unavailable or confirm doubtful aspects.

The proposed methodology is also comparatively less susceptible to criminal distortion. Several traffic parameters can be determined from the resultant RTA photographs or by further adaptation of the proposed methodology (Garner and Uren [1973]). Both the current and proposed methodologies are labour intensive as ideally at least three traffic officers are required at an RTA scene. Under the proposed methodology the susceptibility of committing blunders is diminished as all measurements are made in the office under favorable ergonomic conditions.

The only drawbacks identified in the proposed methodology are twofold. Firstly, compared to the current practice, the new methodology is more expensive unless implemented in total. Expenses are incurred in the photography, enlargement of photographs, photocoordinate measurements, data processing etc. Secondly, it is relatively more difficult to train new personnel in this proposed methodology. However, the advantages of this new methodology greatly outweigh

these disadvantages. Moreover, if optimised well the expenses incurred could be significantly reduced.

In brief, therefore, this methodology when compared with the conventional RTA analysis techniques would significantly improve the collection, accuracy, preservation, and presentation of metric RTA data. On a local framework it would definitely provide an insight into understanding how RTAs occur and how to handle them appropriately.

The proposed photogrammetric RTA analysis methodology has attempted to explain how RTAs occur. However, it may have not directly explained why RTAs occur, where and when they do so. But as argued in the hypothesis of this study, the proposed methodology certainly provides a benchmark from whence these questions may further be addressed.

7.2 Recommendations.

Listed here-under are some of the recommendations emphatically considered appropriate by the author. This list encompasses both technical and administrative recommendations and includes the following;

1. As a practical observation it was felt that a minimum of 2 stereo pairs should be made at each RTA scene. The purpose of the second stereo pair would be to enhance reliability through trinocular vision.
2. In the very near future, a rigorous pilot project study should be done locally on the possibility of using metric and/or non-metric cameras for RTA reconstruction.
3. For the class of RTAs ranging from serious to fatal, photographs should be taken in order to ensure that the scene is mapped from all possible different perspective views. However, this stringent requirement

may be relaxed for minor RTAs.

4. In order to have an upto date analysis of RTAs in Kenya an RTA database should be set up. This would not only highlight the classification but also portray the macro- and micro-distribution of RTAs in this country. The use of photographs for RTA analysis is particularly apt as these would only require to be digitized before being incorporated into such a database.
5. There is an urgent need for a Photogrammetry Department to be established in the Kenya Police. Such an endeavour would not only provide an avenue for dealing with RTA analyses under the proposed methodology, but also one for criminological, pathological and forensic investigations. This would in the long run save this country a considerable amount of revenue that is currently used to import expatriate technical service.
6. In order that such a department is set up, the Department of Surveying and Photogrammetry at the University of Nairobi could be requested to chip in to provide technical expertise through organization of relevant short courses, seminars and/or lecture programmes.

REFERENCES AND BIBLIOGRAPHY.

Abbreviations used:

- ACSM: American Congress on Surveying and Mapping
ASP: American Society of Photogrammetry
ASPRS: American Society of Photogrammetry and Remote Sensing
AJGPS: Australian Journal of Geodesy, Photogrammetry and Surveying
CISM: Canadian Institution of Surveying and Mapping
CMMV: Close-Range Photogrammetry Meets Machine Vision
IAP: International Archives of Photogrammetry
IAPRS: International Archives of Photogrammetry and Remote Sensing
ISP: International Society for Photogrammetry
ISPRS: International Society for Photogrammetry and Remote Sensing
PE: Photogrammetric Engineering
PERS: Photogrammetric Engineering and Remote Sensing
PR: The Photogrammetric Record
UI: University of Illinois at Urbana-Champaign
UON: University of Nairobi

1. Abdel-Aziz, Y.I., and Karara, H.M., 1971. Direct Linear Transformation from comparator coordinates into Object-Space Coordinates, Proc. ASP/UI Symposium on Close-Range Photogrammetry, Urbana, Illinois.
2. Abdel-Aziz, Y.I., 1974. Photogrammetric Potentials of Non-metric cameras, Ph.D. dissertation, UI.
3. Adams, L.P., 1980. The use of non-metric cameras in short range photogrammetry. Presented paper at the 14th Congress of the ISP, Hamburg.
4. Agoki, G.S., 1988. Characteristics of Road Traffic Accidents in Kenya, Ph.D. dissertation, UON.

5. Atkinson, J.K., 1990. Highway Maintenance Handbook, Thomas Telford Ltd, London. pp 295-301; pp 314-334.
6. Ayeni, O.O., 1985. Photogrammetry as a tool for national development. PERS, Vol.51, No.4, pp 444-455.
7. Bannister A., and Raymond S., 1986. Surveying. Longman Group Ltd., pp 223-226.
8. Bopp, H., and Krauss, H., 1978. Extension of the 11-parameter solution for the On-the-job-calibrations of non-metric cameras. IAP, Vol.22, Part 5, Stockholm.
9. Brown, D.C., 1971. Analytical calibration of close-range cameras. Symposium on close-range photogrammetry, UI.
10. Bruhn, H., and Schneider, C.T., 1990. Optical measurement of vehicle body-shapes in the wind tunnel. A paper presented at the CMMV Symposium, Zurich.
11. Faig, W., 1975. Calibration of Close-Range Photogrammetric systems: mathematical-formulation. PERS, 41(12).
12. Faig, W., 1976. Photogrammetric potentials of non-metric cameras. Report of ISP working group v/2, 13th ISP Congress, Helsinki.
13. Faig, W., Shih, T.Y., and Deng, D., 1990. The Enlarger-Digitizer Approach: Accuracy and Reliability. PERS, Vol.56, No.2, pp 243-246.
14. Faig, W., Wilson, F.R., and Shih, T.Y., 1992. Photogrammetry: A practical tool for car collision investigation. CISM Journal, Vol.46, No.1, pp 31-40.
15. Fraser, C.S., 1980. Accuracy aspects of multiple focal setting self-calibration applied to non-metric cameras. Presented paper at the 14th Congress of the ISP, Hamburg.
16. Fraser, C.S., 1982. On the use of non-metric cameras in analytical close-range photogrammetry. Canadian Surveyor, 36(3), pp 259-279.

17. Fryer, J.G., and Mitchell H.L., 1987. Radial distortion and Close-Range Stereo photogrammetry. AJGPS. Nos 46 & 47, pp 123-138.
18. Fryer, J.G., Knits, H.T., and Donnelly, B.E., 1990. Radial lens distortion and film unflatness in 35mm cameras. AJGPS. No 53, pp 15-28.
19. Garner, J.B., and Uren, J., 1973. The use of photographic methods for traffic data collection. PR, 7(41), pp 555-567.
20. Ghosh, S.K., 1979. Analytical Photogrammetry, Pergamon Press Inc., USA. pp 20-21.
21. Ghosh, S.K., 1981. Photogrammetry for Police use: Experience in Japan. PERS, Vol.46, No.3, pp 329-332.
22. Ghosh, S.K., Rahimi, M., and Shi, Z., 1990. Calibration of amateur cameras for various object distances. Presented paper at the 14th Congress of the ISP, Hamburg.
23. Hashimoto, T., and Murai, S., 1990. Traffic flow measurement by video Image Processing. Presented paper at the CMMV Symposium, Zurich.
24. Hatzopoulos, J.N., 1985. An analytical system for Close-Range Photogrammetry. PERS, Vol.51, No.10, pp 1583-1588.
25. Highway Research Board: Highway Capacity Manual, 1965. Special Report 1987, Washington D.C., 1965.
26. Hottier, P., 1976. Accuracy of Close-Range analytical restitutions: Practical experiments and prediction. PERS, Vol.42, No.3, pp 345-375.
27. Karara, H.M., 1967. Universal Stereo metric Systems. PE, Vol.33, No.11, pp 1303-1313.
28. Karara, H.M., and Faig, W., 1980. An expose on photographic data acquisition systems in Close Range Photogrammetry. Presented paper at the 14th Congress of the ISP, Hamburg.

29. Karara, H.M., 1985. Close-Range Photogrammetry: where are we and where are we heading? PERS, Vol.51, No.5, pp 536-543.
30. Kenefick, J.F., 1971. Ultra-precise analytics. PE, Vol.37, No.10, pp 1167-1187.
31. Kenefick, J.F., Gyer, M.S., and Harp, B.F., 1972. Analytical Self Calibration. PERS, Vol.38, No.11. 31.
32. Kobelin, J., 1976. Mapping street intersections using Close range photogrammetry. PERS, Vol.52, No.8, pp 1083-1089.
33. Koch, K.R., 1988. Parameter Estimation and Hypothesis Testing in Linear Models. Springer-Verlag Berlin Heidelberg, pp 175-230.
34. Kolbl, O., 1976. Metric or Non-metric. Invited paper, comm. V, 13th ISP Congress, Helsinki.
35. Kubik, K., and Merchant, D., 1987. Photogrammetric work without blunders, Tech. papers Vol.2, ASPRS-ACSM Annual Conv. pp 200-207.
36. Kwamina, J.W., Noel, L.P., and Soin, S.S., 1976. A review of Road Traffic Accidents in Nairobi, Kenya, 1968-1972. The Nigerian Engineer, Vol.11, No.3.
37. Lillesand, T.M., and Clapp, J.L., 1971. The utility of stereo metric systems in Traffic Accident Investigation. Proceedings symposium on Close-range photogrammetry. Urbana, Illinois, pp 259-276.
38. Maina, B.R., 1978. Road Safety in Nairobi: an analysis of Road accidents on Nairobi road network, M.A Thesis, UON.
39. Mang'oli, M.K.W., 1979. Traffic flow modelling and a new traffic signal control system for the city of Nairobi, M.Sc Thesis, UON.
40. Mikhail, E.M., and Ackerman, F., 1982. Observations and Least Squares, University Press of America Inc., pp 53-59.

41. Miyanji, O.M., 1976. Road Traffic Accidents (RTAs) in Kenya and in the capital city, Nairobi, with special emphasis on RTAs to children under twelve years of age in Nairobi during 1975 and on road safety and preventive aspects, M.Med Thesis, UON.
42. Mufturglu, O., and Aytac, M., 1980. Calibration of non-metric cameras from single photograph and pair of photographs. Presented paper at the 14th Congress of the ISP, Hamburg.
43. Murai, S., Nakamura, H., and Suzuki, Y., 1980. Analytical orientation for non-metric cameras in the application to terrestrial photogrammetry. Presented paper at the 14th Congress of the ISP, Hamburg.
44. Murai, S., Matsuoka, R., and Okuda, T., 1984. A Study on analytical calibration of non-metric cameras and accuracy of three dimensional measurement. Presented paper at the 15th ISPRS Congress, Rio de Janeiro.
45. Nagaraja, H.N., 1988. An application study for mapping cracks in buildings. Presented paper at the 16th ISPRS Congress, Kyoto.
46. Quinn, A.O., 1979. Admissibility in court of photogrammetric products. PERS, Vol.45, No.2, pp 167-170.
47. Quinn, A.O., 1984. Legal aspects of photogrammetric measurements for Surveying and Mapping. PERS, Vol.50, No.4, pp 453-456.
48. Robertson, G., 1990(a). Aircraft crash analysis utilizing a photogrammetric approach. A paper presented at the CMMV Symposium, Zurich.
49. Robertson, G., 1990(b). Instrumentation requirements for forensic analysis. A paper presented at the CMMV Symposium, Zurich.
50. Rogers, H.H.M., 1981. Vertical refraction on very short lines. Survey Review No.199. Vol.26 pp 32-35.

51. Salley, J.R., 1964. Close range photogrammetry - a useful tool in traffic accident investigation. PE, Vol.30, No.4, pp 568-573.
52. Salmenpera, H., 1980. A procedure for close range camera calibration. Presented paper at the 14th Congress of the ISP, Hamburg.
53. Schernhorst, J.N., 1967. Close Range Instrumentation. PE, Vol.33, No.4, pp 377-381.
54. Shortis, M.R., 1983. Deformation analysis and monitoring by Close Range Photogrammetry. Paper presented at the Surveillance of Engineering Structures Symposium at the Dept. of Surveying, University of Melbourne, Australia.
55. Simonsson, G., 1980. Some means to cost-effective non-topographic photogrammetry. Invited paper at the 14th Congress of the ISP, Hamburg.
56. The Kenya Police, Road Traffic Accident Statistics, 1992.
57. The Traffic Act. Chapter 403 of the Laws of Kenya. Revised Edition, 1988. Printed and published by the Government Printer, Nairobi.
58. Torlegard, K., 1981. Accuracy improvement in Close range photogrammetry, Instut fur photogrammetrie, Munichen, Germany.
59. Turpin, R.D., and Lee, C.E., 1961. Use of photogrammetric methods in traffic studies. PE, Vol.27, No.1, pp 79-83.
60. Waldhausl, P., and Kager, H., 1984. Metric restitution of traffic scenes from non-metric photographs. IAPRS, 25(A5):732-739.
61. Wolf, P.R., 1983. Elements of Photogrammetry, McGraw-Hill, Inc., Singapore. pp 74-83.
62. Zolfaghari, M., 1980. A direct method for measurement of coordinates of a three dimensional test

field. Presented paper at the 14th Congress of ISP,
Hamburg.

APPENDIX A.

A.1 The DLT formulation.

The collinearity condition is expressed by the well-known projective transformation relationship as follows:

$$\begin{bmatrix} \bar{x} - x_p \\ \bar{y} - y_p \\ -C \end{bmatrix} = \lambda \begin{bmatrix} m_{11} & m_{12} & m_{13} \\ m_{21} & m_{22} & m_{23} \\ m_{31} & m_{32} & m_{33} \end{bmatrix} \begin{bmatrix} X - X_0 \\ Y - Y_0 \\ Z - Z_0 \end{bmatrix} \quad (\text{A.1})$$

where the above parameters are as defined in section 3.2

The refined photo coordinates \bar{x} , \bar{y} are the result of an image refinement process which corrects the observed comparator coordinates for lens distortion, linear film deformation, and comparator errors. In the process, also the comparator coordinates are transformed into the photo coordinate system defined by the fiducial marks in the camera. This transformation and the correction for linear film deformation, linear lens distortion and comparator errors are obtained in the following:

$$\begin{aligned} \bar{x} - x_p &= a_1 + a_2 x + a_3 y \\ \bar{y} - y_p &= a_4 + a_5 x + a_6 y \end{aligned} \quad (\text{A.2})$$

where again the parameters are as defined before.

Equations (A.2) apply only to metric cameras, with or without reseau, and to non-metric cameras which have been modified by constructing fiducial marks into them. In this case, the fiducial marks, or the reseau points are used to establish the photo coordinate system and to obtain the parameters for correcting linear film deformation, lens distortion, and comparator errors. For non-metric cameras that have not been modified, the absence of fiducial marks

will not allow the use of equations (A.2). Without loss of generality however, the photo coordinate system may be assumed parallel to the comparator coordinate system and the transformation and correction formulas will take the following form:

$$\begin{aligned}\bar{x} - x_p &= \lambda_x (x + \Delta x - x_o) \\ \bar{y} - y_p &= \lambda_y (y + \Delta y - y_o)\end{aligned}\tag{A.3}$$

where λ_x, λ_y = scale factors which allow for a different scale in the two axes

x_o, y_o = coordinates of the principal point referred to the comparator coordinate system.

$\Delta x, \Delta y$ = systematic errors in coordinates.

In Equations (A.1), dividing the first and second equations by the third, and substituting Equations (A.3) in the resulting relationships, one obtains

$$x + \Delta x - x_o = -C_x \frac{m_{11}(X - X_o) + m_{12}(Y - Y_o) + m_{13}(Z - Z_o)}{m_{31}(X - X_o) + m_{32}(Y - Y_o) + m_{33}(Z - Z_o)}\tag{A.4}$$

$$y + \Delta y - y_o = -C_y \frac{m_{21}(X - X_o) + m_{22}(Y - Y_o) + m_{23}(Z - Z_o)}{m_{31}(X - X_o) + m_{32}(Y - Y_o) + m_{33}(Z - Z_o)}$$

Simplifying Equation (A.4), one gets

$$x + \Delta x = \frac{L_1 X + L_2 Y + L_3 Z + L_4}{L_9 X + L_{10} Y + L_{11} Z + 1}\tag{A.5}$$

$$y + \Delta y = \frac{L_5 X + L_6 Y + L_7 Z + L_8}{L_9 X + L_{10} Y + L_{11} Z + 1}$$

where all the above parameters are as defined in section 3.3

Equations (A.5) are the basic formulas derived by Abdel-Aziz and Karara [1971] for the Direct Linear Transformation (DLT)

$$\Delta x = x' (K_1 r^2 + K_2 r^4 + K_3 r^6 + \dots) + P_1 (r^2 + 2x'^2) + 2P_2 x' y' \quad (\text{A.8})$$

$$\Delta y = y' (K_1 r^2 + K_2 r^4 + K_3 r^6 + \dots) + P_2 (r^2 + 2y'^2) + 2P_1 x' y'$$

where

$$\begin{aligned} x' &= x - x_0 \\ y' &= y - y_0 \\ r^2 &= x'^2 + y'^2 \end{aligned}$$

K 's = coefficients of symmetrical lens distortion

P 's = coefficients of asymmetrical lens distortion

For each point i in photo j , therefore, equation (A.7) can be rewritten using matrix notation as

$$\begin{bmatrix} V_{x_l} \\ V_{y_l} \end{bmatrix} + \begin{bmatrix} B_{x_1} & B_{x_2} & \dots & B_{x_{16}} \\ B_{y_1} & B_{y_2} & \dots & B_{y_{16}} \end{bmatrix} \begin{bmatrix} L_1 \\ L_2 \\ L_3 \\ \vdots \\ L_{11} \\ K_1 \\ K_2 \\ K_3 \\ P_1 \\ P_2 \end{bmatrix} + \begin{bmatrix} D_{x_l} \\ D_{y_l} \end{bmatrix} = 0 \quad (\text{A.9})$$

where

$$\begin{aligned} D_{x_l} &= x_l / A_l \\ B_{x_1} &= -X_l / A_l \\ B_{x_2} &= -Y_l / A_l \\ B_{x_3} &= -Z_l / A_l \\ B_{x_4} &= -1 / A_l \\ B_{x_5} &= 0 \end{aligned}$$

$$\begin{aligned} D_{y_l} &= y_l / A_l \\ B_{y_1} &= 0 \\ B_{y_2} &= 0 \\ B_{y_3} &= 0 \\ B_{y_4} &= 0 \\ B_{y_5} &= -X_l / A_l \end{aligned}$$

$$\begin{aligned}
B_{x_6} &= 0 & B_{y_6} &= -Y_l / A_l \\
B_{x_7} &= 0 & B_{y_7} &= -Z_l / A_l \\
B_{x_8} &= 0 & B_{y_8} &= -1 / A_l \\
B_{x_9} &= x_l X_l / A_l & B_{y_9} &= y_l X_l / A_l \\
B_{x_{10}} &= x_l Y_l / A_l & B_{y_{10}} &= y_l Y_l / A_l \\
B_{x_{11}} &= x_l Z_l / A_l & B_{y_{11}} &= y_l Z_l / A_l \\
B_{x_{12}} &= x_l r_l^2 & B_{y_{12}} &= y_l r_l^2 \\
B_{x_{13}} &= x_l r_l^4 & B_{y_{13}} &= y_l r_l^4 \\
B_{x_{14}} &= x_l r_l^6 & B_{y_{14}} &= y_l r_l^6 \\
B_{x_{15}} &= r_l^2 + 2x_l^2 & B_{y_{15}} &= 2x_l y_l \\
B_{x_{16}} &= 2x_l y_l & B_{y_{16}} &= r_l^2 + 2y_l^2 \\
x_l' &= x_l - x_0 & y_l' &= y_l - y_0 \\
r_l^2 &= (x_l - x_0)^2 + (y_l - y_0)^2
\end{aligned}$$

The pair of condition equations that can be written for a point i in photo j therefore, can be expressed as

$$V_l + B_l \Delta_j + D_l = 0 \tag{A.10.1}$$

where

$$V_l = \begin{bmatrix} v_{x_l} \\ v_{y_l} \end{bmatrix} ; \quad D_l = \begin{bmatrix} D_{x_l} \\ D_{y_l} \end{bmatrix}$$

B_l = matrix of B_{x_l} 's and B_{y_l} 's

Δ_j = matrix of unknowns for photo j

For n control points, one can write

$$\begin{bmatrix} V_1 \\ V_2 \\ V_3 \\ \vdots \\ \vdots \\ \vdots \\ V_n \end{bmatrix} + \begin{bmatrix} B_1 \\ B_2 \\ B_3 \\ \vdots \\ \vdots \\ \vdots \\ B_n \end{bmatrix} \Delta_j + \begin{bmatrix} D_1 \\ D_2 \\ D_3 \\ \vdots \\ \vdots \\ \vdots \\ D_n \end{bmatrix} = 0 \quad (\text{A.10.2})$$

or

$$\begin{matrix} V & + & B & \Delta_j & + & D & = & 0 \\ 2n \times 1 & & 2n \times 1 & 1 & & 1 & & 2n \times 1 \end{matrix}$$

$$V = -(B \Delta_j + D) \text{ giving } V^T = -(\Delta_j^T B^T + D^T)$$

Then the sum of the squares of the residuals is given by

$$V^T W V = \Delta_j^T B^T W B \Delta_j + \Delta_j^T B^T W D + D^T W B \Delta_j + D^T W D \quad (\text{A.11})$$

From section 6.1.1 the least squares solution postulates that the sum of the squares of the weighted residuals be a minimum. Thus taking the partial derivative of Equations (A.11) with respect to the unknowns gives

$$\frac{\partial V^T W V}{\partial \Delta_j} = B^T W B + B^T W D = 0 \quad (\text{A.12})$$

where W = weight matrix for the condition equations.

A least squares solution, therefore, will give

$$\begin{aligned} \Delta_j &= -(B^T W B)^{-1} B^T W D \\ &= -N^{-1} D^* \end{aligned} \quad (\text{A.13})$$

where $N = B^T W B$ and $D^* = B^T W D$

Premultiplying Equation (A.12) by Δ_j^T , one obtains

$$\Delta_j^T B^T W B \Delta_j + \Delta_j^T B^T W D = 0 \quad (\text{A.14})$$

Substituting Equation (A.14) into (A.11) gives

$$V^T W V = D^T W B \Delta_j + D^T W D \quad (\text{A.15})$$

Equation (A.15) is a convenient form for the computation of the sum of the residuals squared. The second term is the contribution of the condition equations, while the first term is the contribution of the normal equations.

A.3 The form of the weight matrix.

Equations (A.7) can be rewritten as follows:

$$F_x = -(L_1 X + L_2 Y + L_3 Z + L_4)/A + x(L_9 X + L_{10} Y + L_{11} Z)/A + \Delta x + x/A = 0$$

$$F_y = -(L_5 X + L_6 Y + L_7 Z + L_8)/A + y(L_9 X + L_{10} Y + L_{11} Z)/A + \Delta y + y/A = 0 \quad (\text{A.16.1})$$

By the law of propagation of variances, assuming independence, equations (A.16.1)

$$m_{F_x}^2 = \left[\frac{xL_9 - L_1}{A} \right]^2 m_X^2 + \left[\frac{xL_{10} - L_2}{A} \right]^2 m_Y^2 + \left[\frac{xL_{11} - L_3}{A} \right]^2 m_Z^2 + m_x^2 \left[\frac{1}{A^2} \right] \quad (\text{A.16.2})$$

$$m_{F_y}^2 = \left[\frac{yL_9 - L_5}{A} \right]^2 m_X^2 + \left[\frac{yL_{10} - L_6}{A} \right]^2 m_Y^2 + \left[\frac{yL_{11} - L_7}{A} \right]^2 m_Z^2 + m_y^2 \left[\frac{1}{A^2} \right]$$

where m_X^2, m_Y^2, m_Z^2 = variances of object space coordinates

m_x^2, m_y^2 = variances of comparator coordinates

$m_{F_x}^2, m_{F_y}^2$ = variances associated with the x and y condition equations, respectively.

resulting number of unknowns.

Systematic Errors corrected	Unknowns	No.	Ref. Equations
Linear components of film deformation, lens distortion and comparator errors	L_1 through L_{11}	11	(A.5)
1st term of symmetrical lens distortion, and linear errors	L_1 through L_{11} , K_1	12	(A.5) and (A.8)
1st three terms of symmetrical lens distortion, and linear errors	L_1 through L_{11} , K_1, K_2, K_3	14	(A.5) and (A.8)
1st three terms of symmetrical, and 1st two terms of asymmetrical, lens distortion and linear errors	L_1 through L_{11} , K_1, K_2, K_3 P_1, P_2	16	(A.5) and (A.8)

A.6 Computation of the interior orientation elements.

$$\begin{aligned}
 1/L^2 &= L_9^2 + L_{10}^2 + L_{11}^2 \\
 x_0 &= (L_1 L_9 + L_2 L_{10} + L_3 L_{11}) L^2 \\
 y_0 &= (L_5 L_9 + L_6 L_{10} + L_7 L_{11}) L^2 \\
 C_x^2 &= -x_0^2 + (L_1^2 + L_2^2 + L_3^2) L^2 \\
 C_y^2 &= -y_0^2 + (L_5^2 + L_6^2 + L_7^2) L^2 \\
 C &= (C_x + C_y) / 2
 \end{aligned}
 \tag{A.22}$$

A.7 Computation of the object space coordinates.

From Equations (A.6), one gets the relationships:

$$\begin{aligned}
 (x + \Delta x)(L_9 X + L_{10} Y + L_{11} Z + 1) - (L_1 X + L_2 Y + L_3 Z + L_4) &= 0 \\
 (y + \Delta y)(L_9 X + L_{10} Y + L_{11} Z + 1) - (L_5 X + L_6 Y + L_7 Z + L_8) &= 0
 \end{aligned}
 \tag{A.23.1}$$

The values of Δx , Δy are computed from Equations (A.8) and applied to the observed coordinates x , y giving,

$$\bar{\bar{x}} = x + \Delta x$$

$$\bar{\bar{y}} = y + \Delta y \quad (\text{A.23.2})$$

where $\bar{\bar{x}}$, $\bar{\bar{y}}$ are the observed comparator coordinates corrected for systematic errors.

Substituting Equations (A.23.2) in (A.23.1) and re-arranging gives

$$(\bar{\bar{x}}L_9 - L_1)X + (\bar{\bar{x}}L_{10} - L_2)Y + (\bar{\bar{x}}L_{11} - L_3)Z + (\bar{\bar{x}} - L_4) = 0$$

$$(\bar{\bar{y}}L_9 - L_5)X + (\bar{\bar{y}}L_{10} - L_6)Y + (\bar{\bar{y}}L_{11} - L_7)Z + (\bar{\bar{y}} - L_8) = 0$$

$$(\text{A.23.3})$$

In each photograph, therefore, one can write for each point one set of equations (A.23.3). If there are P photographs used in the solution, there results $2P$ number of equations to compute for the unknowns X, Y, Z , the object space coordinates of a point. The number of degrees of freedom will be

$$DF = 2P - 3$$

In matrix notation, from Equation (A.23.3), the pair of condition equations that one can write for a point i in photo j are

$$V_j + B_j \Delta_i + C_j = 0 \quad (\text{A.24})$$

where

$$V_j = \begin{bmatrix} v_x \\ v_y \end{bmatrix} \quad \Delta_i = \begin{bmatrix} X \\ Y \\ Z \end{bmatrix}_i$$

$$B_j^T = \begin{bmatrix} (\bar{\bar{x}}L_9 - L_1) & (\bar{\bar{y}}L_9 - L_5) \\ (\bar{\bar{x}}L_{10} - L_2) & (\bar{\bar{y}}L_{10} - L_6) \\ (\bar{\bar{x}}L_{11} - L_3) & (\bar{\bar{y}}L_{11} - L_7) \end{bmatrix}_j$$

$$C_j = \begin{bmatrix} \bar{x} - L_4 \\ \bar{y} - L_0 \end{bmatrix}$$

For P photographs, Equation (A.24) becomes

$$V + B \Delta_l + C = 0 \quad (A.25)$$

A least squares solution will again give

$$\begin{aligned} \Delta_l &= -(B^T W B)^{-1} B^T W C \\ &= -N^{-1} C^* \end{aligned} \quad (A.26)$$

where $N = B^T W B$

$$C^* = B^T W C$$

$W =$ associated weight matrix.

Again, $V^T W V = C^T W B \Delta_l + C^T W C$

The variance of unit weight will be

$$m_0^2 = \frac{V^T W V}{DF} \quad (A.27)$$

The variance-covariance matrix of the computed coordinates will be

$$m_{\Delta_l}^2 = m_0^2 N^{-1}$$

The weight associated with each condition equation is obtained as follows:

From Equations (A.6) assuming 16 unknowns, i.e., 11 DLT parameters, first three terms of symmetrical lens distortion and the first two terms of asymmetrical lens distortion, will be carried in the solution, there results

$$F_l = B_l \Delta_l + D_l \quad (A.28)$$

where

$$F_l = \begin{bmatrix} F_x \\ F_y \end{bmatrix} \quad D_l = \begin{bmatrix} Ax_l \\ Ay_l \end{bmatrix}$$

$$\Delta_j^T = [L_1 \ L_2 \ L_3 \ \dots \ L_{11} \ K_1 \ K_2 \ K_3 \ P_1 \ P_2]$$

$$B_l^T = \begin{bmatrix} -X & 0 \\ -Y & 0 \\ -Z & 0 \\ -1 & 0 \\ 0 & -X \\ 0 & -Y \\ 0 & -Z \\ 0 & -1 \\ xX & yX \\ xY & yY \\ xZ & yZ \\ Ax' r^2 & Ay' r^2 \\ Ax' r^4 & Ay' r^4 \\ Ax' r^6 & Ay' r^6 \\ A(r^2 + 2x'^2) & 2Ax' y' \\ 2Ax' y' & A(r^2 + 2y'^2) \end{bmatrix}$$

By the law of propagation of variances, one obtains

$$m_{F_l} = \begin{bmatrix} m_{F_x}^2 & m_{F_x F_y} \\ m_{F_x F_y} & m_{F_y}^2 \end{bmatrix}$$

$$= B_l m_{\Delta_j} B_l^T + A^2 \begin{bmatrix} m_x^2 & 0 \\ 0 & m_y^2 \end{bmatrix}$$

(A.29)

where m_{F_i} = variance-covariance matrix associated with the two condition equations

m_{Δ_j} = variance-covariance matrix of the unknowns carried in the solution.

m_x^2, m_y^2 = variances of comparator coordinates

$$A = L_{9} X + L_{10} Y + L_{11} Z + 1$$

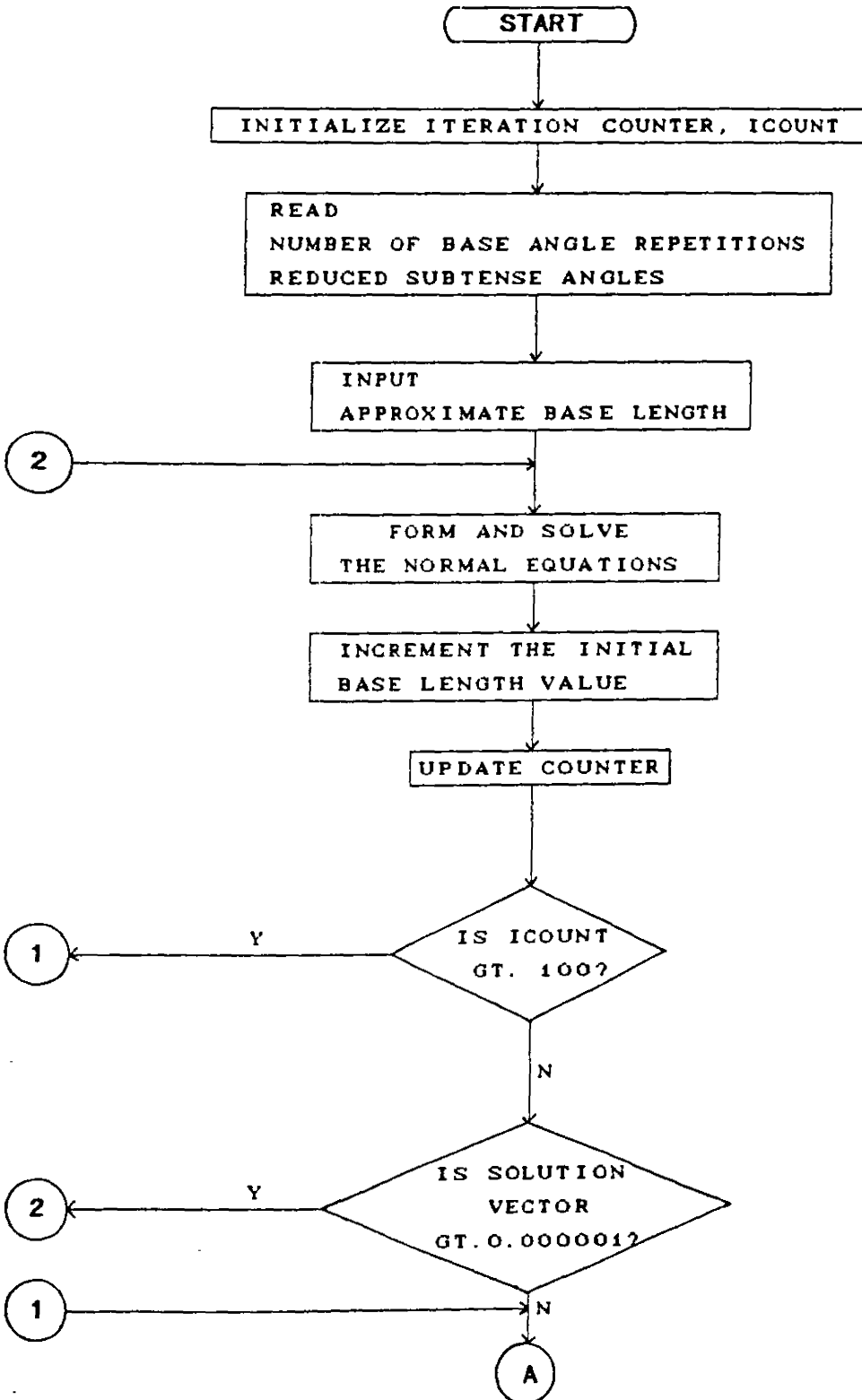
The weights associated with the condition equations will be

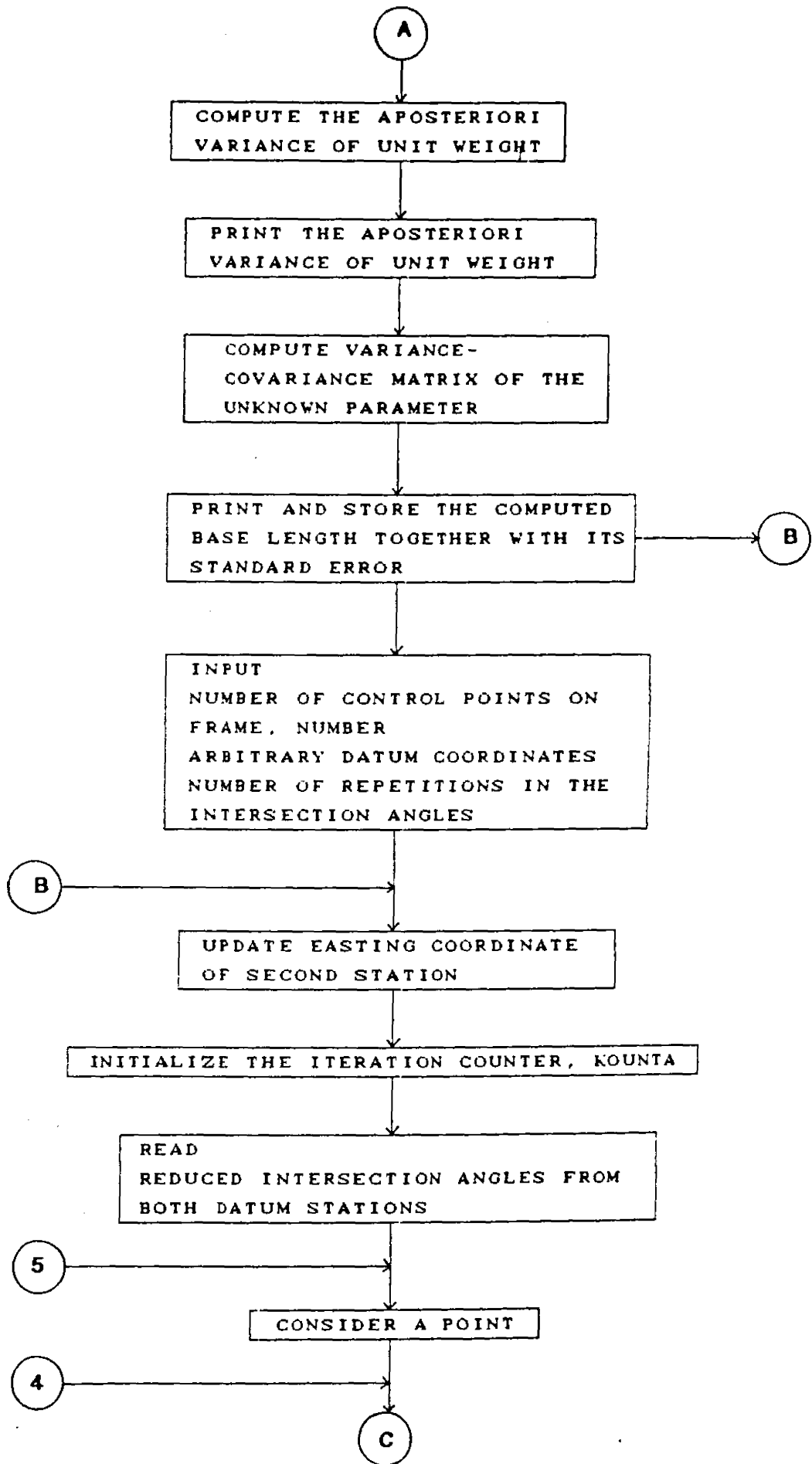
$$W_x = \frac{1}{m_{F_x}^2} \qquad W_y = \frac{1}{m_{F_y}^2} \qquad (A.30)$$

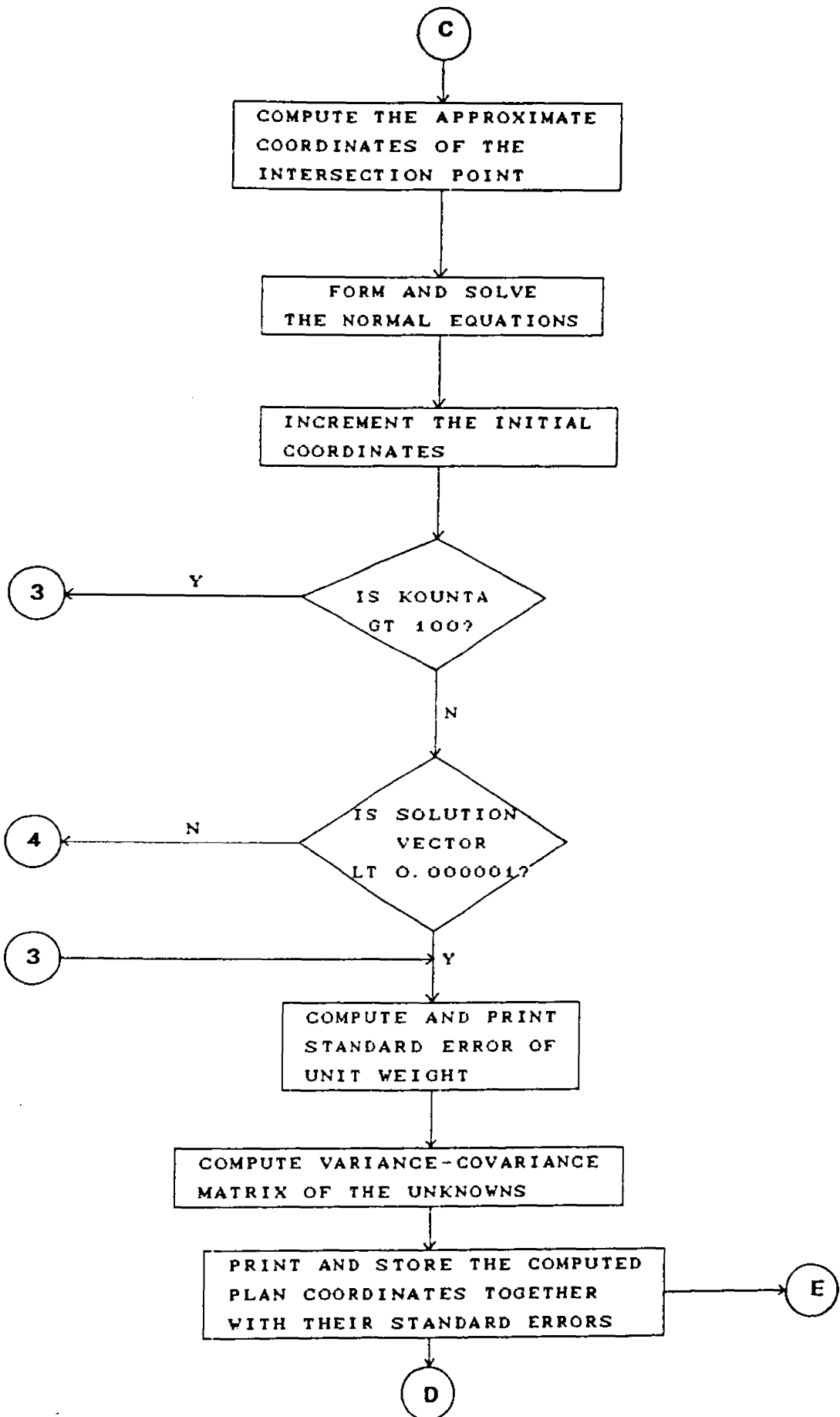
APPENDIX B.

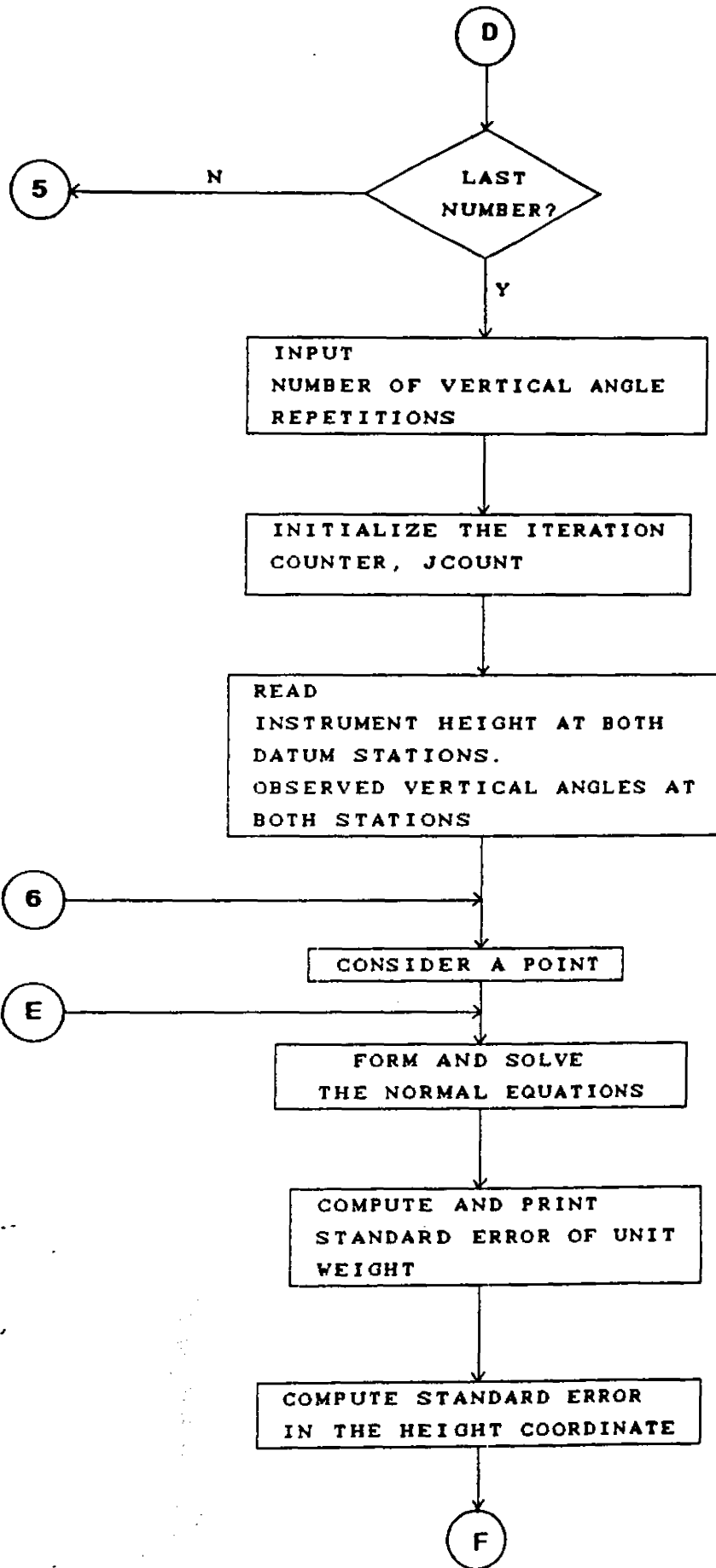
PROGRAM FLOW CHARTS.

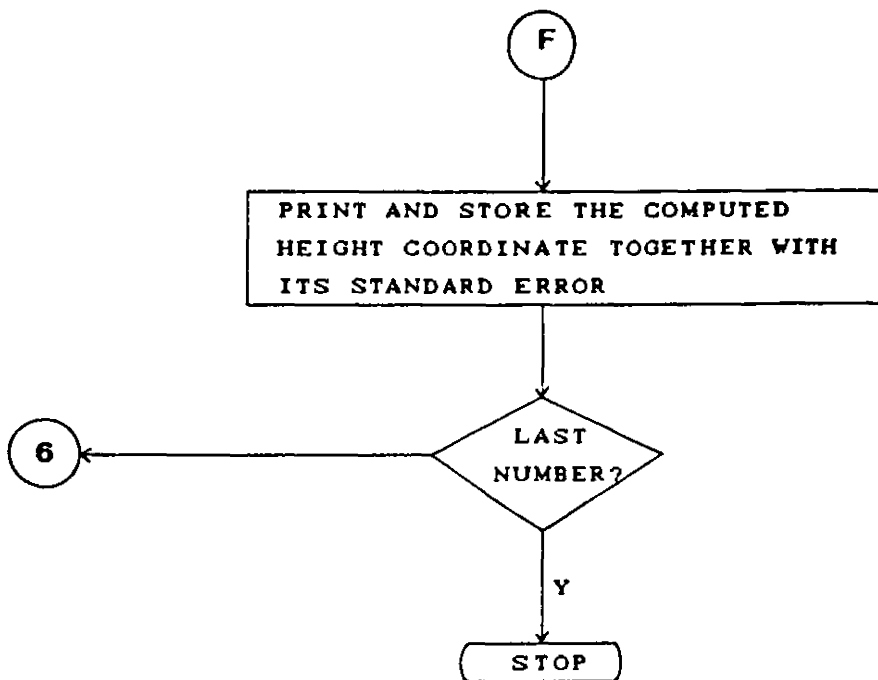
B.1 Main program COORD.



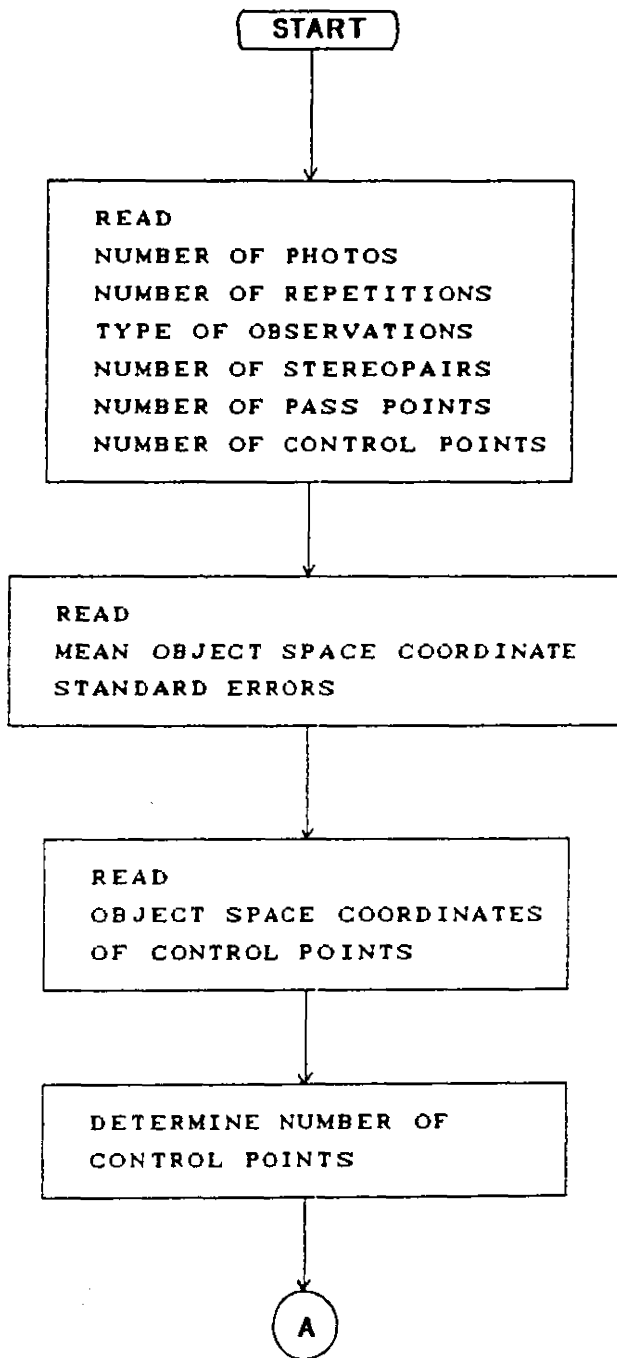


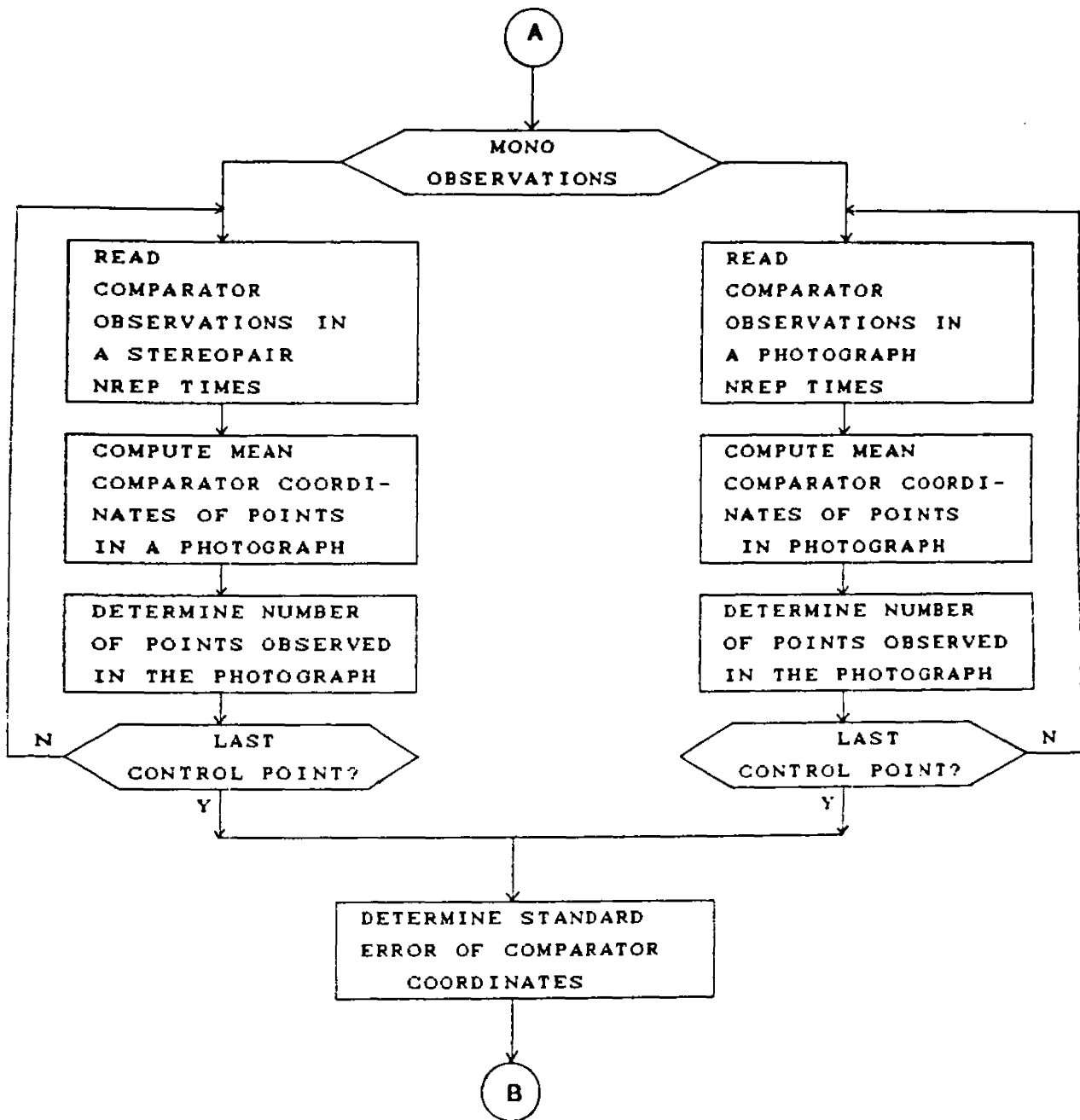


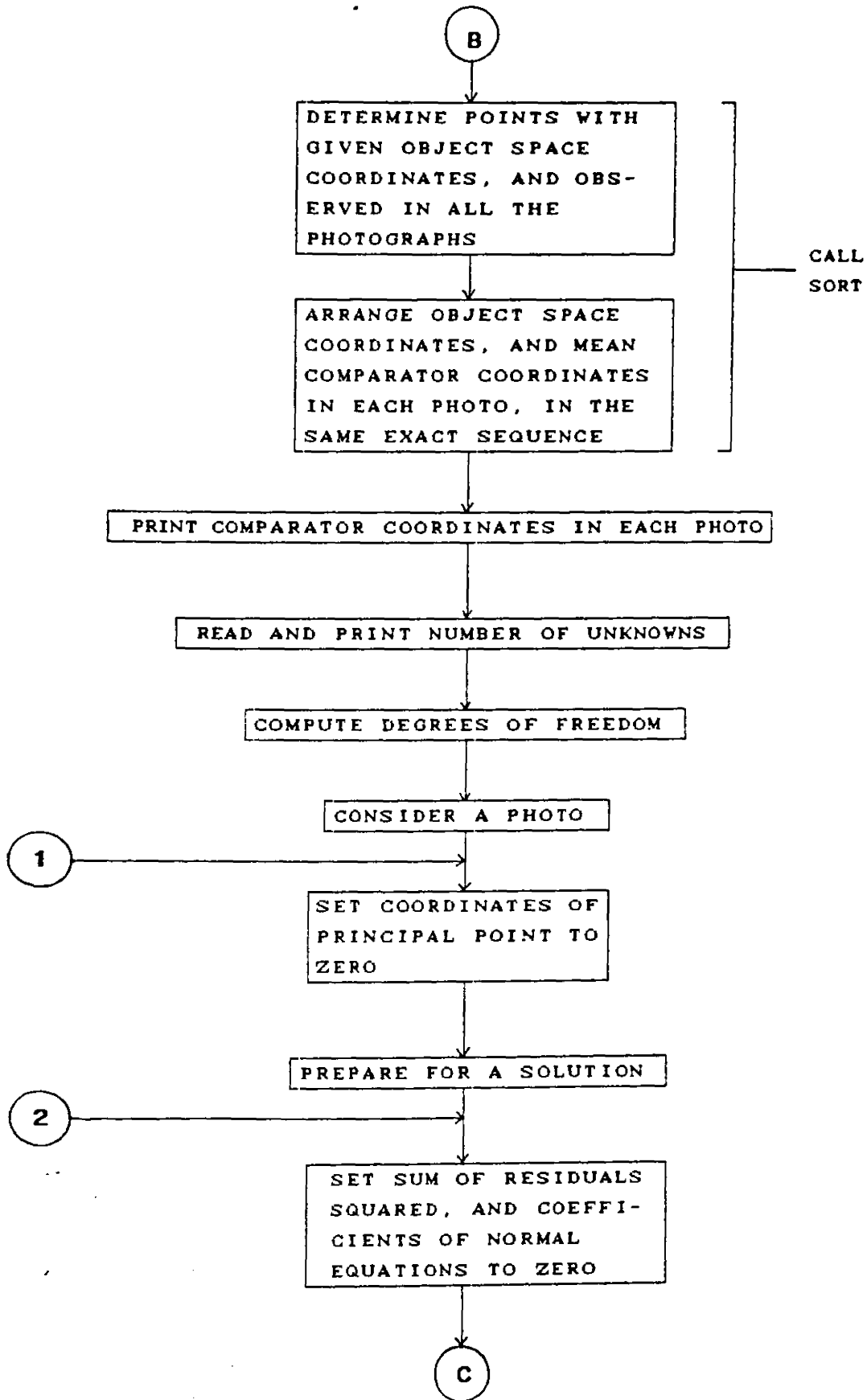


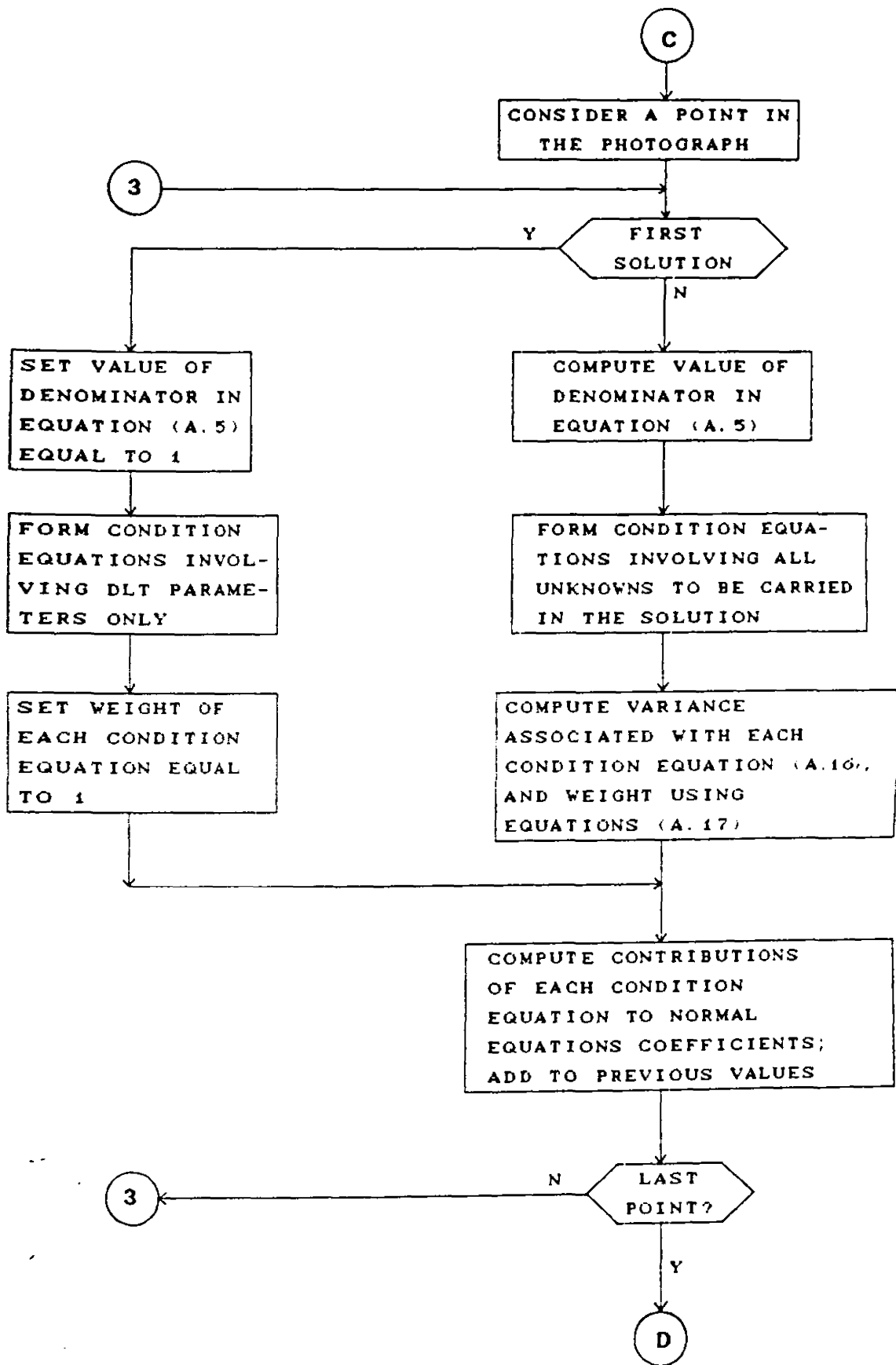


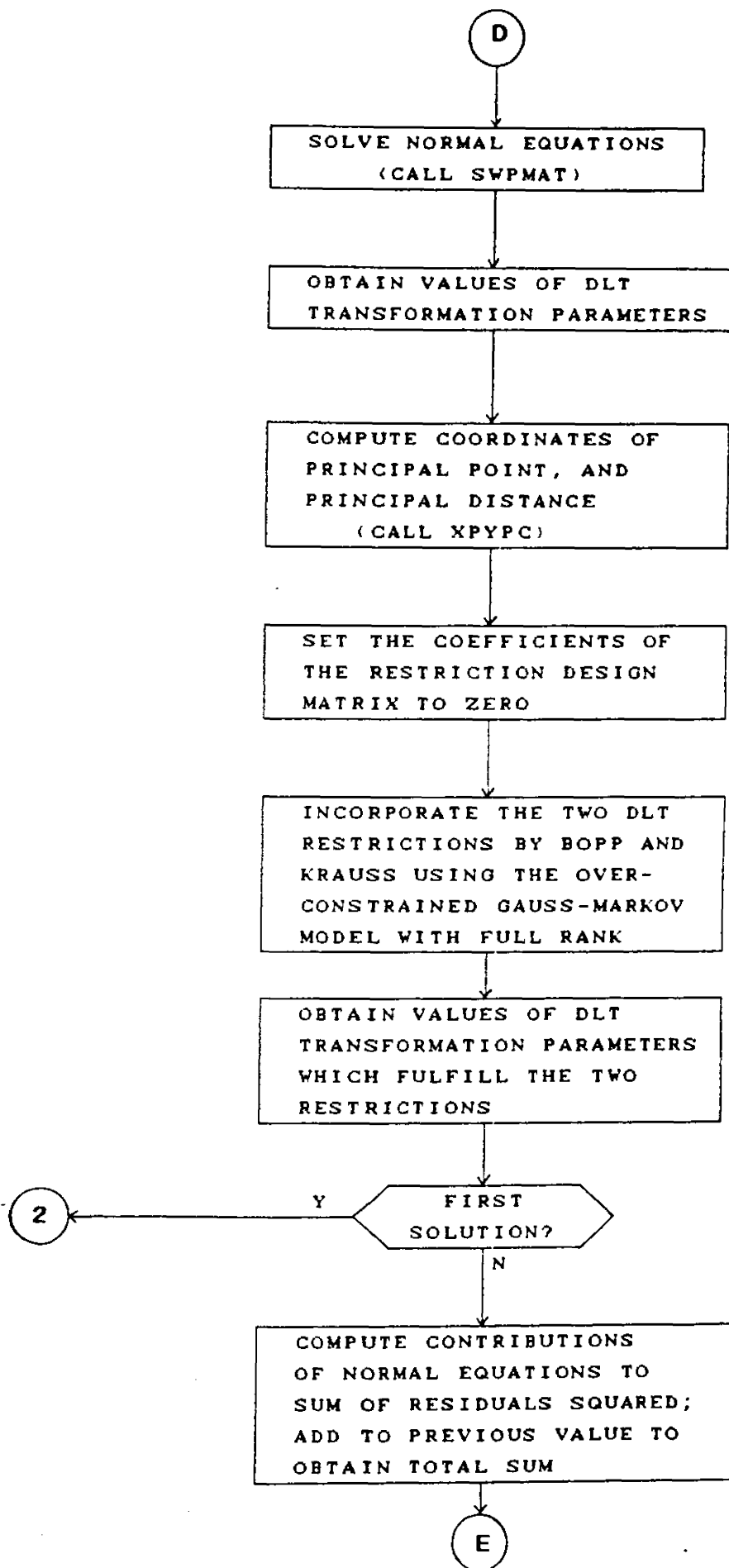
B.2 Main program DLT.

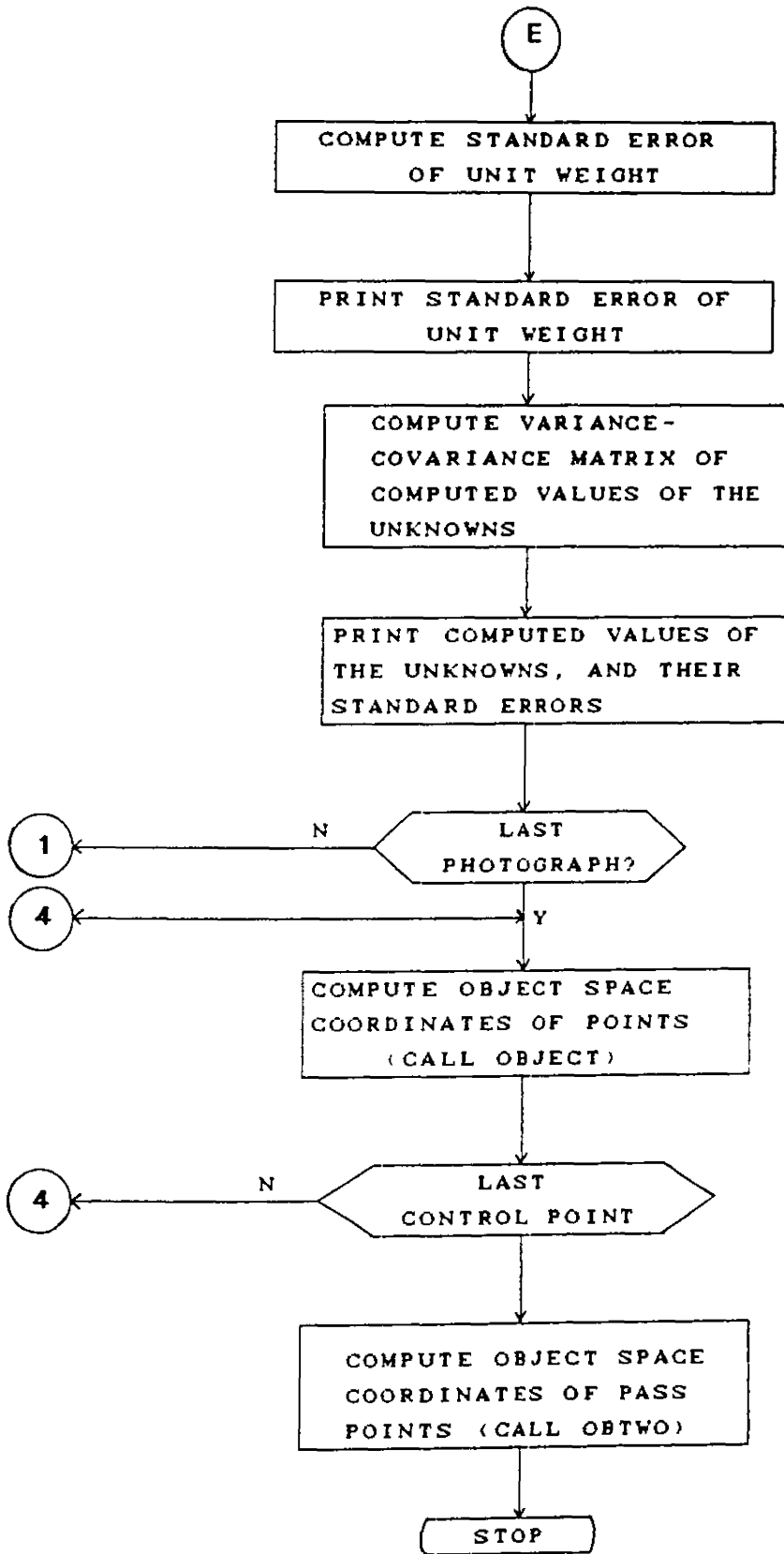




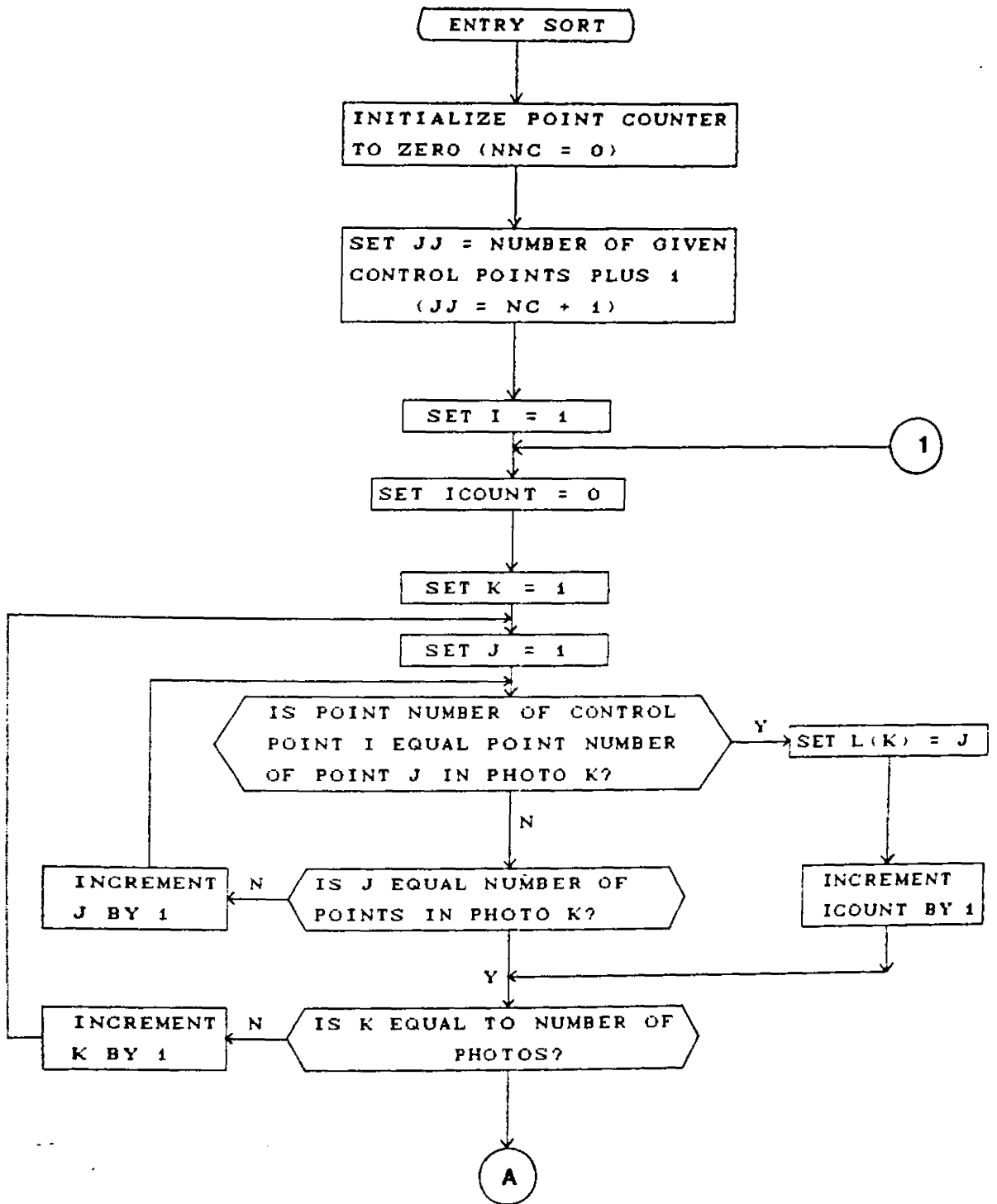


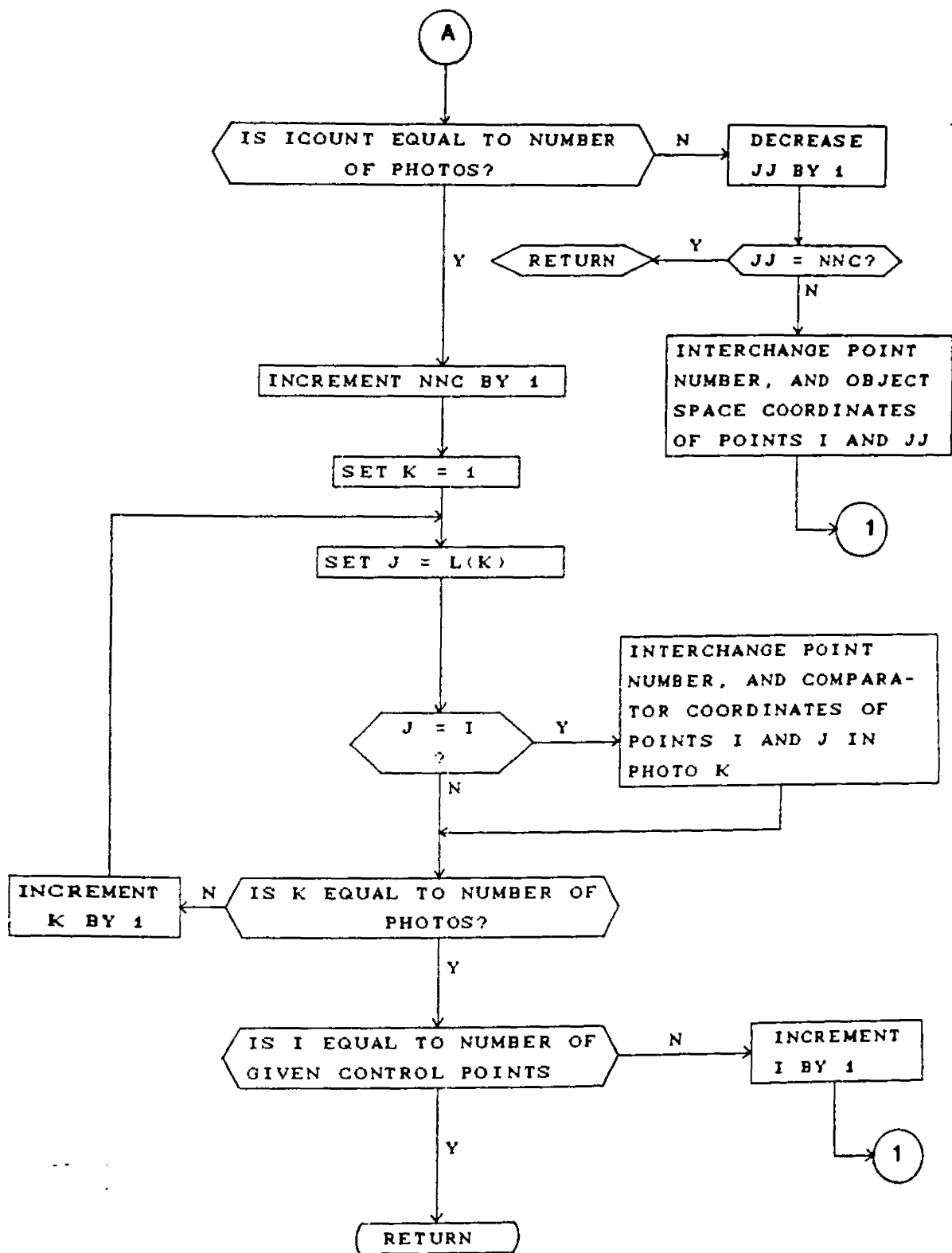




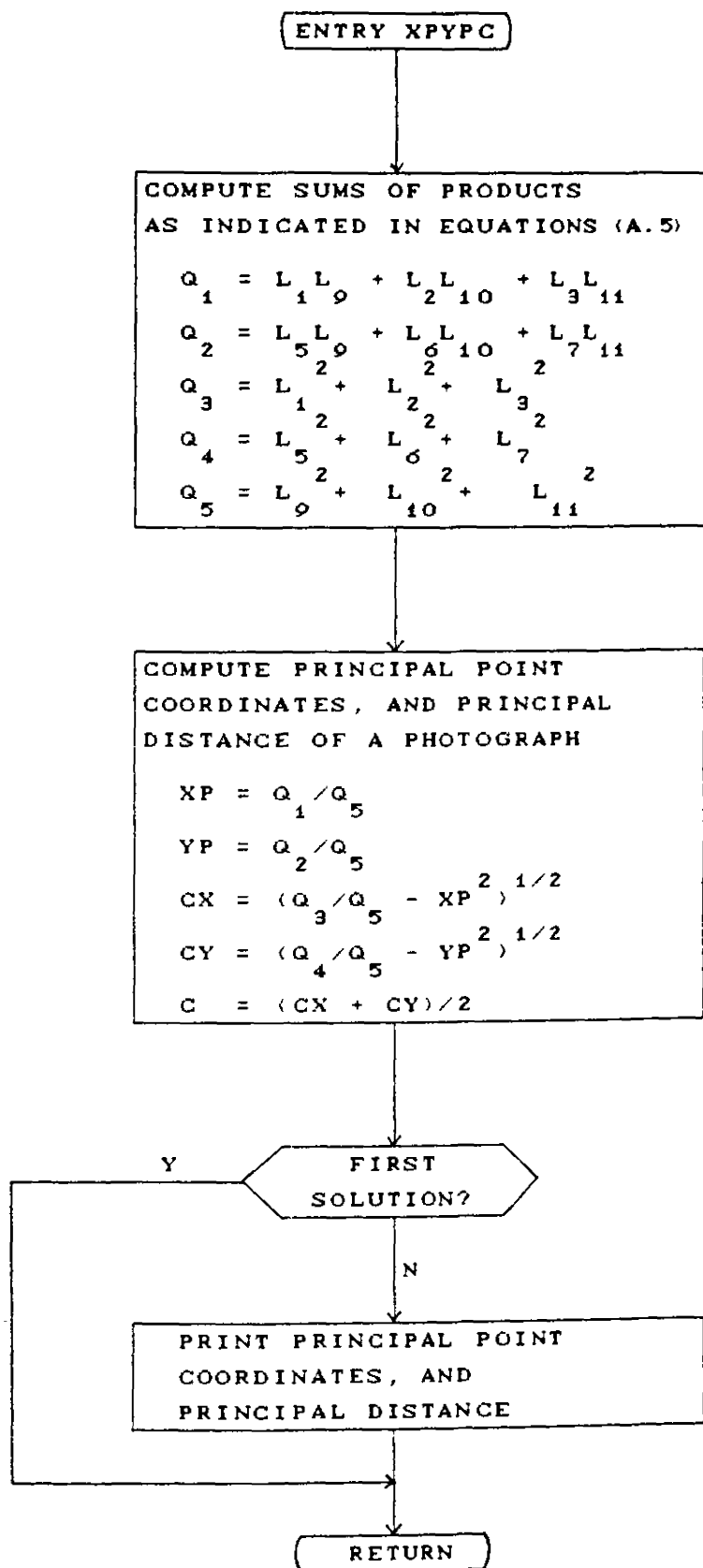


B.3 Subroutine SORT.

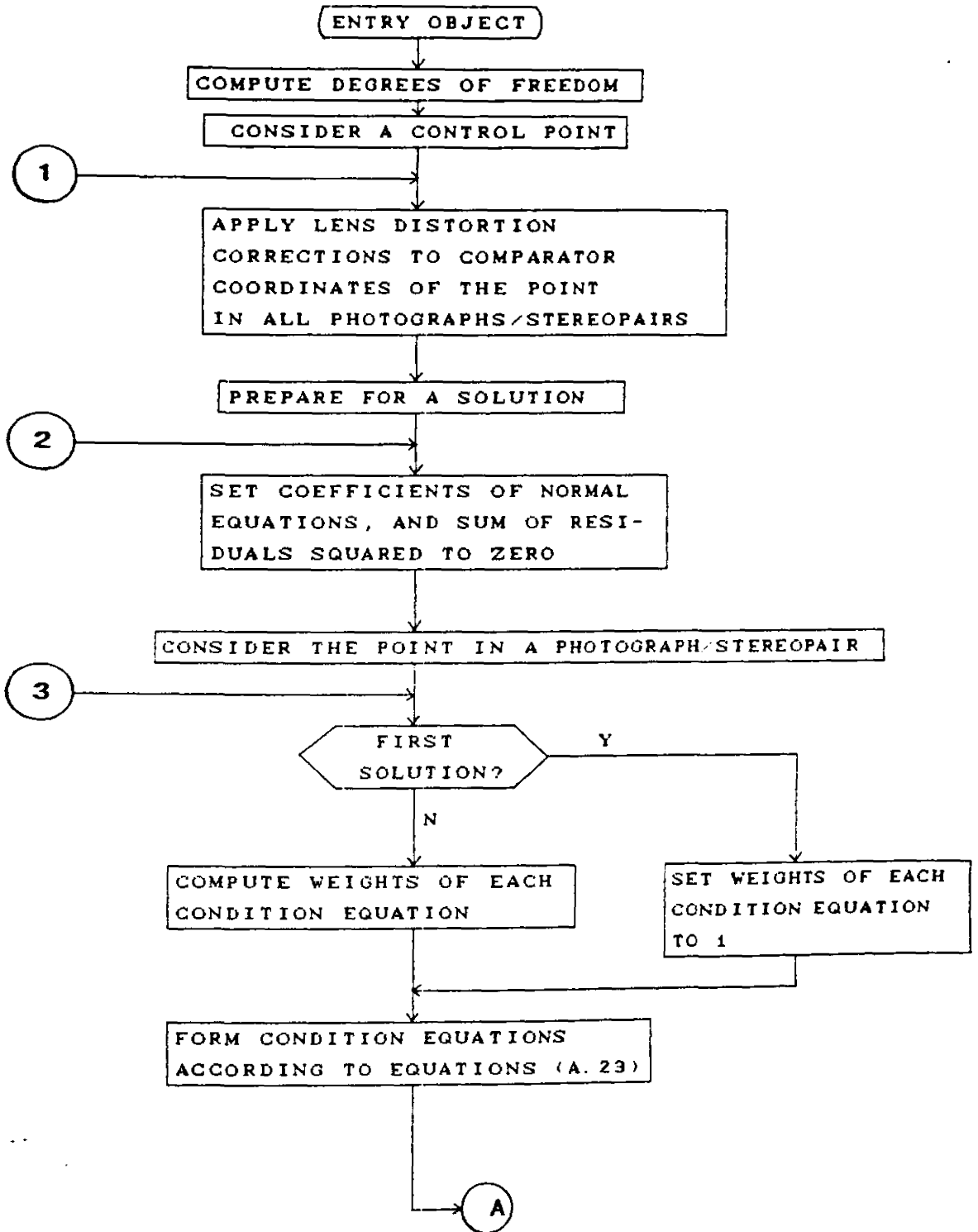


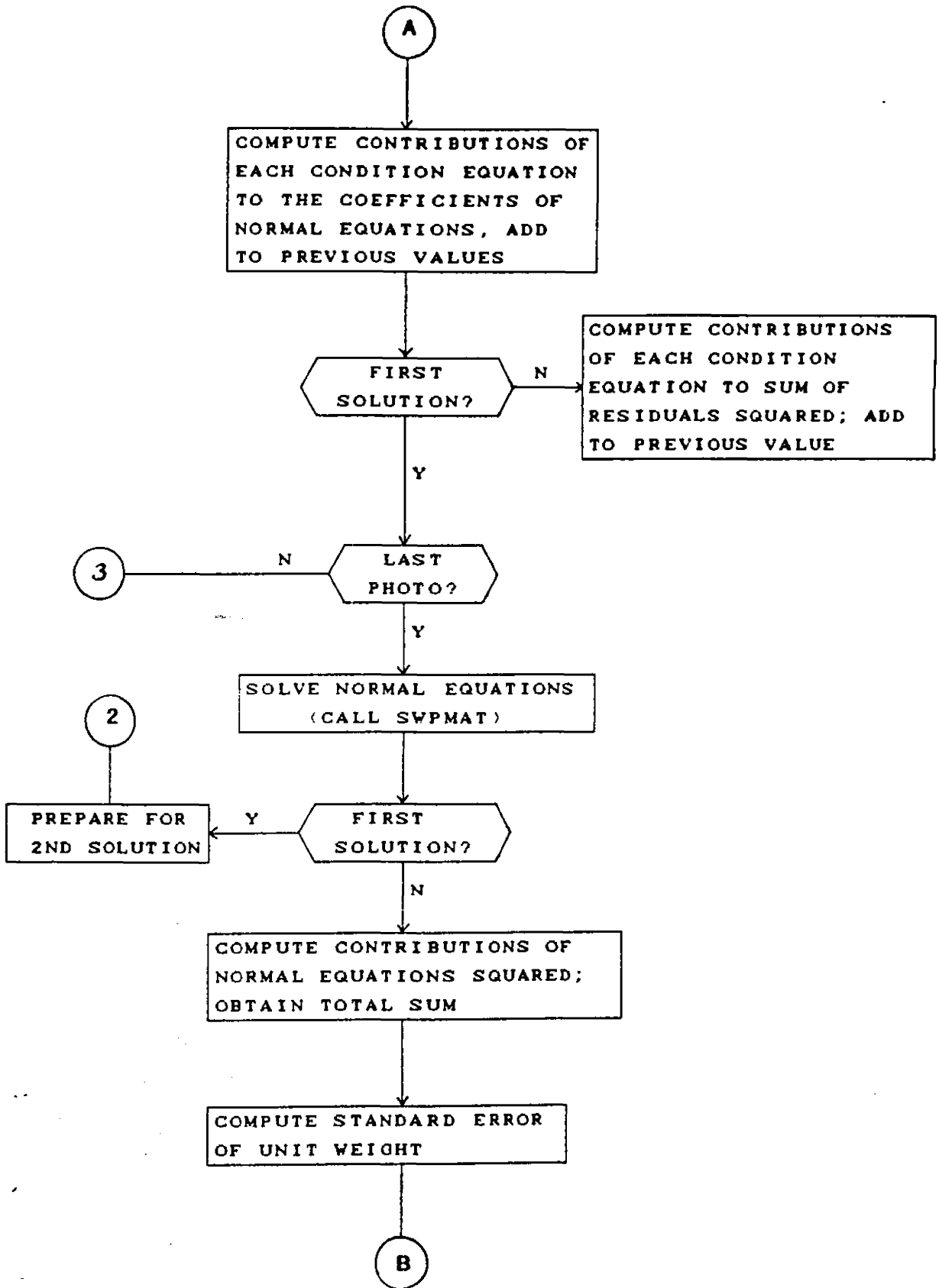


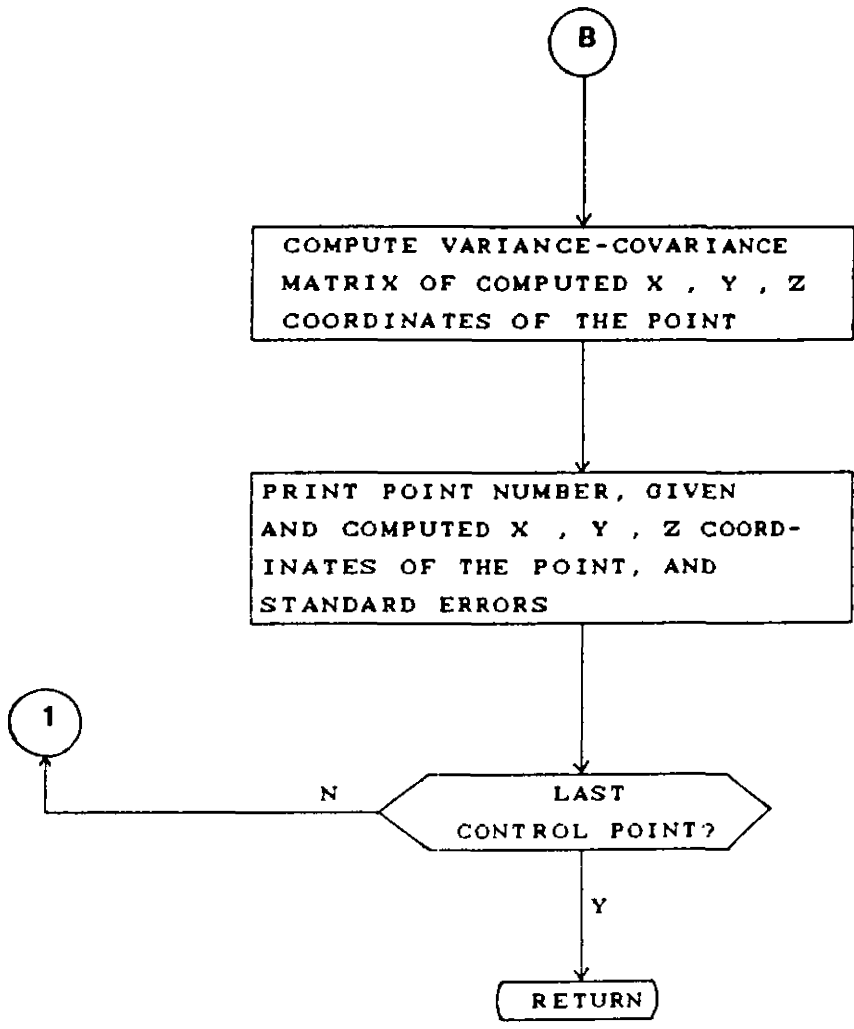
B.4 Subroutine XPYPC.



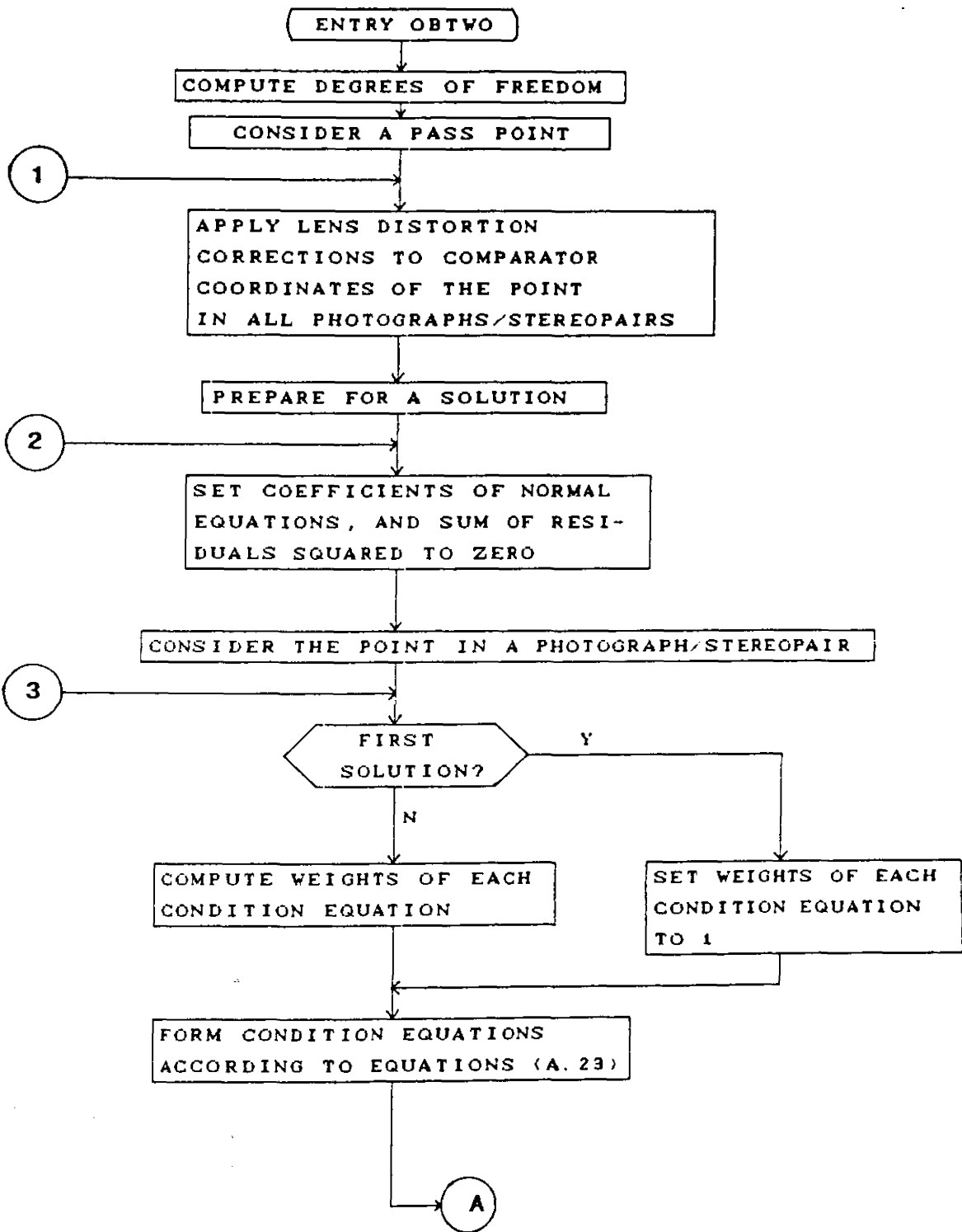
B.5 Subroutine OBJECT.

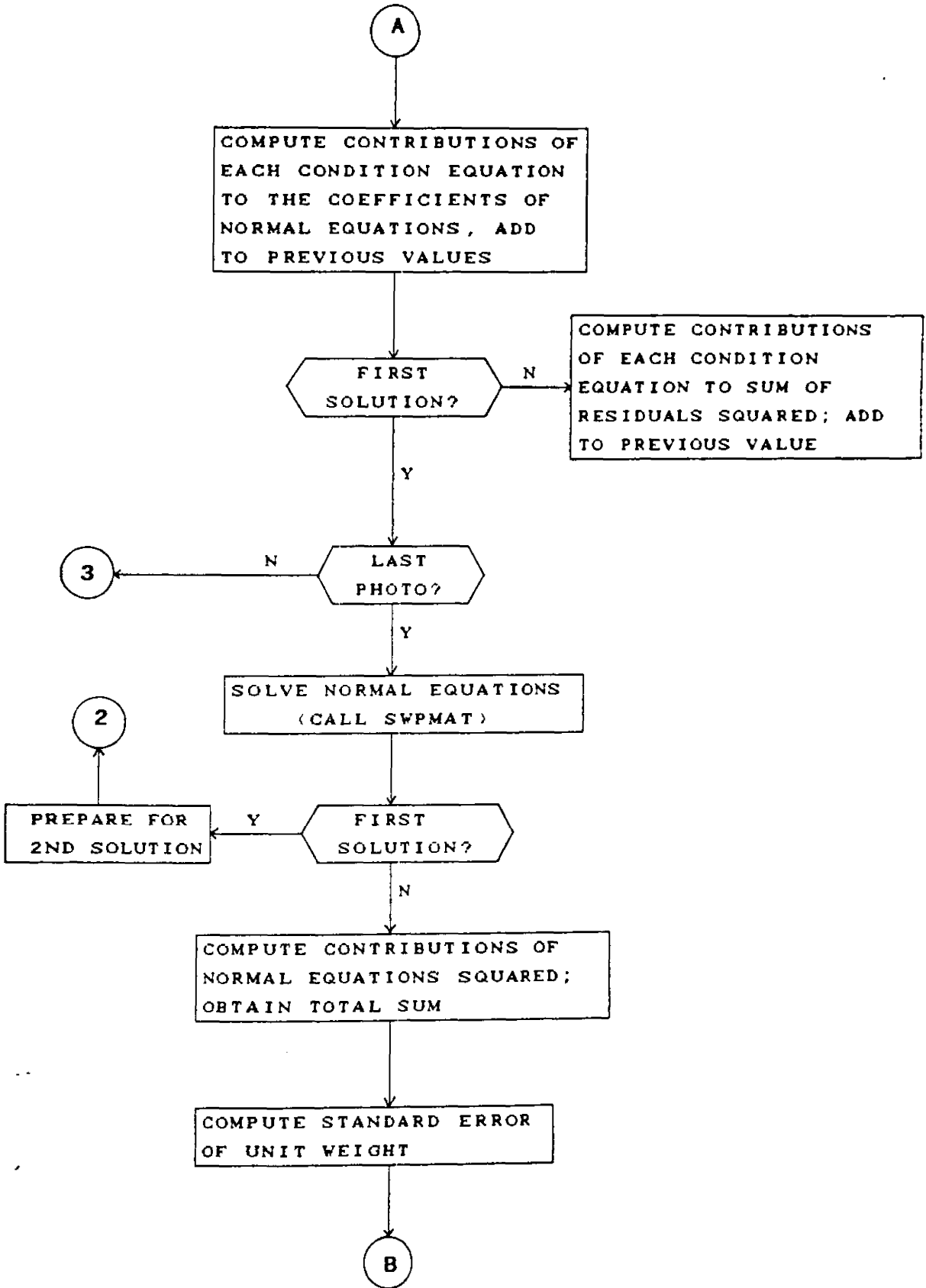


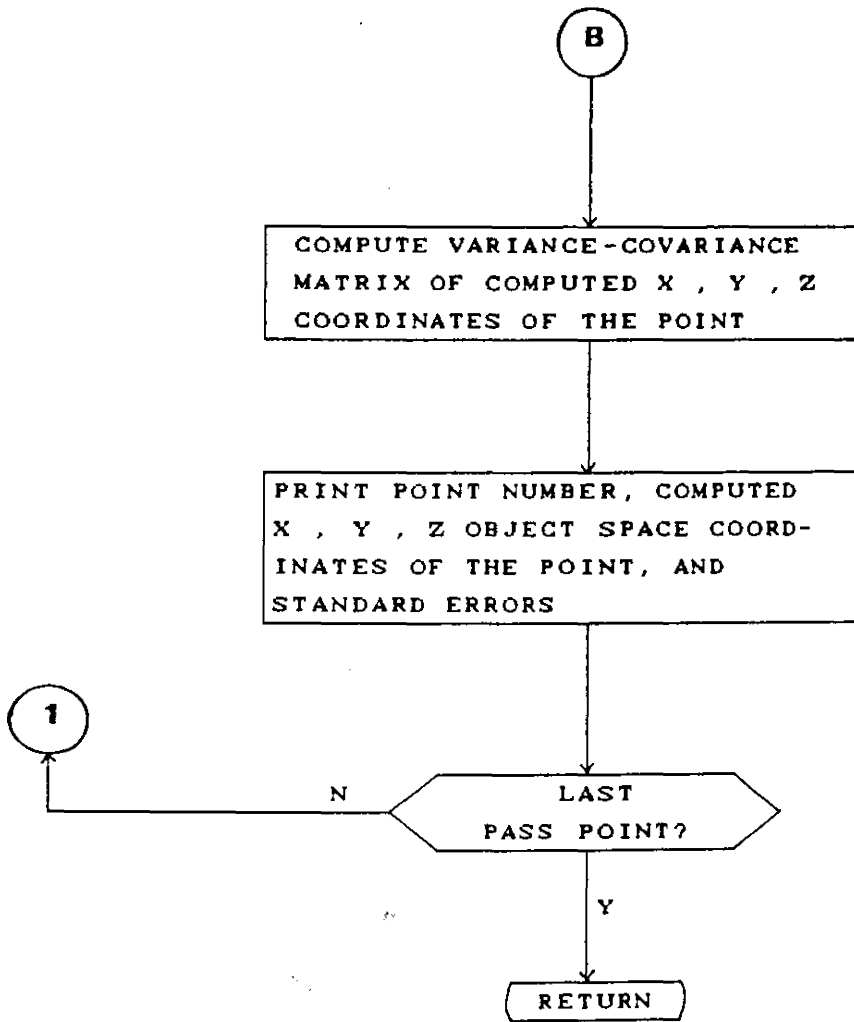




B.6 SUBROUTINE OBTWO.







APPENDIX C.

C.1 Simplified version of the DLT restrictions.

According to section 3.7 the two DLT restrictions are:

$$r_1 = (L_1^2 + L_2^2 + L_3^2) - (L_5^2 + L_6^2 + L_7^2) + \frac{C^2 - B^2}{D} = 0 \quad (C.1.1)$$

$$r_2 = A - \frac{B.C}{D} = 0 \quad (C.1.2)$$

where

$$A = L_1 L_5 + L_2 L_6 + L_3 L_7$$
$$B = L_1 L_9 + L_2 L_{10} + L_3 L_{11}$$
$$C = L_5 L_9 + L_6 L_{10} + L_7 L_{11}$$
$$D = L_9^2 + L_{10}^2 + L_{11}^2$$

Simplifying the above restrictions gives:

$$r_1 = (L_2^2 + L_3^2 - L_6^2 - L_7^2)L_9^2 + (L_1^2 + L_3^2 - L_5^2 - L_7^2)L_{10}^2 \\ + (L_1^2 + L_2^2 - L_5^2 - L_6^2)L_{11}^2 + 2(L_5 L_6 - L_1 L_2)L_9 L_{10} \\ + 2(L_5 L_7 - L_1 L_3)L_9 L_{11} + 2(L_6 L_7 - L_2 L_3)L_{10} L_{11} = 0 \quad (C.1.3)$$

$$r_2 = (L_9^2 + L_{11}^2)L_2 L_6 + (L_9^2 + L_{10}^2)L_3 L_7 + (L_{10}^2 + L_{11}^2)L_1 L_5 \\ - (L_2 L_5 + L_1 L_6)L_9 L_{10} - (L_3 L_5 + L_1 L_7)L_9 L_{11} \\ - (L_3 L_6 + L_2 L_7)L_{10} L_{11} = 0 \quad (C.1.4)$$

C.2 The elements of the restriction design matrix.

As defined in section 6.2 the individual elements of the restriction design matrix are given as follows;

$$\frac{\partial r_1}{\partial L_1} = 2(L_1 L_{10}^2 + L_1 L_{11}^2 - L_2 L_9 L_{10} - L_3 L_9 L_{11})$$

$$\frac{\partial r_1}{\partial L_2} = 2(L_2 L_9^2 + L_2 L_{11}^2 - L_1 L_9 L_{10} - L_3 L_{10} L_{11})$$

$$\frac{\partial r_1}{\partial L_3} = 2(L_3 L_9^2 + L_3 L_{10}^2 - L_1 L_9 L_{11} - L_2 L_{10} L_{11})$$

$$\frac{\partial r_1}{\partial L_4} = 0$$

$$\frac{\partial r_1}{\partial L_5} = 2(L_6 L_9 L_{10} + L_7 L_9 L_{11} - L_5 L_{10}^2 - L_5 L_{11}^2)$$

$$\frac{\partial r_1}{\partial L_6} = 2(L_5 L_9 L_{10} + L_7 L_{10} L_{11} - L_6 L_9^2 - L_6 L_{11}^2)$$

$$\frac{\partial r_1}{\partial L_7} = 2(L_6 L_{10} L_{11} + L_5 L_9 L_{11} - L_7 L_9^2 - L_7 L_{10}^2)$$

$$\frac{\partial r_1}{\partial L_8} = 0$$

$$\frac{\partial r_1}{\partial L_9} = 2(L_2^2 L_9 + L_3^2 L_9 - L_6^2 L_9 - L_7^2 L_9 + L_5 L_6 L_{10} + L_5 L_7 L_{11} - L_1 L_2 L_{10} - L_1 L_3 L_{11})$$

$$\frac{\partial r_1}{\partial L_{10}} = 2(L_1^2 L_{10} + L_3^2 L_{10} - L_5^2 L_{10} - L_7^2 L_{10} + L_5 L_6 L_9 + L_6 L_7 L_{11} - L_1 L_2 L_9 - L_2 L_3 L_{11})$$

$$\frac{\partial r_1}{\partial L_{11}} = 2(L_1^2 L_{11} + L_2^2 L_{11} - L_5^2 L_{11} - L_6^2 L_{11} + L_6 L_7 L_{10} + L_5 L_7 L_9 - L_1 L_3 L_9 - L_2 L_3 L_{10})$$

$$\frac{\partial r_2}{\partial L_1} = L_5 L_{10}^2 + L_5 L_{11}^2 - L_6 L_9 L_{10} - L_7 L_9 L_{11}$$

$$\frac{\partial r_2}{\partial L_2} = L_6 L_9^2 + L_6 L_{11}^2 - L_5 L_9 L_{10} - L_7 L_{10} L_{11}$$

$$\frac{\partial r_2}{\partial L_3} = L_7 L_9^2 + L_7 L_{10}^2 - L_5 L_9 L_{11} - L_6 L_{10} L_{11}$$

$$\frac{\partial r_2}{\partial L_4} = 0$$

$$\frac{\partial r_2}{\partial L_5} = L_1 L_{10}^2 + L_1 L_{11}^2 - L_2 L_9 L_{10} - L_3 L_9 L_{11}$$

$$\frac{\partial r_2}{\partial L_6} = L_2 L_9^2 + L_2 L_{11}^2 - L_1 L_9 L_{10} - L_3 L_{10} L_{11}$$

$$\frac{\partial r_2}{\partial L_7} = L_3 L_9^2 + L_3 L_{10}^2 - L_1 L_9 L_{11} - L_2 L_{10} L_{11}$$

$$\frac{\partial r_2}{\partial L_8} = 0$$

$$\frac{\partial r_2}{\partial L_9} = 2(L_2 L_6 L_9 + L_3 L_7 L_9) - L_1 L_6 L_{10} - L_1 L_7 L_{11} - L_2 L_5 L_{10} - L_3 L_5 L_{11}$$

$$\frac{\partial r_2}{\partial L_{10}} = 2(L_1 L_5 L_{10} + L_3 L_7 L_{10}) - L_1 L_6 L_9 - L_2 L_5 L_9 - L_2 L_7 L_{11} - L_3 L_6 L_{11}$$

$$\frac{\partial r_2}{\partial L_{11}} = 2(L_{1511} L_{11} + L_{2611} L_{11}) - L_{179} L_{11} - L_{2710} L_{11} - L_{359} L_{11} - L_{3610} L_{11}$$

C.3 Coordinate list of the control frame.

STN	Y(M)	X(M)	Z(M)	POS (mm)
	RMS (mm)			
F1	994.933	1002.201	1001.842	4.887
	0.392	0.392	4.855	
F2	994.940	1002.425	1001.843	4.662
	0.393	0.393	4.629	
F3	994.947	1002.673	1001.844	4.387
	0.408	0.408	4.349	
F4	994.954	1002.923	1001.843	4.046
	0.367	0.367	4.013	
F5	994.960	1003.170	1001.844	3.799
	0.369	0.369	3.763	
F6	994.965	1003.421	1001.844	3.540
	0.394	0.394	3.496	
F7	994.969	1003.672	1001.846	3.197
	0.389	0.389	3.149	
F8	994.976	1003.922	1001.849	2.898
	0.389	0.389	2.845	
F9	994.981	1004.173	1001.852	2.527
	0.370	0.370	2.472	
F10	994.987	1004.421	1001.856	2.242
	0.377	0.377	2.178	
F11	994.994	1004.672	1001.861	1.897
	0.376	0.376	1.821	
F12	994.998	1004.923	1001.862	1.623
	0.375	0.375	1.534	
F13	995.002	1005.173	1001.862	1.296
	0.379	0.379	1.180	
F14	995.004	1005.428	1001.863	1.054
	0.393	0.393	0.895	
F15	995.006	1005.660	1001.864	0.784
	0.395	0.395	0.550	
F16	995.003	1005.670	1001.575	0.781
	0.404	0.404	0.532	
F17	995.001	1005.673	1001.276	0.809
	0.435	0.435	0.526	
F18	995.001	1005.672	1000.975	0.783
	0.418	0.418	0.514	

STN	Y(M)	X(M)	Z(M)	POS (mm)
	RMS (mm)			
F19	994.998	1005.672	1000.676	0.752
	0.393	0.393	0.507	
F20	994.995	1005.672	1000.376	0.762
	0.389	0.389	0.527	
F21	994.992	1005.647	1000.077	0.800
	0.416	0.416	0.542	
F22	994.986	1005.430	1000.078	0.991
	0.392	0.392	0.821	
F23	994.980	1005.180	1000.079	1.294
	0.392	0.392	1.169	
F24	994.974	1004.932	1000.082	1.536
	0.386	0.386	1.436	
F25	994.968	1004.681	1000.084	1.853
	0.376	0.376	1.775	
F26	994.961	1004.432	1000.083	2.147
	0.381	0.381	2.078	
F27	994.954	1004.183	1000.082	2.475
	0.371	0.371	2.419	
F28	994.947	1003.934	1000.081	2.842
	0.409	0.409	2.783	
F29	994.940	1003.685	1000.078	3.111
	0.395	0.395	3.060	
F30	994.931	1003.436	1000.078	3.376
	0.416	0.416	3.324	
F31	994.922	1003.187	1000.075	3.710
	0.427	0.427	3.661	
F32	994.912	1002.938	1000.069	3.916
	0.442	0.442	3.866	
F33	994.902	1002.688	1000.064	4.246
	0.400	0.400	4.208	
F34	994.892	1002.439	1000.059	4.487
	0.410	0.410	4.449	
F35	994.884	1002.218	1000.056	4.797
	0.487	0.487	4.747	
F36	994.890	1002.185	1000.346	4.865
	0.442	0.442	4.825	
F37	994.899	1002.183	1000.647	4.942
	0.489	0.489	4.893	
F38	994.909	1002.182	1000.946	4.956
	0.464	0.464	4.912	
F39	994.916	1002.183	1001.246	4.961
	0.455	0.455	4.919	
F40	994.924	1002.182	1001.545	4.913
	0.474	0.474	4.867	

STN	Y(M)	X(M)	Z(M)	POS (mm)
	RMS (mm)			
M1	994.458	1002.665	1001.608	4.269
	0.488	0.488	4.213	
M2	994.465	1002.905	1001.606	4.029
	0.463	0.463	3.975	
M3	994.472	1003.171	1001.602	3.695
	0.455	0.455	3.639	
M4	994.478	1003.430	1001.602	3.374
	0.449	0.449	3.313	
M5	994.484	1003.688	1001.602	3.104
	0.454	0.454	3.037	
M6	994.490	1003.947	1001.602	2.828
	0.482	0.482	2.745	
M7	994.497	1004.205	1001.605	2.460
	0.450	0.450	2.376	
M8	994.504	1004.464	1001.607	2.160
	0.445	0.445	2.066	
M9	994.510	1004.712	1001.611	1.862
	0.432	0.432	1.759	
M10	994.516	1004.983	1001.615	1.528
	0.440	0.440	1.396	
M11	994.521	1005.221	1001.620	1.276
	0.446	0.446	1.109	
M12	994.516	1005.236	1001.364	1.277
	0.434	0.434	1.120	
M13	994.511	1005.235	1001.102	1.235
	0.428	0.428	1.077	
M14	994.507	1005.235	1000.842	1.544
	0.448	0.448	1.092	
M15	994.502	1005.237	1000.584	1.228
	0.416	0.416	1.078	
M16	994.497	1005.218	1000.332	1.711
	0.426	0.426	1.161	
M17	994.491	1004.988	1000.336	1.458
	0.404	0.404	1.341	
M18	994.485	1004.718	1000.340	2.461
	0.432	0.432	1.740	
M19	994.478	1004.457	1000.341	2.144
	0.447	0.447	2.049	
M20	994.470	1004.198	1000.341	2.436
	0.432	0.432	2.358	
M21	994.461	1003.938	1000.340	2.774
	0.437	0.437	2.704	
M22	994.454	1003.680	1000.338	3.081
	0.447	0.447	3.015	

STN	Y(M)	X(M)	Z(M)	POS (mm)
	RMS (mm)			
M23	994.447	1003.420	1000.335	3.355
	0.489	0.489	3.283	
M24	994.440	1003.167	1000.332	3.652
	0.456	0.456	3.595	
M25	994.432	1002.904	1000.326	3.932
	0.465	0.465	3.877	
M26	994.424	1002.669	1000.319	4.199
	0.472	0.472	4.146	
M27	994.431	1002.651	1000.572	4.200
	0.474	0.474	4.146	
M28	994.440	1002.651	1000.832	4.253
	0.457	0.457	4.204	
M29	994.448	1002.650	1001.091	4.322
	0.496	0.496	4.265	
M30	994.454	1002.648	1001.351	4.304
	0.514	0.514	4.242	
R1	993.976	1003.051	1001.267	3.735
	0.502	0.502	3.667	
R2	993.985	1003.349	1001.268	3.405
	0.514	0.514	3.326	
R3	993.994	1003.648	1001.269	3.057
	0.500	0.500	2.974	
R4	994.003	1003.946	1001.268	2.695
	0.443	0.443	2.621	
R5	994.011	1004.245	1001.269	2.335
	0.446	0.446	2.248	
R6	994.019	1004.544	1001.268	1.994
	0.456	0.456	1.887	
R7	994.027	1004.852	1001.268	1.661
	0.446	0.446	1.537	
R8	994.026	1004.893	1001.174	1.646
	0.474	0.474	1.503	
R9	994.021	1004.891	1000.961	1.654
	0.467	0.467	1.516	
R10	994.015	1004.893	1000.775	1.604
	0.463	0.463	1.464	
R11	994.012	1004.851	1000.681	1.671
	0.472	0.472	1.532	
R12	994.004	1004.551	1000.681	1.971
	0.461	0.461	1.860	
R13	993.996	1004.248	1000.680	2.308
	0.514	0.514	2.191	
R14	993.988	1003.947	1000.680	2.651
	0.472	0.472	2.566	

STN	Y(M)	X(M)	Z(M)	POS (mm)
	RMS (mm)			
R15	993.980	1003.649	1000.679	2.946
	0.526	0.526	2.851	
R16	993.972	1003.350	1000.679	3.332
	0.523	0.523	3.249	
R17	993.963	1003.049	1000.678	3.720
	0.543	0.543	3.640	
R18	993.964	1003.007	1000.772	3.685
	0.543	0.543	3.604	
R19	993.969	1003.008	1000.772	3.711
	0.531	0.531	3.634	
R20	993.973	1003.007	1000.994	3.795
	0.544	0.544	3.716	

FIG. 2-1. Copy "A" - Original for the file

THE KENYA POLICE - TRAFFIC DEPARTMENT ACCIDENT REPORT FORM										Acc. Reg. No.		
Police Division			Police Station			On - Reg. No.		U.B. No.				
Day, date and time of accident			Road Authority <input type="checkbox"/> MOTC <input type="checkbox"/> Municipality <input type="checkbox"/> Other			<input type="checkbox"/> Urban <input type="checkbox"/> Rural		Speed limit				
Location of accident (indicate milestone or nearest known place with distance)						Road No.		Total number of vehicles				
Types of vehicles and other participants involved			Register Number		Name and address of owner/driver (state which)			Nature/extent/seriousness of damages				
1 <input type="checkbox"/> JSC <input type="checkbox"/> PU <input type="checkbox"/> LO <input type="checkbox"/> LT <input type="checkbox"/> BU <input type="checkbox"/> MA <input type="checkbox"/> MC <input type="checkbox"/> BC <input type="checkbox"/> OT <input type="checkbox"/> PED												
2 <input type="checkbox"/> JSC <input type="checkbox"/> PU <input type="checkbox"/> LO <input type="checkbox"/> LT <input type="checkbox"/> BU <input type="checkbox"/> MA <input type="checkbox"/> MC <input type="checkbox"/> BC <input type="checkbox"/> OT <input type="checkbox"/> PED												
3 <input type="checkbox"/> JSC <input type="checkbox"/> PU <input type="checkbox"/> LO <input type="checkbox"/> LT <input type="checkbox"/> BU <input type="checkbox"/> MA <input type="checkbox"/> MC <input type="checkbox"/> BC <input type="checkbox"/> OT <input type="checkbox"/> PED												
Name and address of injured person					Type of injury Fat. Ser. Sli.		Veh/part. ref. No.	Class of person	Age	Sex	Position in vehicle	Safety belt usage
Certificate of competence			Vehicle/Particip. No. 1		Vehicle/Particip. No. 2		Vehicle/Particip. No. 3		Pedestrian accidents only			
Driving licence No. valid/not valid									If pedestrian was crossing the road he/she was: <input type="checkbox"/> on pedestrian crossing <input type="checkbox"/> 1-25m from pedestrian crossing <input type="checkbox"/> over 25m			
Road licence No. valid/not valid									If pedestrian was walking along the road he/she was walking: <input type="checkbox"/> in the direction of traffic <input type="checkbox"/> towards the traffic Comments about pedestrian movement:			
Insurance company												
Ins. certificate No. valid/not valid												
P.S.V. licence No. valid/not valid												
Road surface		Width of surface	Condition of road at the accident site							Surface was		
<input type="checkbox"/> tarmac <input type="checkbox"/> murrum <input type="checkbox"/> earth		_____m	<input type="checkbox"/> damaged If damaged, tick below as appropriate <input type="checkbox"/> not damaged <input type="checkbox"/> potholes <input type="checkbox"/> damaged edges <input type="checkbox"/> corrugated <input type="checkbox"/> loose stones on the surface							<input type="checkbox"/> met <input type="checkbox"/> dry		
Accident site was:		Junction accidents only			Traffic signs and signals at junction				Railway level crossing			
<input type="checkbox"/> junction <input type="checkbox"/> not junction		Junction type was: <input type="checkbox"/> T-junction <input type="checkbox"/> 4-leg junction <input type="checkbox"/> roundabout <input type="checkbox"/> other junction			<input type="checkbox"/> give way <input type="checkbox"/> stop <input type="checkbox"/> no signs <input type="checkbox"/> no traffic light signals If there were traffic light signals, were they: <input type="checkbox"/> operating <input type="checkbox"/> not operating				<input type="checkbox"/> uncontrolled <input type="checkbox"/> controlled <input type="checkbox"/> no railway crossing			
Road works at the accident site		Weather conditions		Illumination				Apparent police cause code No.				
<input type="checkbox"/> yes <input type="checkbox"/> no		<input type="checkbox"/> clear <input type="checkbox"/> cloudy <input type="checkbox"/> foggy <input type="checkbox"/> rainy		<input type="checkbox"/> daylight <input type="checkbox"/> night time 6.45p.m.-6.15a.m. <input type="checkbox"/> street lights on <input type="checkbox"/> no street lights								
State who was primarily responsible for the accident										Alcohol involved		
										<input type="checkbox"/> yes <input type="checkbox"/> no		

Class of person
 "PS" Front seat
 "RS" Rear seat
 "ST" Standing (inside)
 "OB" On open body
 "M" Motor-cycle
 "B" Bicycle
 "O" Other vehicle
 "P" Pedestrian
 "H" Pick-up, van
 "L" Lorry + trailer
 "B" Bus

Class of person
 "PS" Front seat
 "RS" Rear seat
 "ST" Standing (inside)
 "OB" On open body

Class of person
 "PS" Front seat
 "RS" Rear seat
 "ST" Standing (inside)
 "OB" On open body
 "M" Motor-cycle
 "B" Bicycle
 "O" Other vehicle
 "P" Pedestrian
 "H" Pick-up, van
 "L" Lorry + trailer
 "B" Bus

Tick where necessary

names and addresses of witnesses

details of accident and remarks of the investigating officer

draw a sketch plan of the accident site

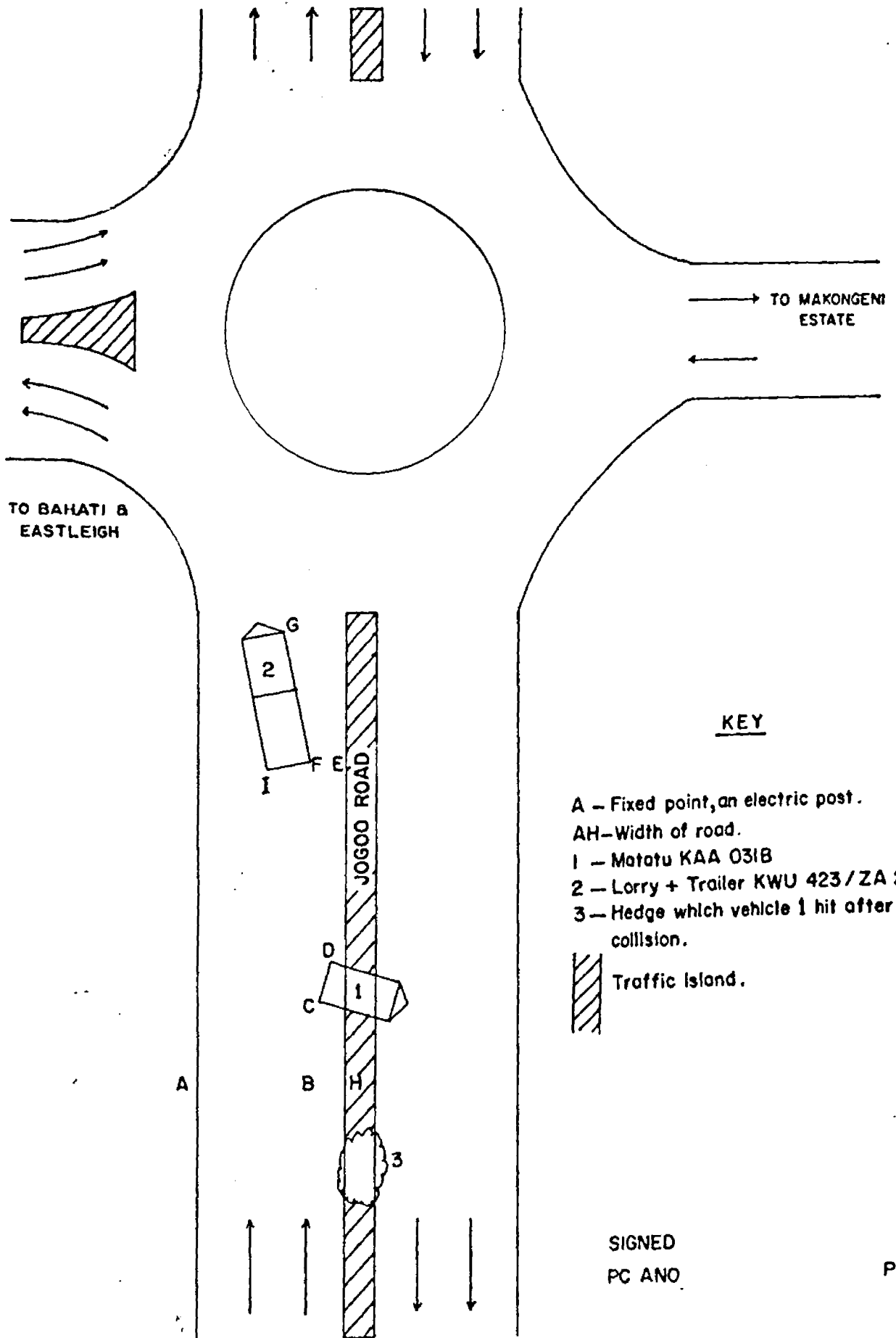
Additional information on types of vehicles.	Tick relevant vehicle/participant reference number	
<input type="checkbox"/> <input type="checkbox"/> <input type="checkbox"/> country bus	<input type="checkbox"/> <input type="checkbox"/> <input type="checkbox"/> GK bus	<input type="checkbox"/> <input type="checkbox"/> <input type="checkbox"/> taxicab
<input type="checkbox"/> <input type="checkbox"/> <input type="checkbox"/> XBS	<input type="checkbox"/> <input type="checkbox"/> <input type="checkbox"/> institutional bus	<input type="checkbox"/> <input type="checkbox"/> <input type="checkbox"/> tanker
<input type="checkbox"/> <input type="checkbox"/> <input type="checkbox"/> other urban bus	<input type="checkbox"/> <input type="checkbox"/> <input type="checkbox"/> mini bus	

Has a notice of intended prosecution been served? yes no


When a police vehicle is involved this form must be despatched to the Commissioner of Police and the Divisional Transport Officer within 24 hours	Despatched to Commissioner of Police P.P.O. } Through O.C.P.D. } D.T.O.	Date
---	--	---------------------------------

Reporting Officer	Officer-in-charge Police Station
Date	Date
Signature	Signature

Fig. 2-3. THE RTA SKETCH PLAN



KEY

- A - Fixed point, an electric post.
- AH - Width of road.
- 1 - Matatu KAA 031B
- 2 - Lorry + Trailer KWU 423 / ZA 274B
- 3 - Hedge which vehicle 1 hit after collision.
-  Traffic Island.

SIGNED
PC ANO

PTO

Measurements

- AB - 20ft
- BH - 6ft 7'
- BC - 24ft 2'
- DC - 6ft 8'
- DE - 82ft
- EF - 10ft 3'
- FG - 55ft 2'
- FI - 10ft 2'

```

*****
*
*
*           THIS PROGRAM PERFORMS
*
*           A   T H R E E   D I M E N S I O N A L
*
*           C O O R D I N A T I O N   O F   A
*
*           C O N T R O L   F R A M E   U S I N G
*
*           A   L E A S T   S Q U A R E S
*
*           A D J U S T M E N T   P R O C E D U R E .
*
*****

```

```

PROGRAM COORD
IMPLICIT REAL*8(A-H,O-Z)
PROGRAM BY KIEMA, J.B.K           F/56/7096/90
DEPARTMENT OF SURVEYING & PHOTOGRAMMETRY
UNIVERSITY OF NAIROBI.
-----

```

DIMENSIONING

```

-----
DIMENSION A(50,1),GC(50,1),GOB(50,1),BRG(50),Y(50,1),SEC(6),
<ATA(1,1),AINV(1,1),ATY(1,1),AX(50,1),E(50,1),CV(1,1),
<ETE(1,1),COVX(1,1),STD(1,1),VBRG(20),YC(20,1),ACT(2,20),
<ACTA(2,2),ACINV(2,2),ACTY(2,1),XC(2,1),AXC(50,1),EC(50,1),
<ETC(1,50),ETCE(1,1),COV(2,2),CD(2,1),AV(50,1),BC(50,1),
<BOB(50,1),YV(50,1),AVT(1,50),AVTA(1,1),AVINV(1,1),AVTY(1,1),
<XV(1,1),AVX(50,1),EV(50,1),EVT(1,50),EVTE(1,1),WBRG(20),
<AC(20,2),IDEG(6),IMIN(6),MDEG(50),MMIN(50),NDEG(50),
<NMIN(50),JDEG(20),JMIN(20),KDEG(20),KMIN(20),AT(1,50),
<ESEC(50),FSEC(50),ANG1(50),ANG2(50),ANG(50),X(1,1),EQ(1,1),
<EAPP(1,1),VSEC(20),S1(200),EX(200,1),HX(200,1),SN(200,1),
<SE(200,1),SH(200,1),EE(1,1),EN(1,1),S2(200),WSEC(20),
<BSA(20),BSB(20),ET(1,50),PCA(20),PCB(20)
INTEGER STN(200),REP,VREP,WREP
REAL NAPP(1,1),NX(200,1),NQ(1,1),MPEE,MPEN,MPEH,NA,NB
-----

```

''P'' IS A FACTOR THAT TRANSFORMS RADIANS INTO SECONDS

P=206264.8063

```

*****
THE FIRST PART OF THIS PROGRAM INVOLVES A LEAST SQUARES
COMPUTATION OF THE BASE BETWEEN THE INTERSECTING STATIONS.
*****

```

```

ICOUNT=ITERATION COUNTER
ICOUNT=1
-----

```

INPUT THE NUMBER OF BASE ANGLE REPETITIONS.

```

WRITE(*,2000)
2000 FORMAT(/5X,'ENTER THE NO. OF BASE ANGLE REPETITIONS')
READ(*,2002)REP
2002 FORMAT(I2)
C -----
C READING IN THE REDUCED BASE ANGLES.
C -----
DO 2006 I=1,REP
READ(96,2008)IDEG(I),IMIN(I),SEC(I)
C -----
C CONVERTING THE REDUCED SUBTENSE ANGLES INTO SECONDS.
C -----
BRG(I)=IDEG(I)*3600.0+IMIN(I)*60.0+SEC(I)
2006 CONTINUE
2008 FORMAT(2X,I3,2X,I2,2X,F5.1)
C -----
C APVUW IS THE APRIORI VARIANCE OF UNIT WEIGHT
APVUW=1.0
C -----
C INITIALISING THE DESIGN MATRIX, A.
C -----
DO 2010 I=1,REP
J=1
2010 A(I,J)=0.0
C -----
C INPUT THE APPROXIMATE BASE LENGTH.
C -----
WRITE(*,2012)
2012 FORMAT(/5X,'INPUT THE APPROXIMATE BASE LENGTH')
READ(*,2014)B
2014 FORMAT(F5.1)
C -----
C FORMING THE DESIGN MATRIX A AND THE VECTOR OF OBSERVATIONS Y.
C -----
2022 DO 2016 I=1,REP
J=1
A(I,J)=(2.0/(1.0+B**2))*(-1.0)
GC(I,J)=2.0*ATAN(1.0/B)
GOB(I,J)=BRG(I)/P
Y(I,J)=GOB(I,J)-GC(I,J)
2016 CONTINUE
C -----
C MATRIX MANIPULATION.
C -----
C THE ASSUMPTION HERE IS THAT THE OBSERVATIONS ARE UNCORRELATED
AND ARE OF EQUAL WEIGHT
C -----
CALL TRANSP(A,AT,REP,1)
CALL MULT(AT,A,ATA,1,REP,1)
CALL MATINV(ATA,AINV,1)
CALL MULT(AT,Y,ATY,1,REP,1)
X(1,1)=AINV(1,1)*ATY(1,1)
C -----

```

```

C   'X' IS THE VECTOR OF CORRECTIONS
C   -----
C   INCREMENT THE INITIAL VALUE.
C   -----
C   BASE=B+X(1,1)
C   -----
C   ITERATION CRITERIA
C   -----
C   ICOUNT=ICOUNT+1
C   IF(ICOUNT.GT.100)GO TO 2018
C   B=BASE
C   IF(ABS(X(1,1)).GT.0.000001)GO TO 2022
C   -----
C   ACCURACY ESTIMATION.
C   E IS THE VECTOR OF RESIDUALS
C   -----
2018 WRITE(97,2034)BASE
2034 FORMAT(/5X,'THE BASE LENGTH= ',F8.4,/5X,40('='))
      DO 2054 I=1,REP
      AX(I,1)=A(I,1)*X(1,1)
2054 CONTINUE
      DO 2024 I=1,REP
2024 E(I,1)=Y(I,1)-AX(I,1)
C   -----
C   CALCULATING THE APOSTERIORI VARIANCE OF UNIT WEIGHT.
C   -----
      CALL TRANSP(E,ET,REP,1)
      CALL MULT(ET,E,ETE,1,REP,1)
C   -----
C   VUW IS THE APOSTERIORI VARIANCE OF UNIT WEIGHT
C   DF ARE THE ASSOCIATED DEGREES OF FREEDOM
C   -----
      DF=REP-1
      VUW=ETE(1,1)/DF
C   -----
C   COMPUTING THE VARIANCE-COVARIANCE MATRIX.
C   COVX IS THE COVARIANCE MATRIX OF THE ESTIMATED PARAMETER
C   -----
      COVX(1,1)=AINV(1,1)*VUW
      STDX(1,1)=DSQRT(COVX(1,1))
      WRITE(97,2036)STDX(1,1)
2036 FORMAT(/5X,'THE STANDARD ERROR IN THE BASE LENGTH= ',F10.8,/3X,
>55('='))
C   *****
C   THE SECOND PART OF THIS PROGRAM INVOLVES AN INTERSECTION FOR
C   THE PROVISION OF HORIZONTAL CONTROL.
C   *****
C   INPUT THE NUMBER OF CONTROL POINTS ON THE FRAME.
C   -----
      WRITE(*,2038)
2038 FORMAT(/5X,'ENTER THE NO. OF CONTROL POINTS ON THE FRAME')
      READ(*,2040)NUMBER
2040 FORMAT(I3)

```

NUMB=1

C INPUTING THE FIXED ARBITRARY DATUM COORDINATES FOR THE
C INTERSECTING STATIONS.
C -----

NA=1000.000
EA=1000.000
ZA=1000.000
NB=1000.000
EB=1000.000+BASE
ZB=999.9881

C ITERATION COUNTER.
C INITIALISE THE COUNTER
C -----

NSTART=1

C INPUT THE NUMBER OF REPETITIONS OF THE INTERSECTION ANGLES
C OBSERVED FOR EACH POINT DENOTED BY NUMERO.
C -----

WRITE(*,2070)

2070 FORMAT(/5X,'ENTER THE NO. OF REPETITIONS FOR THE INTERSECTION
< ANGLES')

READ(*,2002)NUMERO
II=1
KOUNTA=1

C READING THE REDUCED INTERSECTION ANGLES FROM BOTH DATUM
C STATIONS.
C -----

200 DO 2042 I=NSTART,NUMERO
READ(96,2044)STN(1),MDEG(I),MMIN(I),ESEC(I),STN(2),NDEG(I),
>NMIN(I),FSEC(I)

C CONVERTING THE REDUCED OBSERVED ANGLES INTO SECONDS THEN
C RADIANS.
C -----

ANG1(I)=MDEG(I)*3600.0+MMIN(I)*60.0+ESEC(I)
ANG2(I)=NDEG(I)*3600.0+NMIN(I)*60.0+FSEC(I)
ANG1(I)=ANG1(I)/P
ANG2(I)=ANG2(I)/P

2042 CONTINUE

2044 FORMAT(2X,I3,2X,I3,2X,I2,2X,F5.1,2X,I3,2X,I3,2X,I2,2X,F5.1)
CD(1,1)=0.0
CD(2,1)=0.0

C COMPUTING THE APPROXIMATE COORDINATES OF THE POINT TO BE
C INTERSECTED
C -----

EAPP(1,1)=(EA/TAN(ANG2(1))+EB/TAN(ANG1(1))+NB-NA)/
<(1.0/TAN(ANG1(1))+1.0/TAN(ANG2(1)))
NAPP(1,1)=(NA/TAN(ANG2(1))+NB/TAN(ANG1(1))+EA-EB)/
<(1.0/TAN(ANG1(1))+1.0/TAN(ANG2(1)))

```

C -----
C FORMING THE DESIGN MATRIX AND THE VECTOR OF OBSERVATIONS.
C -----
C INITIALISING THE DESIGN MATRIX, AC(I,J)
C -----
  NUM=NUMERO*2
  DO 10 I=1,NUM
  DO 10 J=1,2
  AC(I,J)=0.0
10 CONTINUE
  DO 20 I=1,NUMERO
  DO 20 J=1,2
  GO TO (30,40)J
30 K1=2*I-1
  GO TO 50
40 K2=2*I
  GO TO 60
50 AC(K1,J)=1.0/(TAN(ANG1(I)))+1.0/(TAN(ANG2(I)))
  AC(K1,J+1)=0.0
  GO TO 20
60 AC(K2,J-1)=0.0
  AC(K2,J)=1.0/(TAN(ANG1(I)))+1.0/(TAN(ANG2(I)))
20 CONTINUE
C -----
C INITIALISING THE VECTOR OF OBSERVATIONS YI(I,J)
C -----
130 DO 70 I=1,NUM
  J=1
  YC(I,J)=0.0
70 CONTINUE
  DO 80 I=1,NUMERO
  J=1
  I1=2*I-1
  I2=2*I
  YC(I1,J)=(EA/TAN(ANG2(I))+EB/TAN(ANG1(I))+NB-NA)
  <-(1.0/TAN(ANG1(I))+1.0/TAN(ANG2(I)))*EAPP(1,1)
  YC(I2,J)=(NA/TAN(ANG2(I))+NB/TAN(ANG1(I))+EA-EB)
  <-(1.0/TAN(ANG1(I))+1.0/TAN(ANG2(I)))*NAPP(1,1)
80 CONTINUE
C -----
C MATRIX MANIPULATION.
C -----
C THE ASSUMPTION HERE IS THAT THE OBSERVATIONS ARE UNCORRELATED
C AND ARE OF EQUAL WEIGHT
C -----
  CALL TRANSP(AC,ACT,NUM,2)
  CALL MULT(ACT,AC,ACTA,2,NUM,2)
  CALL MATINV(ACTA,ACINV,2)
  CALL MULT(ACT,YC,ACTY,2,NUM,1)
  CALL MULT(ACINV,ACTY,XC,2,2,1)
C ''XC'' IS THE VECTOR OF CORRECTIONS
C -----
C INCREMENT THE APPROXIMATE COORDINATES.

```

EQ(1,1)=EAPP(1,1)+XC(1,1)
NQ(1,1)=NAPP(1,1)+XC(2,1)

ITERATION CRITERIA

KOUNTA=KOUNTA+1
IF(KOUNTA.GT.100)GO TO 110
EAPP(1,1)=EQ(1,1)
NAPP(1,1)=NQ(1,1)
DO 120 I=1,2
120 IF(ABS(XC(I,1))-ABS(CD(I,1))).LT.0.000001)GO TO 110
CD(1,1)=XC(1,1)
CD(2,1)=XC(2,1)
GO TO 130

ACCURACY ESTIMATION.
EC IS THE VECTOR OF RESIDUALS

STORING THE COMPUTED COORDINATES.

110 EX(II,1)=EQ(1,1)
NX(II,1)=NQ(1,1)
CALL MULT(AC,XC,AXC,NUM,2,1)
DO 160 I=1,NUM
160 EC(I,1)=YC(I,1)-AXC(I,1)

CALCULATING THE APOSTERIORI VARIANCE OF UNIT WEIGHT.

CALL TRANSP(EC,ETC,NUM,1)
CALL MULT(ETC,EC,ETCE,1,NUM,1)
DFM=NUMERO-1
AVUW=ETCE(1,1)/DFM

COMPUTING THE VARIANCE-COVARIANCE MATRIX.

DO 180 I=1,2
DO 180 J=1,2
COV(I,J)=ACINV(I,J)*AVUW
180 CONTINUE
EE(1,1)=DSQRT(COV(1,1))
EN(1,1)=DSQRT(COV(2,2))

STORING THE STANDARD ERRORS

SE(II,1)=EE(1,1)
SN(II,1)=EN(1,1)
II=II+1
NUMB=NUMB+1
IF(NUMB.EQ.(NUMBER+1))GO TO 210
IF(NUMB.LT.(NUMBER+1))GO TO 200

THE THIRD PART OF THIS PROGRAM INVOLVES THE DETERMINATION OF

```

C THE Z-COORDINATE THROUGH TRIGONOMETRIC HEIGHTING.
C *****
210 NU=1
C -----
C INPUT THE NUMBER OF VERTICAL ANGLE REPETITIONS.
C -----
WRITE(*,400)
400 FORMAT(/5X,'ENTER THE NO. OF VERTICAL ANGLE REPETITIONS')
READ(*,2002)VREP
WREP=VREP*2
C -----
C READING IN THE BACKSIGHT READINGS AND DETERMINING THE HEIGHT
C OF THE COLLIMATION LINE (PC) AT BOTH INSTRUMENT STATIONS.
C -----
III=1
DO 410 I=1,VREP
READ(96,401)BSA(I),BSB(I)
PCA(I)=ZB+BSA(I)
PCB(I)=ZB+BSB(I)
410 CONTINUE
401 FORMAT(3X,F6.4,3X,F6.4)
SUBT=90.0*3600.0
C -----
C READING IN THE OBSERVED VERTICAL ANGLES.
C -----
450 DO 404 I=1,VREP
READ(96,2009)JDEG(I),JMIN(I),VSEC(I),KDEG(I),KMIN(I),WSEC(I)
2009 FORMAT(2X,I3,2X,I2,2X,F5.1,2X,I3,2X,I2,2X,F5.1)
C -----
C CONVERTING THE REDUCED VERTICAL ANGLES INTO SECONDS THEN
C RADIANS.
C -----
VBRG(I)=(JDEG(I)*3600.0+JMIN(I)*60.0+VSEC(I))
VBRG(I)=SUBT-VBRG(I)
VBRG(I)=VBRG(I)/P
WBRG(I)=(KDEG(I)*3600.0+KMIN(I)*60.0+WSEC(I))
WBRG(I)=SUBT-WBRG(I)
WBRG(I)=WBRG(I)/P
404 CONTINUE
C -----
C INITIALISING THE DESIGN MATRIX, AV
C -----
DO 408 I=1,WREP
J=1
408 AV(I,J)=0.0
S1(NU)=DSQRT((EX(NU,1)-EA)**2+(NX(NU,1)-NA)**2)
S2(NU)=DSQRT((EX(NU,1)-EB)**2+(NX(NU,1)-NB)**2)
C -----
C FORMING THE DESIGN MATRIX, AV AND THE VECTOR OF OBSERVATION, YV.
C -----
DO 510 I=1,WREP
510 AV(I,1)=1.0
DO 512 I=1,VREP

```

```

      YV(I,1)=PCA(I)+S1(NU)*TAN(VBRG(I))
512 CONTINUE
      VREP=VREP+1
      DO 513 I=VREP,WREP
        J=1
        YV(I,1)=PCB(J)+S2(NU)*TAN(WBRG(J))
        J=J+1
513 CONTINUE
      VREP=VREP-1
C -----
C MATRIX MANIPULATION.
C -----
C THE ASSUMPTION HERE IS THAT THE OBSERVATIONS ARE UNCORRELATED
C AND ARE OF EQUAL WEIGHT
C -----
      CALL TRANSP(AV,AVT,WREP,1)
      CALL MULT(AVT,AV,AVTA,1,WREP,1)
      CALL MATINV(AVTA,AVINV,1)
      CALL MULT(AVT,YV,AVTY,1,WREP,1)
      XV(1,1)=AVINV(1,1)*AVTY(1,1)
C -----
C ACCURACY ESTIMATION.
C EV IS THE VECTOR OF RESIDUALS
C -----
C STORING THE Z COORDINATE.
C -----
      HX(III,1)=XV(1,1)
      DO 514 I=1,WREP
        AVX(I,1)=AV(I,1)*XV(1,1)
514 CONTINUE
      DO 516 I=1,WREP
516 EV(I,1)=YV(I,1)-AVX(I,1)
C -----
C CALCULATING THE APOSTERIORI VARIANCE OF UNIT WEIGHT.
C -----
      CALL TRANSP(EV,EVT,WREP,1)
      CALL MULT(EVT,EV,EVTE,1,WREP,1)
      DFV=WREP-1
      VVUW=EVTE(1,1)/DFV
C -----
C COMPUTING THE VARIANCE-COVARIANCE MATRIX.
C -----
      COVX(1,1)=AVINV(1,1)*VVUW
      STDV(1,1)=DSQRT(COVX(1,1))
      SH(III,1)=STDV(1,1)
      III=III+1
      NU=NU+1
      IF(NU.EQ.(NUMBER+1))GO TO 470
      IF(NU.LT.(NUMBER+1))GO TO 450
470 WRITE(97,499)
499 FORMAT(///5X,'THE THREE DIMENSIONAL COORDINATES OF THE CONTROL
< FRAME',/2X,60('='),// 4X,'STN',5X,'NORTHING',10X,'EASTING',
< 10X,'HEIGHT',/)

```

```

DO 399 I=1,NUMBER
WRITE(97,498)I,NX(I,1),EX(I,1),HX(I,1)
WRITE(97,496)SN(I,1),SE(I,1),SH(I,1)
399 CONTINUE
498 FORMAT(3X,I3,4X,F10.3,8X,F10.3,7X,F10.3)
496 FORMAT(6X,F12.8,8X,F12.8,8X,F12.8)
C -----
C COMPUTING THE MEAN POSITIONAL ERRORS
C -----
MPEN=0.0
MPEE=0.0
MPEH=0.0
DO 502 I=1,NUMBER
MPEN=MPEN+SN(I,1)
MPEE=MPEE+SE(I,1)
MPEH=MPEH+SH(I,1)
502 CONTINUE
MPEN=MPEN/NUMBER
MPEE=MPEE/NUMBER
MPEH=MPEH/NUMBER
WRITE(97,307)
307 FORMAT(///5X,'THE MEAN POSITIONAL ERRORS (m)',/2X,36('='))
WRITE(97,308)MPEN,MPEE,MPEH
308 FORMAT(/5X,'NORTHING= ',F12.8,/5X,'EASTING= ',F13.8,/5X,
<'HEIGHT= ',F14.8)
STOP
END
C -----
C SUBROUTINES
C -----
SUBROUTINE MULT(A,B,C,L,M,N)
SUBROUTINE FOR MATRIX MULTIPLICATION
C -----
IMPLICIT REAL*8(A-H,O-Z)
DIMENSION A(L,M),B(M,N),C(L,N)
DO 50 I=1,L
DO 50 J=1,N
C(I,J)=0.0
DO 50 K=1,M
C(I,J)=C(I,J)+A(I,K)*B(K,J)
50 CONTINUE
RETURN
END
SUBROUTINE TRANSP(A,B,M,N)
SUBROUTINE FOR MATRIX TRANSPOSITION
C -----
IMPLICIT REAL*8(A-H,O-Z)
DIMENSION A(M,N),B(N,M)
DO 30 I=1,N
DO 30 J=1,M
30 B(I,J)=A(J,I)
RETURN
END

```

```

SUBROUTINE MATINV(G,GINV,N)
SUBROUTINE FOR MATRIX INVERSION
-----
IMPLICIT REAL*8(A-H,O-Z)
DIMENSION G(N,N),GINV(N,N),B(50,100)
DO 1 I=1,N
DO 1 J=1,N
1 B(I,J)=G(I,J)
J1=N+1
J2=2*N
DO 2 I=1,N
DO 2 J=J1,J2
2 B(I,J)=0.0
DO 3 I=1,N
J=I+N
3 B(I,J)=1.0
DO 610 K=1,N
KP1=K+1
IF(K.EQ.N)GO TO 500
L=K
DO 400 I=KP1,N
400 IF(ABS(B(I,K)).GT.ABS(B(L,K))) L=I
IF(L.EQ.K) GO TO 500
DO 410 J=K,J2
TEMP=B(K,J)
B(K,J)=B(L,J)
410 B(L,J)=TEMP
500 DO 501 J=KP1,J2
501 B(K,J)=B(K,J)/B(K,K)
IF(K.EQ.1) GO TO 600
KM1=K-1
DO 510 I=1,KM1
DO 510 J=KP1,J2
510 B(I,J)=B(I,J)-B(I,K)*B(K,J)
IF(K.EQ.N) GO TO 700
600 DO 610 I=KP1,N
DO 610 J=KP1,J2
610 B(I,J)=B(I,J)-B(I,K)*B(K,J)
700 DO 701 I=1,N
DO 701 J=1,N
K=J+N
701 GINV(I,J)=B(I,K)
RETURN
END

```

```

C *****
C PROGRAM DLT
C PROGRAM DLT IS THE DIRECT LINEAR TRANSFORMATION METHOD
C OF SOLVING THE COLLINEARITY CONDITION OF PHOTOGRAMMETRY.
C IT CAN HANDLE REPEATED OBSERVATIONS OF COMPARATOR
C COORDINATES FOR EITHER MONO OR STEREO OBSERVATIONS.
C AS PRESENTLY WRITTEN, IT CAN HANDLE UP TO FOUR
C PHOTOGRAPHS BUT CAN BE MADE TO HANDLE AS MANY PHOTOGRAPHS
C AS ARE USED IN THE SOLUTION BY SIMPLY CHANGING THE
C DIMENSIONS OF THE VARIABLES AFFECTED BY THE NUMBER
C OF PHOTOGRAPHS.
C DEPENDING ON THE EXTENT OF THE LENS DISTORTION CORRECTION,
C IT IS SET UP TO SOLVE FOR ANY OF FOUR GROUPS OF UNKNOWNNS-
C 11, INVOLVING THE ELEVEN DLT PARAMETERS, IN WHICH LINEAR FILM
C DEFORMATION AND LENS DISTORTION ARE IMPLICIT,
C 12, INVOLVING THE DLT PARAMETERS PLUS THE COEFFICIENT
C OF THE 1ST TERM OF SYMMETRICAL LENS DISTORTION,
C 14, INVOLVING THE DLT PARAMETERS PLUS THE COEFFICIENTS OF
C THE 1ST, 2ND, AND 3RD TERMS OF SYMMETRICAL LENS
C DISTORTION,
C 16, INVOLVING THE 14 UNKNOWNNS ABOVE PLUS THE COEFFICIENTS
C OF THE FIRST TWO TERMS OF ASYMMETRICAL LENS DISTORTION.
C *****
C IMPLICIT REAL*8(A-H,O-Z)
C DIMENSION Q(20),SD(20),A(4),R(2,20),RT(20,2),WRT(20,2),
C <WK(2,2),WKR(2,20),RTK(20,20),WRK(20,20),WC(20,20),DX(20,1),
C <XRR(20,1),WRKW(20,20),WKI(2,2),WS(20,20)
C COMMON/DATA/ NNC,NNC1,NPHOT,NUM(100),NUM1(100),E(100,3),
C <X(100,4),Y(100,4),NPOINT,NCONT
C COMMON/TRANS/ D(4,20),XP(4),YP(4),W(20,20)
C COMMON/NUMBER/ NC,NPC(4),NP(100,4)
C
C TOL = 1.D-6
C -----
C TOL=TEST FOR SINGULARITY OF NORMAL EQUATION MATRIX
C -----
C READ(21,9) NPHOT,NREP,NTYPE,NPAIR,NPOINT,NCONT
C WRITE(*,1002)NPHOT,NREP,NTYPE,NPAIR,NPOINT,NCONT
C 9 FORMAT(5X,I1,4X,I1,4X,I1,4X,I1,2X,I3,3X,I3)
C 1002 FORMAT(5X,'NPHOT= ',I1,2X,'NREP= ',I1,2X,'NTYPE= ',I1,2X,
C <'NPAIR= ',I1,2X,'NPOINT= ',I3,2X,'NCONT= ',I3)
C -----
C NPHOT = NUMBER OF PHOTOS USED IN SOLUTION
C NREP = NUMBER OF REPETITIONS IN COMPARATOR
C COORDINATE OBSERVATIONS
C NTYPE = TYPE OF COMPARATOR OBSERVATIONS, 0=MONO, 1=STEREO
C NPAIR = NUMBER OF STEREO PAIRS OBSERVED
C NPOINT = TOTAL NUMBER OF POINTS MEASURED IN COMPARATOR. THIS
C EXCLUDES THE CONTROL POINTS.
C NCONT = NUMBER OF CONTROL POINTS OBSERVED IN THE SCHEME.
C -----
C READ(21,10) SX,SY,SZ
C WRITE(*,1000)SX,SY,SZ
C 10 FORMAT(3(3X,F7.5))
C 1000 FORMAT(5X,'SX= ',F7.5,3X,'SY= ',F7.5,3X,'SZ= ',F7.5)
C
C SX,SY,SZ = STANDARD ERRORS OF OBJECT SPACE COORDINATES
C
C READ OBJECT SPACE COORDINATES OF CONTROL POINTS
C -----

```

```

NC=0
DO 5 I=1,NCONT
READ(21,15)NUM(I),(E(I,J),J=1,3)
15 FORMAT(I6,F10.3,F10.3,F10.3)
IF(NUM(I).EQ.0) GO TO 16
NC = NC+1
5 CONTINUE

```

```

-----
NUM(I)=NUMBER OF POINT I
E(I,J) = OBJECT SPACE COORDINATES OF POINT I,
        J=1,X, J=2,Y, J=3,Z.
-----

```

```

16 CONTINUE
SVV=0.0
ICOUNT=0
DF= (NREP-1)
IF(NREP.EQ.1) DF = 1.0
IF(NTYPE.EQ.1) GO TO 19

```

```

-----
READ OBSERVED COMPARATOR COORDINATES OF CONTROL POINTS IN ALL
PHOTOS FOR MONO-OBSERVATIONS, AND COMPUTE MEAN COORDINATES
-----

```

```

DO 20 K=1,NPHOT
NPC(K)=0
DO 22 I=1,NCONT
X(I,K)= 0.0
Y(I,K)= 0.0
VV=0.0
DO 25 J=1,NREP
READ(21,151)NO,XC,YC
IF(NO.EQ.0)GO TO 20
ICOUNT=ICOUNT+1
X(I,K)=X(I,K)+XC
Y(I,K)=Y(I,K)+YC
VV=VV+XC*XC+YC*YC

```

```

25 CONTINUE
151 FCRMAT(I6,F11.2,F11.2)
NPC(K)=NPC(K)+1
NP(I,K)=NO
VV=VV-(X(I,K)**2+Y(I,K)**2)/NREP
SVV=SVV+DABS(VV)
X(I,K)=X(I,K)/NREP
Y(I,K)=Y(I,K)/NREP
22 CONTINUE
20 CONTINUE
GO TO 28

```

```

-----
NPC(K) = NUMBER OF POINTS OBSERVED IN PHOTO K
NP(I,K) = POINT NUMBER OF POINT I IN PHOTO K
X(I,K),Y(I,K) = COMPARATOR COORDINATES OF POINT I IN PHOTO K.
-----

```

```

READ OBSERVED COMPARATOR COORDINATES OF CONTROL POINTS IN ALL
PHOTOS FOR STEREO-OBSERVATIONS, AND COMPUTE MEAN COORDINATES
-----

```

```

19 CONTINUE
DO 21 K=1,NPAIR
M=2*K
L=M-1
NPC(L)=0
NPC(M)=0
DO 23 I=1,NCONT

```

```

X(I,L)=0.0
Y(I,L)=0.0
X(I,M)=0.0
Y(I,M)=0.0
VV=0.0
DO 24 J=1,NREP
READ(21,152)NO,XC,YC,PX,PY
152 FORMAT(I6,4(F11.2))
IF(NO.EQ.0)GO TO 21
ICOUNT=ICOUNT+2
XD=PX-1000.0
YD=PY-1000.0
XC=XC-1000.0
YC=YC-1000.0
X(I,L)=X(I,L)+XC
Y(I,L)=Y(I,L)+YC
X(I,M)=X(I,M)+XD
Y(I,M)=Y(I,M)+YD
VV=VV+XC*XC+YC*YC+XD*XD+YD*YD
24 CONTINUE
NPC(L)=NPC(L)+1
NPC(M)=NPC(M)+1
NP(I,L)=NO
NP(I,M)=NO
SUML=X(I,L)**2+Y(I,L)**2
SUMM=X(I,M)**2+Y(I,M)**2
VV=VV-(SUML+SUMM)/NREP
SVV=SVV+DABS(VV)
X(I,L)=X(I,L)/NREP
Y(I,L)=Y(I,L)/NREP
X(I,M)=X(I,M)/NREP
Y(I,M)=Y(I,M)/NREP
23 CONTINUE
21 CONTINUE
28 CONTINUE

```

```

-----
COMPUTE STANDARD ERROR OF COMPARATOR COORDINATES
-----

```

```

SP=SVV/(2.0*DF*ICOUNT)
SP=DSQRT(SP)
WRITE(22,150)
150 FORMAT(1H0,2X,'DIRECT LINEAR TRANSFORMATION
(PROGRAM SOLUTION'//)
WRITE(22,32)SP
32 FORMAT(1H0,5X,'STANDARD ERRORS OF COMPARATOR COORDINATES'
, D15.5,//)

```

```

-----
SP = STANDARD ERRORS OF COMPARATOR COORDINATES
-----

```

```

*****

```

```

DETERMINE THE POINTS WHICH HAVE GIVEN OBJECT SPACE
COORDINATES AND WHICH WERE OBSERVED IN ALL THE PHOTOS
AND ARRANGE ACCORDING TO POINT NUMBERS, OBJECT SPACE
COORDINATES AND COMPARATOR COORDINATES IN EACH PHOTO
OF THESE POINTS IN THE SAME EXACT SEQUENCE.

```

```

*****

```

```

CALL SORT

```



```

C
DO 26 K=1,NPHOT
WRITE(22,98)K
98 FORMAT(//5X,'COMPARATOR COORDINATES, PHOTO',I3,/)
DO 27 I=1,NNC
WRITE(22,155)NP(I,K),X(I,K),Y(I,K)
155 FORMAT(I10,2D18.9)
27 CONTINUE
26 CONTINUE

```

```

C
WRITE(22,533)
533 FORMAT(//)
READ(21,1010)IP
1010 FORMAT(4X,I2)

```

```

C
-----
C
IP = NUMBER OF UNKNOWNNS TO BE CARRIED IN SOLUTION
C
-----

```

```

C
WRITE(22,101)IP
101 FORMAT('1',10X,'NUMBER OF UNKNOWNNS= ',I4)
IPP1 = IP+1
IPM1 = IP-1
IF(IP.LT.13)GO TO 29
IPM2 = IP-2
IF(IP.EQ.14)GO TO 29
IPM3 = IP-3
IPM4 = IP-4
29 CONTINUE

```

```

C
-----
C
COMPUTE DEGREES OF FREEDOM
C
-----

```

```

DF=2.0*NNC+2-IP

```

```

DO 30 L=1,NPHOT
XP(L) = 0.0
YP(L) = 0.0

```

```

C
-----
C
XP(L),YP(L) = COMPARATOR COORDINATES OF PRINCIPAL
POINT OF PHOTO L
C
-----

```

```

DO 31 LL=1,5
VV = 0.0

```

```

C
-----
C
VV = SUM OF RESIDUALS SQUARED
C
-----

```

```

C
INITIALIZE NORMAL EQUATIONS
C
-----

```

```

DO 35 I=1,IP
DO 35 J=1,IPP1
W(I,J) = 0.0
35 CONTINUE

```

```

DO 40 K=1,NNC

```

```

C
-----
C
MODELLING OUT OF LENS DISTORTIONS USING THE COMPLETE
POLYNOMIAL AND CONRADY'S THEORY FOR THE SYMMETRICAL
AND ASYMMETRICAL DISTORTIONS RESPECTIVELY.
C
-----

```

```

IF(IP.EQ.11) GO TO 49
XR = X(K,L) - XP(L)
YR = Y(K,L) - YP(L)
R1 = XR**2

```

```

R3 = YR**2
R2 = DSQRT(R1+R3)
IF(IP.EQ.12) GO TO 49
R4 = R2*R2
R6 = R4*R2
IF(IP.EQ.14) GO TO 49
R7 = 2.0*R1 + R4
R8 = 2.0*R3 + R4
R9 = 2.0*XR*YR
49 CONTINUE
DO 50 III = 1,2

```

```

-----
INITIALIZE CONDITION EQUATION
-----

```

```

DO 60 I=1,IP
Q(I) = 0.0
60 CONTINUE

```

```

AB = 1.0
A(L) = 1.0
IF(LL.EQ.1) GO TO 73
DO 74 I=1,3
A(L) = A(L) + D(L,I+8)*E(K,I)
74 CONTINUE

```

```

-----
D(L,I) = UNKNOWN NUMBER I IN PHOTO L.
        IF I=1,11, DLT PARAMETERS
        IF I=12,16, COEFFICIENTS OF LENS DISTORTION
-----

```

```

GO TO (61,62),III
61 B1 = (D(L,9)*X(K,L) - D(L,1))
   B2 = (D(L,10)*X(K,L) - D(L,2))
   B3 = (D(L,11)*X(K,L) - D(L,3))
   GO TO 63
62 B1=(D(L,9)*Y(K,L)-D(L,5))
   B2=(D(L,10)*Y(K,L) - D(L,6))
   B3=(D(L,11)*Y(K,L) - D(L,7))
63 CONTINUE
AB=((SP)**2+(B1*SX)**2+(B2*SY)**2+(B3*SZ)**2)/
<(A(L)**2)

```

```

-----
AB = VARIANCE ASSOCIATED WITH CONDITION EQUATION
-----

```

```

AB = DSQRT(AB)
73. CONTINUE
GO TO (71,72),III

```

```

-----
FORM X-CONDITION EQUATION
-----

```

```

71 DO 70 I=1,3
   Q(I) = E(K,I)
   Q(I+8) = -1.0*E(K,I)*X(K,L)
70 CONTINUE
Q(4)=1.0
Q(IPP1)=X(K,L)
IF(IP.EQ.11)GO TO 75
IF(IP.EQ.12) GO TO 77
IF(IP.EQ.14) GO TO 81
Q(IPM4) = XR*R2*A(L)
Q(IPM3) = XR*R4*A(L)
Q(IPM2) = XR*R6*A(L)

```

```

      Q(IPM1) = R7*A(L)
      Q(IP) = R9*A(L)
      GO TO 75
81  CONTINUE
      Q(IPM2) = XR*R2*A(L)
      Q(IPM1) = XR*R4*A(L)
      Q(IP) = XR*R6*A(L)
      GO TO 75
77  Q(IP) = XR*R2*A(L)
      GO TO 75

```

 C C C FORM Y-CONDITION EQUATION

```

72  DO 80 I=1,3
      Q(I+4) = E(K,I)
      Q(I+8) = -1.0*E(K,I)*Y(K,L)
80  CONTINUE
      Q(8) = 1.0
      Q(IPP1) = Y(K,L)
      IF(IP.EQ.11) GO TO 75
      IF(IP.EQ.12) GO TO 78
      IF(IP.EQ.14) GO TO 82
      Q(IPM4) = YR*R2*A(L)
      Q(IPM3) = YR*R4*A(L)
      Q(IPM2) = YR*R6*A(L)
      Q(IPM1) = R3*A(L)
      Q(IP) = R3*A(L)
      GO TO 75
92  CONTINUE
      Q(IPM2) = YR*R2*A(L)
      Q(IPM1) = YR*R4*A(L)
      Q(IP) = YR*R6*A(L)
      GO TO 75
78  Q(IP) = YR*R2*A(L)
75  CONTINUE

```

 C C C APPLY WEIGHT TO CONDITION EQUATION

```

      DO 76 I=1,IPP1
      Q(I) = Q(I)/(AB*A(L))
76  CONTINUE

```

 C C C COMPUTE CONTRIBUTIONS OF CONDITION EQUATION TO SUM OF
 RESIDUALS SQUARED, AND OBTAIN CUMULATIVE SUM

```

      VW = VW + Q(IPP1)*Q(IPP1)

```

 C C C FORM NORMAL EQUATIONS

```

      DO 80 I=1,IP
      DO 80 J=1,IPP1
      W(I,J) = W(I,J) + Q(J)*Q(I)
80  CONTINUE
      DO 89 I=1,IPM1
      KL=I+1
      DO 89 J=KL,IP
      W(J,I)=W(I,J)
89  CONTINUE
50  CONTINUE
40  CONTINUE

```

```

DO 91 I=1,IP
Q(I)=W(I,IPP1)
91 CONTINUE

```

```

*****
SOLVE NORMAL EQUATIONS
*****

```

```

CALL SWPMAT(W,1,IP,IPP1,KERR,TOL)

```

```

-----
OBTAIN VALUES OF THE UNKNOWNNS, COMPUTE CONTRIBUTIONS OF NORMAL
EQUATIONS TO SUM OF RESIDUALS SQUARED, AND OBTAIN TOTAL SUM.
-----

```

```

DO 105 I=1,IP
D(L,I) = W(I,IPP1)
VV = VV - Q(I)*W(I,IPP1)
105 CONTINUE

```

```

*****
COMPUTE RESIDUALS OF PRINCIPAL POINT,
AND PRINCIPAL DISTANCE FOR PHOTO L
*****

```

```

CALL XPYPC(L,LL)

```

```

*****
INCORPORATE THE TWO DLT RESTRICTIONS AS DEFINED BY BOFP AND
KRAUSS. EXACT PRIOR INFORMATION USING THE OVER-CONSTRAINED
GAUSS-MARKOV MODEL WITH FULL RANK IS THE ESTIMATION
PROCEDURE ADOPTED.
*****

```

```

-----
INITIALIZE THE RESTRICTION DESIGN MATRIX, R
-----

```

```

DO 510 I=1,2
DO 510 J=1,IP
R(I,J)=0.0
510 CONTINUE

```

```

-----
FORMING THE DESIGN RESTRICTION MATRIX, R
-----

```

```

R(1,1)=2.0*(D(L,1)*D(L,10)*D(L,10)+D(L,1)*D(L,11)*D(L,11)
<-D(L,9)*D(L,2)*D(L,10)-D(L,9)*D(L,3)*D(L,11))
R(1,2)=2.0*(D(L,2)*D(L,9)*D(L,9)+D(L,2)*D(L,11)*D(L,11)
<-D(L,1)*D(L,9)*D(L,10)-D(L,10)*D(L,3)*D(L,11))
R(1,3)=2.0*(D(L,3)*D(L,9)*D(L,9)+D(L,3)*D(L,10)*D(L,10)
<-D(L,1)*D(L,9)*D(L,11)-D(L,2)*D(L,10)*D(L,11))
R(1,4)=0.0
R(1,5)=2.0*(D(L,9)*D(L,6)*D(L,10)+D(L,9)*D(L,7)*D(L,11)
<-D(L,5)*D(L,10)*D(L,10)-D(L,5)*D(L,11)*D(L,11))
R(1,6)=2.0*(D(L,5)*D(L,9)*D(L,10)+D(L,10)*D(L,7)*D(L,11)
<-D(L,6)*D(L,9)*D(L,9)-D(L,6)*D(L,11)*D(L,11))
R(1,7)=2.0*(D(L,6)*D(L,10)*D(L,11)+D(L,5)*D(L,9)*D(L,11)
<-D(L,7)*D(L,9)*D(L,9)-D(L,7)*D(L,10)*D(L,10))
R(1,8)=0.0
R(1,9)=2.0*(D(L,2)*D(L,2)*D(L,9)+D(L,3)*D(L,3)*D(L,9)+
<D(L,5)*D(L,6)*D(L,10)+D(L,5)*D(L,7)*D(L,11)-
<D(L,6)*D(L,6)*D(L,9)-D(L,7)*D(L,7)*D(L,9)-
<D(L,1)*D(L,2)*D(L,10)-D(L,1)*D(L,3)*D(L,11))
R(1,10)=2.0*(D(L,1)*D(L,1)*D(L,10)+D(L,3)*D(L,3)*D(L,10)+

```

```

<D(L,5)*D(L,9)*D(L,6)+D(L,6)*D(L,7)*D(L,11)-
<D(L,5)*D(L,5)*D(L,10)-D(L,7)*D(L,7)*D(L,10)-
<D(L,1)*D(L,9)*D(L,2)-D(L,2)*D(L,3)*D(L,11)
R(1,11)=2.0*(D(L,1)*D(L,11)+D(L,2)*D(L,2)*D(L,11)+
<D(L,6)*D(L,10)*D(L,7)+D(L,5)*D(L,9)*D(L,7)-
<D(L,5)*D(L,5)*D(L,11)-D(L,6)*D(L,6)*D(L,11)-
<D(L,1)*D(L,9)*D(L,3)-D(L,2)*D(L,10)*D(L,3)
R(2,1)=D(L,5)*D(L,10)*D(L,10)+D(L,5)*D(L,11)*D(L,11)-
<D(L,9)*D(L,6)*D(L,10)-D(L,9)*D(L,7)*D(L,11)
R(2,2)=D(L,6)*D(L,3)*D(L,9)+D(L,6)*D(L,11)*D(L,11)-
<D(L,10)*D(L,5)*D(L,9)-D(L,10)*D(L,7)*D(L,11)
R(2,3)=D(L,7)*D(L,9)*D(L,9)+D(L,7)*D(L,10)*D(L,10)-
<D(L,11)*D(L,5)*D(L,9)-D(L,11)*D(L,6)*D(L,10)
R(2,4)=0.0
R(2,5)=D(L,1)*D(L,10)*D(L,10)+D(L,1)*D(L,11)*D(L,11)-
<D(L,2)*D(L,10)*D(L,9)-D(L,3)*D(L,11)*D(L,9)
R(2,6)=D(L,2)*D(L,9)*D(L,9)+D(L,2)*D(L,11)*D(L,11)-
<D(L,1)*D(L,9)*D(L,10)-D(L,3)*D(L,11)*D(L,10)
R(2,7)=D(L,3)*D(L,9)*D(L,9)+D(L,3)*D(L,10)*D(L,10)-
<D(L,1)*D(L,9)*D(L,11)-D(L,2)*D(L,10)*D(L,11)
R(2,8)=0.0
R(2,9)=2.0*(D(L,2)*D(L,6)*D(L,9)+D(L,3)*D(L,7)*D(L,9))-
<D(L,1)*D(L,6)*D(L,10)-D(L,1)*D(L,7)*D(L,11)-
<D(L,2)*D(L,10)*D(L,5)-D(L,3)*D(L,11)*D(L,5)
R(2,10)=2.0*(D(L,1)*D(L,5)*D(L,10)+D(L,3)*D(L,7)*D(L,10))-
<D(L,1)*D(L,9)*D(L,6)-D(L,2)*D(L,5)*D(L,9)-
<D(L,2)*D(L,7)*D(L,11)-D(L,3)*D(L,11)*D(L,6)
R(2,11)=2.0*(D(L,1)*D(L,5)*D(L,11)+D(L,2)*D(L,6)*D(L,11))-
<D(L,1)*D(L,9)*D(L,7)-D(L,2)*D(L,10)*D(L,7)-
<D(L,3)*D(L,5)*D(L,9)-D(L,3)*D(L,6)*D(L,10)
DO 519 I=1,IP
DO 519 J=1,IP
IF(W(I,J).NE.W(J,I))GO TO 31

```

MATRIX MANIPULATION

CALL TRANSP(R,RT,2,IP)
 CALL MULT(W,RT,WRT,IP,IP,2)
 CALL MULT(R,WRT,WK,2,IP,2)
 CALL MATINV(WK,WKI,2)
 CALL MULT(WKI,R,WKR,2,2,IP)
 CALL MULT(RT,WKR,RTK,IP,2,IP)
 CALL MULT(W,RTK,WRK,IP,IP,IP)

DO 520 I=1,IP
 DO 520 J=1,IP
 IF(I.EQ.J)GO TO 524
 WC(I,J)=-1.0*WRK(I,J)

GO TO 520
 524 WC(I,J)=1.0-WRK(I,J)
 520 CONTINUE

DO 540 I=1,IP
 J=1

DX(I,J)=D(L,I)
 540 CONTINUE

CALL MULT(WC,DX,XRR,IP,IP,1)
 DO 560 I=1,IP
 J=1

D(L,I)=XRR(I,J)
 560 CONTINUE

```

DO 583 I=1,IP
DO 583 J=1,IP
WS(I,J)=W(I,J)
583 CONTINUE
IF(LL.EQ.1) GO TO 31
-----
C
C COMPUTE, STORE AND PRINT STANDARD ERROR OF UNIT WEIGHT
C
-----
VV=DABS(VV/DF)
STD=DSQRT(VV)
WRITE(22,112)STD
112 FORMAT(11X,'STANDARD ERROR OF UNIT WEIGHT =',F20.4 )
31 CONTINUE
WRITE(22,109) L
109 FORMAT(1H0,5X'COMPUTED VALUES OF UNKNOWNNS AND STANDARD ERRORS,
<PHOTO',I3,/PH/,16X'DLT PARAMETERS',5X'STANDARD ERRORS',/)
-----
C
C COMPUTE VARIANCE-COVARIANCE MATRIX OF
C COMPUTED VALUES OF THE UNKNOWNNS
C
-----
CALL MULT(WRK,W,WRKW,IP,IP,IP)
DO 580 I=1,IP
DO 580 J=1,IP
W(I,J)=W(I,J)-WRKW(I,J)
580 CONTINUE
DO 110 I=1,IP
DO 111 J=1,IP
W(I,J) = W(I,J)*VV
111 CONTINUE
SD(I) = DSQRT(ABS(W(I,I)))
110 CONTINUE
-----
C
C PRINT VALUES OF THE UNKNOWNNS,
C AND THEIR RESPECTIVE STANDARD ERRORS.
C
-----
DO 120 I=1,11
WRITE(22,300) D(L,I),SD(I)
300 FORMAT(10X,2D20.8)
120 CONTINUE
WRITE(22,533)
IF(IP.EQ.11) GO TO 30
-----
C
WRITE(22,119)
119 FORMAT(1H0,5X'LENS DISTORTION COEFFICIENTS',2X'STANDARD ERRORS',/)
DO 130 I = 12,IP
WRITE(22,300) D(L,I), SD(I)
130 CONTINUE
30 CONTINUE
-----
C
C *****
C COMPUTE THE OBJECT SPACE COORDINATES OF CONTROL POINTS
C *****
CALL OBJECT(IPM4,IPM3,IPM2,IPM1,IP,SP)
ICOUNT=0
SVV=0.0
IF(NTYPE.EQ.1)GO TO 115
-----
C
C READ OBSERVED COMPARATOR COORDINATES OF IMAGE POINTS IN ALL
C PHOTOS FOR MONO-OBSERVATIONS, AND COMPUTE MEAN COORDINATES
C
-----

```

```

NO=0
XC=0
YC=0
DO 210 K=1,NPHOT
NPC(K)=0
DO 220 I=1,NPOINT
X(I,K)=0.0
Y(I,K)=0.0
NP(I,K)=0
VV=0.0
DO 250 J=1,NREP
READ(21,151)NO,XC,YC
IF(NO.EQ.999) GO TO 99
IF(NO.EQ.0) GO TO 210
ICOUNT=ICOUNT+1
X(I,K)=X(I,K)+XC
Y(I,K)=Y(I,K)+YC
VV=VV+XC*XC+YC*YC
250 CONTINUE
C
NPC(K)=NPC(K)+1
NP(I,K)=NO
NNC1=NPC(K)
NUM1(I)=0
NUM1(I)=NC
VV=VV-(X(I,K)**2 + Y(I,K)**2)/NREP
SVV=SVV+DABS(VV)
X(I,K)=X(I,K)/NREP
Y(I,K)=Y(I,K)/NREP
220 CONTINUE
210 CONTINUE
GO TO 430

```

```

C
C -----
C READ OBSERVED COMPARATOR COORDINATES OF IMAGE POINTS IN ALL
C PHOTOS FOR STEREO-OBSERVATIONS, AND COMPUTE MEAN COORDINATES
C -----

```

```

115 CONTINUE
DO 420 K=1,NPAIR
M=2*K
L=M-1
NPC(L)=0
NPC(M)=0
DO 422 I=1,NPOINT
X(I,L)=0.0
Y(I,L)=0.0
X(I,M)=0.0
Y(I,M)=0.0
VV=0.0
DO 424 J=1,NREP
READ(21,152)NO,XC,YC,PX,PY
IF(NO.EQ.999)GO TO 99
IF(NO.EQ.0)GO TO 420
ICOUNT=ICOUNT+2
XD=PX-1000.0
YD=PY-1000.0
XC=XC-1000.0
YC=YC-1000.0
X(I,L)=X(I,L)+XC
Y(I,L)=Y(I,L)+YC
X(I,M)=X(I,M)+XD
Y(I,M)=Y(I,M)+YD

```



```
<X(100,4),Y(100,4),NPOINT,NCONT  
COMMON/NUMBER/ NC,NPC(4),NP(100,4)
```

```
C  
NNC = 0  
JJ = NC + 1
```

```
C  
DO 10 I=1,NC  
11 CONTINUE  
ICOUNT = 0  
DO 20 K=1,NPHOT  
M=NPC(K)  
DO 30 J=1,M  
IF(NUM(I).NE.NP(J,K)) GO TO 30  
L(K) = J  
ICOUNT = ICOUNT + 1  
GO TO 20  
30 CONTINUE  
20 CONTINUE
```

```
C  
IF(ICOUNT.EQ.NPHOT) GO TO 40  
JJ = JJ - 1  
IF(JJ.EQ.NNC) GO TO 60  
NTEMP = NUM(JJ)  
XTEMP = E(JJ,1)  
YTEMP = E(JJ,2)  
ZTEMP = E(JJ,3)  
NUM(JJ)=NUM(I)  
E(JJ,1)=E(I,1)  
E(JJ,2)=E(I,2)  
E(JJ,3)=E(I,3)  
NUM(I)=NTEMP  
E(I,1)=XTEMP  
E(I,2)=YTEMP  
E(I,3)=ZTEMP  
GO TO 11
```

```
C  
40 CONTINUE  
NNC=NNC+1  
DO 50 K=1,NPHOT  
J=L(K)  
IF(J.EQ.I) GO TO 50  
NTEMP=NP(J,K)  
XTEMP=X(J,K)  
YTEMP=Y(J,K)  
NP(J,K)=NP(I,K)  
X(J,K)=X(I,K)  
Y(J,K)=Y(I,K)  
NP(I,K)=NTEMP  
X(I,K)=XTEMP  
Y(I,K)=YTEMP  
50 CONTINUE  
10 CONTINUE  
60 CONTINUE
```

```
C  
RETURN  
END  
SUBROUTINE XPYPC(L,LL)
```

```
C  
C  
C *****  
C  
C SUBROUTINE XPYPC COMPUTES THE COORDINATES OF THE PRINCIPAL
```

C POINT, XP AND YP, AND THE PRINCIPAL DISTANCE, C, OF A
 C PHOTOGRAPH FROM THE DIRECT LINEAR TRANSFORMATION PARAMETERS
 C OBTAINED FOR THE PHOTOGRAPH

IMPLICIT REAL*8(A-H,O-Z)
 DIMENSION Q(5)
 COMMON/TRANS/ D(4,20),XP(4),YP(4),W(20,20)

DO 10 I=1,5
 Q(I) = 0.0
 10 CONTINUE

DO 30 I=1,3
 J=I+8
 K=I+4
 Q(1) = Q(1) + D(L,I)*D(L,J)
 Q(2) = Q(2) + D(L,K)*D(L,J)
 Q(3) = Q(3) + D(L,I)*D(L,I)
 Q(4) = Q(4) + D(L,K)*D(L,K)
 Q(5) = Q(5) + D(L,J)*D(L,J)
 30 CONTINUE

XP(L) = Q(1)/Q(5)
 YP(L) = Q(2)/Q(5)
 CX= Q(3)/Q(5) - XP(L)*XP(L)
 CY= Q(4)/Q(5) - YP(L)*YP(L)
 CX=DSQRT(CX)
 CY=DSQRT(CY)
 C=(CX+CY)*0.5

IF(LL.EQ.1) GO TO 40
 WRITE(22,100)L
 100 FORMAT(1H0,10X'INNER ORIENTATION, PHOTO'13)
 WRITE(22,300)XP(L),YP(L),C
 300 FORMAT(15X'XP=',F10.4,5X'YP=',F10.4,5X'C=',F10.4)
 40 CONTINUE

RETURN
 END
 SUBROUTINE OBJECT (IPM4,IPM3,IPM2,IPM1,IP,SP)

SUBROUTINE OBJECT APPLIES LENS DISTORTION CORRECTIONS TO THE
 OBSERVED COMPARATOR COORDINATES OF CONTROL POINTS, AND RECOMPUTES
 THE OBJECT SPACE COORDINATES OF THESE POINTS AGAIN USING AS MANY
 PHOTOGRAPHS AS WERE USED IN THE SOLUTION.

IMPLICIT REAL*8(A-H,O-Z)
 DIMENSION Q(10),T(20,20),XX(4),YY(4),R(20),F(20),AX(4),AY(4),
 \A(4),XCC(3),SE(4),SSE(4)
 COMMON/DATA/ NNC,NNC1,NPHOT,NUM(100),NUM1(100),E(100,3),
 \X(100,4),Y(100,4),NPOINT,NCONT
 COMMON/TRANS/ D(4,20),XP(4),YP(4),W(20,20)
 COMMON/NUMBER/ NC,NPC(4),NP(100,4)

TOL = 1.D-6

C PRINT HEADING FOR TABULATION OF COMPUTED DATA
C-----

WRITE(22,126)NPHOT

126 FORMAT('1',1X,'COMPUTATIONS FOR',I4,2X,'-PHOTO DLT',//
\",4X,'POINT',17X,'GIVEN',38X,'COMPUTED',
\\//2(14X,'X',14X,'Y',14X,'Z'),//)

C INITIALIZE AVERAGE STANDARD ERRORS,
C AND COMPUTE DEGREES OF FREEDOM
C-----

DO 5 I=1,4

SSE(I)=0.0

5 CONTINUE

DF=2*NPHOT-3

C APPLY LENS DISTORTION CORRECTION TO OBSERVED COMPARATOR
C COORDINATES. USE IS MADE OF THE COMPLETE POLYNOMIAL AND
C CONRADY'S THEORY FOR THE SYMMETRYCAL AND ASYMMETRICAL
C LENS DISTORTIONS RESPECTIVELY.
C-----

DO 10 K=1,NNC

DO 15 L=1,NPHOT

AX(L) = 1.0

AY(L) = 1.0

IF(IP.EQ.11) GO TO 12

XXX = X(K,L)-XP(L)

YYY = Y(K,L)-YP(L)

R1 = XXX**2

R3 = YYY**2

R2 = DSQRT(R1+R3)

IF(IP.EQ.12) GO TO 14

R4 = R2*R2

R6 = R4*R2

IF(IP.EQ.14) GO TO 17

DK = D(L,IPM4)*R2 + D(L,IPM3)*R4 + D(L,IPM2)*R6

R7 = 2.0*R1 + R4

R8 = 2.0*R3 + R4

R9 = 2.0*XXX*YYY

XX(L) = X(K,L) - (XXX*DK + D(L,IPM1)*R7 + D(L,IP)*R9)

YY(L) = Y(K,L) - (YYY*DK + D(L,IPM1)*R8 + D(L,IP)*R9)

C XX(L),YY(L) = PLATE COORDINATES CORRECTED FOR LENS DISTORTION
C-----

GO TO 15

17 CONTINUE

DK = D(L,IPM2)*R2 + D(L,IPM1)*R4 + D(L,IP)*R6

GO TO 18

14 CONTINUE

DK=D(L,IP)*R2

18 CONTINUE

XX(L) = X(K,L)-XXX*DK

YY(L) = Y(K,L)-YYY*DK

GO TO 15

12 CONTINUE

XX(L) = X(K,L)

YY(L) = Y(K,L)

15 CONTINUE

C COMPUTE WEIGHTS ASSOCIATED WITH CONDITION EQUATIONS
C-----

```

0 -----
DO 20 M=1,2
IF(M.EQ.1) GO TO 80
DO 25 L=1,NPHOT
XXX = X(K,L) - XP(L)
YYY = Y(K,L) - YP(L)
A(L) = 1.0
DO 30 I=1,3
A(L) = A(L)+D(L,I+8)*XCC(I)
30 CONTINUE

DO 35 II=1,2
GG = 0.0
DO 40 I=1,IP
R(I) = 0.0
F(I) = 0.0
40 CONTINUE

IF(II.EQ.2) GO TO 50
DO 45 I=1,3
J = I+8
R(I) = XCC(I)
R(J) = -1.0*XCC(I)*X(K,L)
45 CONTINUE
R(4) = 1.0
IF(IP.EQ.11)GO TO 60
R(12)=-1.0*A(L)*XXX(L)*R2
IF(IP.EQ.12)GO TO 60
R(13)=-1.0*A(L)*XXX(L)*R4
R(14)=-1.0*A(L)*XXX(L)*R6
IF(IP.EQ.14)GO TO 60
R(15)=-1.0*A(L)*R7
R(16)=-1.0*A(L)*R9
GO TO 60

50 CONTINUE
DO 55 I=5,7
J = I+4
JU = I-4
R(I) = XCC(JU)
R(J) = -1.0*XCC(JU)*Y(K,L)
55 CONTINUE
R(8) = 1.0
IF(IP.EQ.11)GO TO 60
R(12)=-1.0*A(L)*YYY(L)*R2
IF(IP.EQ.12)GO TO 60
R(13)=-1.0*A(L)*YYY(L)*R4
R(14)=-1.0*A(L)*YYY(L)*R6
IF(IP.EQ.14)GO TO 60
R(15)=-1.0*A(L)*R9
R(16)=-1.0*A(L)*R8
60 CONTINUE
AB = (A(L)*SP)**2

DO 65 I=1,IP
DO 70 J=1,IP
F(I) = F(I) + R(J)*W(I,J)
70 CONTINUE
GG = GG + F(I)*R(I)
85 CONTINUE
IF(II.EQ.2) GO TO 75

```

```

AX(L) = GG+AB
-----
AX(L) = VARIANCE ASSOCIATED WITH X-CONDITION EQUATION
-----
AX(L) = DSQRT(AX(L))
GO TO 35
75 AY(L) = GG+AB
-----
AY(L) = VARIANCE ASSOCIATED WITH Y-CONDITION EQUATION
-----
AY(L) = DSQRT(AY(L))
35 CONTINUE
35 CONTINUE
90 CONTINUE
-----
INITIALIZE NORMAL EQUATIONS, AND SUM OF RESIDUALS SQUARED
-----
DO 85 I=1,3
DO 85 J=1,4
T(I,J) = 0.0
85 CONTINUE
VV = 0.0

DO 90 L=1,NPNOT
DO 95 II=1,2
GO TO (91,92),II
-----
FORM X-CONDITION EQUATION
-----
91 DO 96 I=1,3
J = I+8
Q(I) = (D(L,J)*XX(L) - D(L,I))/AX(L)
96 CONTINUE
Q(4) = (D(L,4)*1.000 - XX(L))/AX(L)
GO TO 100
-----
FORM Y-CONDITION EQUATION
-----
92 DO 97 I=1,3
J = I+8
JJ=I+4
Q(I) = (D(L,J)*YY(L) - D(L,JJ))/AY(L)
97 CONTINUE
Q(4) = (D(L,8)*1.000 - YY(L))/AY(L)
100 CONTINUE
-----
COMPUTE CONTRIBUTIONS OF CONDITION EQUATION TO SUM OF RESIDUALS
SQUARED, AND OBTAIN CUMULATIVE SUM
-----
VV = VV + Q(4)**2
-----
FORM NORMAL EQUATIONS
-----
DO 105 I=1,3
DO 105 J=1,4
T(I,J) = T(I,J) + Q(I)*Q(J)
105 CONTINUE
95 CONTINUE
90 CONTINUE
DO 110 I=1,3

```

```

Q(I) = T(I,4)
110 CONTINUE

*****
SOLVE NORMAL EQUATIONS
*****

CALL SWPMAT(T,1,3,4,KERR,TOL)
-----
OBTAIN COMPUTED OBJECT SPACE COORDINATES OF A POINT, XCC(I),
I=1,3 I=1,X, I=2,Y, I=3,Z
COMPUTE CONTRIBUTIONS OF NORMAL EQUATIONS TO SUM OF RESIDUALS
SQUARED, AND OBTAIN TOTAL SUM
-----
DO 115 I=1,3
XCC(I)=T(I,4)
VV = VV - Q(I)*T(I,4)
115 CONTINUE
IF(M.EQ.1) GO TO 20
VV = DABS(VV/DF)
-----
COMPUTE STANDARD ERROR OF UNIT WEIGHT
-----
SEUW = DSQRT(VV)
SE(4)=0.0
-----
COMPUTE VARIANCE-COVARIANCE MATRIX OF COMPUTED COORDINATES
-----
DO 120 I=1,3
DO 125 J=1,3
T(I,J)=VV*(T(I,J))
125 CONTINUE
SE(I) = T(I,I)
SE(4) = SE(4) + SE(I)
120 CONTINUE
20 CONTINUE
-----
COMPUTE SUMS OF VARIANCES, AND STANDARD ERRORS OF COORDINATES
-----
DO 130 I=1,4
SSE(I) = SSE(I) + SE(I)
SE(I) = DSQRT(SE(I))
130 CONTINUE
-----
PRINT CONTROL POINT NUMBER, GIVEN AND COMPUTED COORDINATES,
AND STANDARD ERRORS, FOR EACH POINT
-----
WRITE(22,200) NUM(K),(E(K,I),I=1,3),(XCC(I),I=1,3)
200 FORMAT(1X,I5,10D15.7)
WRITE(22,255)
255 FORMAT(26X,'RMS',27X'POS',/)
WRITE(22,256)(SE(I),I=1,4)
256 FORMAT(6X,4D15.7,/)

10 CONTINUE
-----
COMPUTE AND PRINT AVERAGE STANDARD ERRORS FOR ALL THE CONTROL
POINTS.
-----
DO 140 I=1,4
SSE(I) = DSQRT(SSE(I)/NMC)

```

140 CONTINUE

WRITE(22,400) NNC,(SSE(I),I=1,4)

400 FORMAT(1H0,9X'AVERAGE MEAN SQUARE ERRORS FOR',I3,2X'POINTS ARE',/
< ,6X,4D15.7,///)

RETURN

END

SUBROUTINE SWPMAT(A,IN,N,M,KERR,TOL)

SUBROUTINE SWPMAT IS A MATRIX INVERSION ROUTINE FOR USE WITH
LEAST SQUARE PROBLEMS.

SWEEPS CLEAR ACROSS MATRIX TO COLUMN M. BY SWEEPING ENTIRE MATRIX
SWPMAT DEVELOPS REGRESSION COEFFICIENTS WITHOUT MATRIX MULTIPLI-
CATION. IN IS THE SUBSCRIPT OF THE FIRST PIVOTAL ELEMENT TO
BE USED BY THE SUBROUTINE. FOR EXAMPLE IN = 2 WILL IGNORE THE
THE FIRST ROW AND COLUMN OF THE MATRIX A. IN = 1 USUALLY.
BY USING M=N IN CALLING SEQUENCE, SWPMAT MAY BE USED FOR
INVERSION ONLY, SWEEPING N COLUMNS AND ROWS.

THE SWEEPED PORTION OF THE MATRIX REPLACES THE ORIGINAL CONTENTS
OF THE A MATRIX, WHICH ARE DESTROYED.

TOL IS THE TEST FOR SINGULARITY- SUGGEST TOL= 1.0D-06 IN
CALLING PROGRAM.

N = NUMBER OF INDEPENDENT VARIABLES.

M = N + NUMBER OF DEPENDENT VARIABLES.

KERR = ERROR SWITCH, ZERO IF MATRIX NOT SINGULAR, HAS ROW OR
COLUMN NUMBER CAUSING SINGULARITY IF SINGULAR.

THE SUBROUTINE IS APPLICABLE TO NON-SYMMETRIC CASES ALSO.

THE PROGRAM WAS DEVELOPED BY THE DEPARTMENT OF AGRONOMY,
UNIVERSITY OF ILLINOIS AT URBANA CHAMPAIGN.

IMPLICIT REAL*8(A-H,O-Z)

DIMENSION A(20,20)

KERR = 0

DO 40 K=IN,N

IF(DABS(A(K,K)) - TOL) 85,85,86

86 X = 1.0/A(K,K)

DO 41 J=IN,M

41 A(K,J) = A(K,J)*X

A(K,K) = X

DO 42 I=IN,N

IF(I-K) 50,42,50

50 Y=A(I,K)

A(I,K)=0.0

DO 43 J=IN,M

43 A(I,J)=A(I,J)-Y*A(K,J)

42 CONTINUE

40 CONTINUE

99 RETURN

85 KERR=K

GO TO 99

END

SUBROUTINE OBTWO(IPM4,IPM3,IPM2,IPM1,IP,SF)

C
 C SUBROUTINE OBtwo APPLIES LENS DISTORTION CORRECTIONS TO THE
 C OBSERVED COMPARATOR COORDINATES OF IMAGE POINTS, AND COMPUTES
 C OBJECT SPACE COORDINATES OF THESE POINTS USING AS MANY PHOTOGRAPHS
 C AS WERE USED IN THE SOLUTION
 C

C
 C IMPLICIT REAL*8(A-H,O-Z)
 C DIMENSION Q(10),T(20,20),XX(4),YY(4),R(20),F(20),AX(4),AY(4),
 C \A(4),XCC(3),SE(4),SSE(4)
 C COMMON/DATA/ NNC,NNC1,NPHOT,NUM(100),NUM1(100),E(100,3),
 C \X(100,4),Y(100,4),NPOINT,NCONT
 C COMMON/TRANS/ D(4,20),XP(4),YP(4),W(20,20)
 C COMMON/NUMBER/ NC,NPC(4),NP(100,4)
 C

TOL=1.D-6

 PRINT HEADING FOR TABULATION OF COMPUTED DATA

C
 C WRITE(22,127)NPHOT
 C 127 FORMAT('1',1X'COMPUTATIONS FOR',I4,2X'-PHOTO DLT',//,1X'POINT',
 C \14X'COMPUTED OBJECT',24X'RMS',
 C \/,10X'SPACE COORDINATES',
 C \//,2(14X'X',14X'Y',14X'Z'),14X'POS',//)
 C

 INITIALIZE AVERAGE STANDARD ERRORS,
 AND COMPUTE DEGREES OF FREEDOM

C
 C DO 305 I=1,4
 C SSE(I)=0.0
 C 305 CONTINUE
 C DF=2*NPHOT-3
 C

 APPLY LENS DISTORTION CORRECTIONS TO OBSERVED COMPARATOR
 COORDINATES. USE IS MADE OF THE COMPLETE POLYNOMIAL AND
 CONRADY'S THEORY FOR THE SYMMETRICAL AND ASYMMETRICAL
 LENS DISTORTIONS RESPECTIVELY.

C
 C DO 310 K=1,NNC1
 C DO 315 L=1,NPHOT
 C AX(L)=1.0
 C AY(L)=1.0
 C IF(IP.EQ.11) GO TO 312
 C XXX = X(K,L) - XP(L)
 C YYY = Y(K,L) - YP(L)
 C R1 =XXX**2
 C R3 =YYY**2
 C R2 =DSQRT(R1+R3)
 C IF(IP.EQ.12) GO TO 314
 C R4 = R2*R2
 C R6 = R4*R2
 C IF(IP.EQ.14) GO TO 317
 C DK = D(L,IPM4)*R2 + D(L,IPM3)*R4 + D(L,IPM2)*R6
 C R7 = 2.0*R1 + R4
 C R8 = 2.0*R3 + R4
 C R9 = 2.0*XXX*YYY
 C XX(L) = X(K,L) - (XXX*DK + D(L,IPM1)*R7 + D(L,IP)*R9)
 C YY(L) = Y(K,L) - (YYY*DK + D(L,IPM1)*R8 + D(L,IP)*R8)
 C

 XX(K),YY(L) = PLATE COORDINATES CORRECTED FOR LENS DISTORTION

```

C -----
  GO TO 315
317 CONTINUE
  DK = D(L,IPM2)*R2 + D(L,IPM1)*R4 + D(L,IP)*R6
  GO TO 318
314 CONTINUE
  DK = D(L,IP)*R2
318 CONTINUE
  XX(L) = X(K,L) - XXX*DK
  YY(L) = Y(K,L) - YYY*DK
  GO TO 315
312 CONTINUE
  XX(L) = X(K,L)
  YY(L) = Y(K,L)
315 CONTINUE

```

```

C -----
C COMPUTE WEIGHTS ASSOCIATED WITH CONDITION EQUATIONS
C -----

```

```

  DO 320 M=1,2
  IF(M.EQ.1) GO TO 380
  DO 325 L=1,NPHOT
  XXX = X(K,L) - XP(L)
  YYY = Y(K,L) - YP(L)
  A(L)=1.0
  DO 330 I=1,3
  A(L) = A(L) + D(L,I+8)*XCC(I)
330 CONTINUE

```

```

  DO 335 II=1,2
  GG=0.0
  DO 340 I=1,IP
  R(I)=0.0
  F(I)=0.0
340 CONTINUE

```

```

  IF(II.EQ.2) GO TO 350
  DO 345 I=1,3
  J = I + 8
  R(I) = XCC(I)
  R(J) = -1.0*XCC(I)*X(K,L)
345 CONTINUE
  R(4)=1.0
  IF(IP.EQ.11)GO TO 360
  R(12)=-1.0*A(L)*XX(L)*R2
  IF(IP.EQ.12)GO TO 360
  R(13)=-1.0*A(L)*XX(L)*R4
  R(14)=-1.0*A(L)*XX(L)*R6
  IF(IP.EQ.14)GO TO 360
  R(15)=-1.0*A(L)*R7
  R(16)=-1.0*A(L)*R9
  GO TO 360

```

```

350 CONTINUE
  DO 355 I=5,7
  J = I + 4
  JJ = I - 4
  R(I) = XCC(JJ)
  R(J) = -1.0*XCC(JJ)*Y(K,L)
355 CONTINUE
  R(8)=1.0
  IF(IP.EQ.11)GO TO 360

```

```

R(12)=-1.0*A(L)*YY(L)*R2
IF(IP.EQ.12)GO TO 360
R(13)=-1.0*A(L)*YY(L)*R4
R(14)=-1.0*A(L)*YY(L)*R6
IF(IP.EQ.14)GO TO 360
R(15)=-1.0*A(L)*R9
R(16)=-1.0*A(L)*R8
360 CONTINUE
AB = (A(L)*SP)**2

```

```

C
DO 365 I=1,IP
DO 370 J=1,IP
F(I) = F(I) + R(J)*W(I,J)
370 CONTINUE
GG = GG + F(I)*R(I)
365 CONTINUE
IF(II.EQ.2) GO TO 375
AX(L) = GG + AB

```

```

-----
AX(L) = VARIANCE ASSOCIATED WITH X-CONDITION EQUATION
-----

```

```

AX(L) = DCQRT(AX(L))
GO TO 335
375 AY(L) = GG + AB

```

```

-----
AY(L) = VARIANCE ASSOCIATED WITH Y-CONDITION EQUATION
-----

```

```

AY(L) = DCQRT(AY(L))
385 CONTINUE
386 CONTINUE
390 CONTINUE

```

```

-----
INITIALIZE NORMAL EQUATIONS, AND SUM OF RESIDUALS SQUARED
-----

```

```

DO 395 I=1,3
DO 395 J=1,4
T(I,J) = 0.0
395 CONTINUE
VY = 0.0

```

```

DO 390 L=1,NPHOT
DO 395 II=1,2
GO TO (391,392),II

```

```

-----
FORM X-CONDITION EQUATION
-----

```

```

391 DO 396 I=1,3
J = I + 3
Q(I) = (D(L,J)*XX(L) - D(L,I))/AX(L)
396 CONTINUE
Q(4) = (D(L,4)*1.000 - XX(L))/AX(L)
GO TO 700

```

```

-----
FORM Y-CONDITION EQUATION
-----

```

```

392 DO 397 I=1,3
J = I + 3
JJ = I + 4
Q(I) = (D(L,J)*YY(L) - D(L,JJ))/AY(L)
397 CONTINUE
Q(4) = (D(L,3)*1.000 - YY(L))/AY(L)

```

```

700 CONTINUE
C -----
C COMPUTE CONTRIBUTIONS OF CONDITION EQUATION TO SUM OF RESIDUALS
C SQUARED, AND OBTAIN CUMULATIVE SUM
C -----
VV = VV + Q(4)**2
C -----
C FORM NORMAL EQUATIONS
C -----
DO 405 I=1,3
DO 405 J=1,4
T(I,J) = T(I,J) + Q(I)*Q(J)
405 CONTINUE
395 CONTINUE
390 CONTINUE
C
DO 410 I=1,3
Q(I) = T(I,4)
410 CONTINUE
C
C *****
C SOLVE NORMAL EQUATIONS
C *****
CALL SWPMAT(T,1,3,4,KERR,TOL)
C -----
C OBTAIN COMPUTED OBJECT SPACE COORDINATES OF A POINT, XCC(I),
C I=1,3 I=1,X, I=2,Y, I=3,Z
C COMPUTED CONTRIBUTIONS OF NORMAL EQUATIONS TO SUM OF RESIDUALS
C SQUARED, AND OBTAIN TOTAL SUM
C -----
DO 415 I=1,3
XCC(I)=T(I,4)
VV = VV - Q(I)*T(I,4)
415 CONTINUE
IF(M.EQ.1) GO TO 320
VV = DABS(VV/DF)
C -----
C COMPUTE STANDARD ERROR OF UNIT WEIGHT
C -----
SEUW = DSQRT(VV)
SE(4) = 0.0
C -----
C COMPUTE VARIANCE-COVARIANCE MATRIX OF COMPUTED COORDINATES
C -----
DO 420 I=1,3
DO 425 J=1,3
T(I,J) = VV*(T(I,J))
425 CONTINUE
SE(I) = T(I,I)
SE(4) = SE(4) + SE(I)
420 CONTINUE
320 CONTINUE
C -----
C COMPUTE SUMS OF VARIANCES, AND STANDARD ERRORS OF COORDINATES
C -----
DO 430 I=1,4
SSE(I) = SSE(I) + SE(I)
SE(I) = DSQRT(SSE(I))
430 CONTINUE
C -----

```

```

C     PRINT POINT NUMBER, COMPUTED COORDINATES,
C     AND STANDARD ERRORS, FOR EACH POINT
C     -----
C     WRITE(22,500) NUM1(K),(XCC(I),I=1,3),(SE(I),I=1,4)
500  FORMAT(1X,I5,10D15.7)
C
C     310 CONTINUE
C     -----
C     COMPUTE AND PRINT AVERAGE STANDARD ERRORS FOR ALL THE POINTS
C     -----
C     DO 440 I=1,4
C     SSE(I) = DSQRT(SSE(I)/NNC1)
440  CONTINUE
C
C     WRITE(22,600) NNC1,(SSE(I),I=1,4)
600  FORMAT(1H0,4X,'AVERAGE MEAN SQUARE ERRORS FOR',I3,
        \2X,'POINTS ARE',/,6X,4D15.7)
C
C     RETURN
C     END
C     SUBROUTINE TRANSP(A,B,M,N)
C     IMPLICIT REAL*8(A-H,O-Z)
C
C     DIMENSION A(M,N),B(N,M)
C     DO 30 I=1,N
C     DO 30 J=1,M
30   B(I,J)=A(J,I)
C
C     RETURN
C     END
C     SUBROUTINE MULT(D,B,C,L,M,N)
C     IMPLICIT REAL*8(A-H,O-Z)
C
C     DIMENSION D(L,M),B(M,N),C(L,N)
C     DO 75 I=1,L
C     DO 75 J=1,N
C     C(I,J)=0.0
C     DO 75 K=1,M
C     C(I,J)=C(I,J)+D(I,K)*B(K,J)
75   CONTINUE
C     RETURN
C     END
C     SUBROUTINE MATINV(A,AINV,N)
C     SUBROUTINE INVERTS A MATRIX OF ORDER N
C     AINV IS THE INVERSE OF A
C     IMPLICIT REAL*8(A-H,O-Z)
C     DIMENSION A(N,N),AINV(N,N),B(50,100)
C     DO 11 I=1,N
C     DO 11 J=1,N
11   B(I,J)=A(I,J)
        J1=N+1
        J2=2*N
        DO 12 I=1,N
        DO 12 J=J1,J2
12   B(I,J)=0.0
        DO 13 I=1,N
        J=I+N
13   B(I,J)=1.0
        DO 610 K=1,N
        KP1=K+1
        IF(K.EQ.N)GO TO 500

```

```

L=K
DO 400 I=KP1,N
400 IF(ABS(B(I,K)).GT.ABS(B(L,K)))L=I
IF(L.EQ.K)GO TO 500
DO 410 J=K,J2
TEMP=B(K,J)
B(K,J)=B(L,J)
410 B(L,J)=TEMP
500 DO 501 J=KP1,J2
501 B(K,J)=B(K,J)/B(K,K)
IF(K.EQ.1)GO TO 600
KM1=K-1
DO 510 I=1,KM1
DO 510 J=KP1,J2
510 B(I,J)=B(I,J)-B(I,K)*B(K,J)
IF(K.EQ.N)GO TO 700
600 DO 610 I=KP1,N
DO 610 J=KP1,J2
610 B(I,J)=B(I,J)-B(I,K)*B(K,J)
700 DO 701 I=1,N
DO 701 J=1,N
K=J+N
701 AINV(I,J)=B(I,K)
RETURN
END

```